MODELLING OF THE RESILIENT AND PERMANENT DEFORMATION BEHAVIOUR OF SUBGRADE SOILS AND UNBOUND GRANULAR MATERIALS

by

Haithem T. Soliman

A Thesis

Submitted to the Faculty of Graduate Studies in Partial Fulfillment of the Requirements for the Degree of

Doctor of Philosophy

Department of Civil Engineering
University of Manitoba
Winnipeg, Manitoba

Abstract

Laboratory characterization of subgrade soils and unbound granular materials is an essential component of the Mechanistic-Empirical Pavement Design Guide (Pavement ME). The design thickness and performance of a pavement structure are highly dependent on the deformation behaviour of subgrade and granular material. Specifications for granular materials vary among transportation agencies based on the availability of materials, climatic conditions, and function. Specifications aim to provide durable materials that meet design requirements and achieve the target design life with cost effective materials.

The objectives of the research are to:

- evaluate resilient modulus of typical fine-grained soils under traffic loading.
- evaluate resilient modulus, permanent deformation, and permeability of typical unbound granular materials.
- evaluate the effect of moisture and fines fraction on the performance of unbound granular materials and subgrade soil.
- develop prediction models for resilient modulus to improve reliability of Level 2 inputs in the Pavement ME.
- provide test data in support of updating Manitoba Infrastructure and Transportation specifications for unbound granular materials to improve the performance of pavement structures.

Resilient modulus tests were conducted on three types of subgrade soil (high plastic clay, sandy clay, and silty sand/sandy silt) at four levels of moisture content. Resilient modulus, permanent deformation and permeability tests were conducted on six gradations representing two types of granular material (100% crushed limestone and gravel) at two levels of moisture content. Prediction models were developed for resilient modulus and compared to the models developed under the Long Term Pavement Performance program. The proposed models provided more reliable predictions with lower root mean square error.

The deformation behaviour of the granular materials was classified according to the shakedown and dissipated energy approaches. Among the tested fines contents, limestone and gravel materials with optimum fines contents of 4.5% and 9%, respectively, had better resistance to plastic deformation and higher resilient modulus. The dissipated energy approach can be used to determine the stress ratio for the boundary between post compaction and stable zones from multistage triaxial testing. Result of permeability tests showed that the hydraulic conductivity of unbound granular material increased as the fines content decreased.

Acknowledgements

I would like to thank my academic advisor, Dr. Ahmed Shalaby, for his professional guidance, support and motivation throughout this research. Sincere thanks to the members of my examination committee, Dr. Marolo Alfaro, Dr. Louay Mohammad, and Dr. Olanrewaju Ojo. I would also like to thank Materials Engineering Branch staff, Manitoba Infrastructure and Transportation, Mr. Said Kass, Mr. Stan Hilderman, and Dr. Alauddin Ahammed, for their contribution toward the development of this research. In addition, I would like to thank Pavement Research Laboratory staff, Mr. Scott Sparrow and Mr. Mohammad Ahmeduzzaman, and Central Laboratory staff, Mr. Gord Konzelman and Mr. Ryan Fleming, for providing the technical support for the laboratory testing in this research.

I would like to acknowledge the support of this research by Manitoba infrastructure and Transportation, National Science and Engineering Research Council of Canada, and Transportation Association of Canada Foundation.

Finally, I would like to extend my sincere gratitude and appreciation to my father, mother, and brothers for their support and continuous encouragement over the course of my study.

Table of Contents

List of Tables

List of Figures

NOTATIONS AND ABBREVIATIONS

% clay	Percentage of clay in the soil sample
% P200	Percentage passing sieve No. 200
%P3/8	Percentage of passing sieve No. 3/8″
%P4	Percentage of passing sieve No. 4
%P40	Percentage of passing sieve No. 40
% Silt	Percentage of silt in the soil sample
AASHTO	Association of State Highway and Transportation Officials
AC	Asphalt Concrete
CBR	California bearing ratio
D_{60}	Particle size at 60% passing
DER	Dissipated energy ratio
GI	Group index
k	Measured hydraulic conductivity
k_{sat}	Saturated hydraulic conductivity from MEPDG model
LL	Liquid limit
LI	Liquidity index
LTPP	Long Term Pavement Performance
MC	Moisture content
MEPDG	Mechanistic Empirical Pavement Design Guide
M_R	Resilient modulus
N	Number of loading cycles

NCHRP	National Cooperative Highway Research Program
OMC	Optimum moisture content
PI	Plasticity index
p-value	The probability associated with the t-test
n_f	Fines fraction porosity
P_a	Atmospheric pressure at sea level
R^2	Coefficient of determination
RMSE	Root mean square error
S_R	Degree of saturation
W_d	Dissipated energy
W_e	Elastic energy
W_h	Hysteretic energy
W_e	Elastic energy
W_p	Plastic energy
W_T	Total energy
UGM	Unbound Granular Material
τ_{oct}	Octahedral shear stress
σ_d	Deviator stress
ε_r	Resilient strain
ε_p	Permanent strain
$\varepsilon_{p,\,3000}$	Permanent strain after 3,000 loading cycles
$\varepsilon_{p,\,5000}$	Permanent strain after 5,000 loading cycles
$\varepsilon_{p,\,13000}$	Permanent strain after 13,000 loading cycles

θ	Bulk stress
σ_1	Total vertical stress
σ_2, σ_3	Horizontal principal stresses
γ_{opt}	Maximum dry density

1 Introduction

1.1 General Overview

Resilient modulus of unbound granular base materials (UGM) and subgrade soils is an essential material property in any mechanistically-based design and analysis procedure for pavements. Resilient modulus is defined as the ratio of the applied cyclic stress to the "recoverable" strain measured during the unloading phase of the loading cycle. The resilient modulus (M_R) is one of the required material properties for the 1993 American Association of State Highway and Transportation Officials (AASHTO) Design Guide which is an empirically-based design procedure (AASHTO 1993). Resilient modulus is also the primary material input parameter for the Mechanistic-Empirical Pavement Design Guide, Pavement ME (NCHRP 2004). M_R of UGM and subgrade soil is a measure of the elastic modulus of the material from a given stress state.

Rutting is a major flexible pavement distress that leads to uneven riding surface and a significant reduction in pavement serviceability and safety level. Pavements experience rutting failure when the pavement materials undergo an excessive amount of permanent, or plastic, deformation. Accumulation of permanent deformation in UGM and subgrade soils contributes to rutting of pavement surface. Laboratory assessment of permanent, or plastic, deformation is an essential performance parameter for UGM and subgrade soils.

Resilient modulus (elastic behaviour) and permanent deformation (plastic behaviour) of UGM and subgrade soils can be measured in the laboratory or estimated from prediction

models in the literature. The values of M_R and permanent deformation depend on the stress state and the physical properties of UGM and subgrade soils. Several relationships have been proposed for determining M_R and permanent deformation for UGM and subgrade soil as a function of its physical properties (LTPP 2001; Mohammad et al. 2007, 2008; Nazarian Puppalaet al. 2014; et al. 2009). These physical properties can be: dry density, moisture content, Atterberg limits, and gradation. A potential benefit of estimating M_R and permanent deformation for UGM and subgrade soil from its physical properties is to address the effect of seasonal variations on pavement performance. Seasonal variations are critical for selecting representative values of M_R for the design of a particular project. Seasonal variations in resilient modulus are also primary input in the Pavement ME.

The available relationships in the literature for estimating resilient modulus and permanent deformation are either generic to fit a wide range of soil types and UGM or are developed for a specific material. The selected values for resilient modulus of UGM and subgrade soils can significantly affect pavement design (Guan et al. 1998). Research studies showed that the available prediction models and default values in the Pavement ME cannot be generalized to predict the response of any UGM/soil. Therefore, transportation agencies should calibrate their own relationships based on soil types and typical UGM in their region.

1.2 Problem Statement

Pavement materials are usually subjected to stress levels that exceed their elastic limits to accommodate the traffic loading with cost-effective design. Pavement structures fail due

to gradual accumulation of permanent deformation, or degradation in materials during their service life, and not due to rapid collapse (Sharp 1985). Physical and chemical properties of UGM determine the suitability of aggregate for different uses in pavement construction and govern aggregates durability and soundness (Tutumluer 2013). Gradation is one of the main factors that influence the elastic and plastic behaviour of UGM (Tian et al. 1998). For the same aggregate source, base materials with coarser gradations have higher resilient modulus than finer gradations (Gudishala 2004; Kancherla 2004; Tian et al. 1998). In addition to mechanical properties, gradation has an influence on the permeability and frost susceptibility of unbound base materials (Bilodeau et al. 2008).

Currently, resilient and permanent deformation behaviour of subgrade soil and UGM is estimated indirectly from empirical relationships. No laboratory tests are conducted in Manitoba to evaluate these properties. There is no standard test for comprehensive evaluation of permanent deformation of subgrade soil and UGM under repeated loading. Several studies have been conducted to evaluate permanent deformation of subgrade soil and UGM (Bilodeau et al. 2011; Cerni et al. 2012; Pérez et al. 2006, Puppala et al. 2009; Werkmeister et al. 2005). Results of these studies cannot be generalized for all subgrade soil and UGM.

Type (plastic or nonplastic) and amount of fines (passing No. 200 sieve) in base materials influence the elastic and plastic response of base materials under traffic loading (Tutumluer 2013). Several studies evaluated the optimum fines content that achieve maximum strength and increase permanent deformation resistance. Based on laboratory

testing of local UGM, Gandara et al. (2005) found that UGM with fines content ranging from 5% to 10% have higher resilient modulus and are less susceptible to moisture variation. Gandara et al. (2005) recommended a fines content limit of 10% for better performance of base materials. For dense-graded crushed limestone base material, Tutumluer and Seyhan (2000) recommended the optimum fines content to be 7%. The optimum fines content varies based on aggregate physical properties and gradation.

The performance of UGM depends on the interaction between aggregate source, gradation, and fines content. In addition to these parameters, there are other factors that have significant effect on base material performance. These factors are plasticity of fines, degree of compaction, moisture content, and aggregate shape, texture and angularity (Lekarp et al. 2000a, 2000b; Bilodeau and Doré 2012a, 2012b; Tutumluer 2013). Specifications for UGM aim to provide a range of locally available durable materials that meet design requirements and achieve the target design life. Specifications for UGM vary among transportation agencies based on:

- the availability of materials,
- climatic conditions, and
- function.

The effective use of locally-available material and targeting long service life are important aspects for design and construction of sustainable and cost-effective pavements (Tutumluer 2013).

1.3 Research Objectives

The objectives of this research are to:

- Evaluate M_R values for typical UGM and fine-grains soils in Manitoba and develop typical M_R values for design and evaluation of pavement structure.
- Evaluate the sensitivity of M_R for UGM and subgrade soil to moisture variation.
- Develop a regression model to estimate M_R values for typical UGM and fine-grained soils from the basic physical properties.
- Evaluate the permanent deformation of typical UGM in Manitoba under repeated traffic loading and the sensitivity of permanent deformation to the change in moisture content, gradation, and percentage of fines (passing #200 sieve).
- Evaluate the permeability of typical base material in Manitoba and its sensitivity to the change in gradation and percentage of fines.
- Provide testing data in support of updating Manitoba specifications for UGM to provide durable long lasting base layers.

1.4 Scope of the Research

The fine gradation of UGM available in Manitoba, and Prairie region, and the high percentage of fines in some materials provided a need for further investigation of the deformation behaviour and develop performance-based specifications for UGM. A laboratory testing program was developed to include evaluation of resilient modulus (material stiffness) and permanent deformation (material stability). Permeability of UGM was also investigated as it affect the drainage and performance of pavement structure.

The effect of moisture variation on the resilient behaviour of fine-grains soils in Manitoba was investigated through laboratory testing. A testing program was developed to evaluate the resilient modulus of fine-grains soils with varying moisture content. Data from laboratory testing was used to develop locally calibrated prediction models for subgrade resilient modulus.

1.5 Impact of the Research

The research will provide laboratory evaluated values for performance parameters of typical subgrade soils and UGM in Manitoba. This laboratory values will be incorporated in design and analysis of pavements. Results of laboratory tests will be used to develop prediction models adapted to local/regional agencies. These prediction models will provide more reliable information about the dynamic response of subgrade soils and UGM with less testing effort and expenses.

The recommendations and findings of the research will be used to update UGM specifications in Manitoba to provide durable and long lasting granular base layers. Having performance-based specifications will optimize the use of limited infrastructure resources by improving design reliability and eliminating the uncertainties associated with soil and UGM condition and resistance to repeated loading. In addition, accurate evaluation of permanent deformation in UGM will improve performance prediction and reduce rehabilitation and maintenance costs. Improving pavement design and management will optimize the utilization of the constrained budgets and increase the availability of more funds for financing other purposes.

1.6 Thesis Organization

This thesis is organized as follows:

- Chapter 1: Introduction

This chapter presents a general overview, problem statement, research objectives, scope of the research, impact of the research, and thesis organization.

- Chapter 2: Literature Review

This chapter outlines the behaviour of subgrade soil and UGM under traffic loading, laboratory testing of resilient modulus, modeling of subgrade soil and UGM resilient modulus, shakedown behaviour of UGM, and summary of environmental scan of UGM specifications.

- Chapter 3: Experimental Program

This chapter presents the physical properties of the tested materials in this research, outline of the experimental program and test procedures, and calibration of test setup.

- Chapter 4: Resilient Behaviour of Subgrade Soils

This chapter presents the results of resilient modulus test for subgrade soils, comparison between the measured resilient modulus and values reported in the literature, and presenting typical resilient modulus values to replace the Pavement ME default values.

- Chapter 5: Resilient Modulus Prediction Models for Fine-Grained Subgrade Soils

This chapter presents the developed models to predict resilient modulus of fine-grained soils from their physical properties, validation of models, and a comparison between the developed models and the models developed under the Long Term Pavement Performance (LTPP) test program.

- Chapter 6: Resilient Behaviour and Permeability of UGM

This chapter outlines the effect of fines content of compaction characteristics of UGM, the results of resilient modulus test for UGM, comparison between the measured resilient modulus and values reported in the literature, typical resilient modulus values to replace the Pavement ME default values, the results of permeability tests, and the effect of fines content on drainage quality.

- Chapter 7: Resilient Modulus Prediction Models for UGM

This chapter presents the developed models to predict resilient modulus of UGM soils from gradation and compaction parameters, validation of models, and a comparison between the developed models and the LTPP models.

- Chapter 8: Permanent Deformation and Shakedown Behaviour of UGM

This chapter discuss the results of permanent deformation test for UGM, modeling of permanent deformation, and classification of UGM behaviour according to the shakedown approach.

- Chapter 9: Assessing the Behaviour of UGM Using the Dissipated Energy Approach

This chapter discuss the dissipated energy approach for UGM, the effect of changing stress ratio on the UGM dissipated energy, and the change in dissipated energy of UGM under extended number of loading cycles.

- Chapter 10: Conclusions and Recommendations

This chapter provides a summary of the thesis, the conclusions, and recommendations for future work.

2 Literature Review

2.1 Introduction

A typical pavement structure consists of (Figure 2.1):

- top layer: Asphalt Concrete (AC) or Portland Cement Concrete (PCC),
- UGM layer: base course, and
- compacted native soil: subgrade soil.

Pavement layers undergo a complex stress pattern due to a moving traffic loading. Figure 2.2 illustrates the stress pulses induced in an element of a pavement structure due to a moving wheel load. In UGM layers and subgrade soil, each element is subjected to positive vertical and horizontal stress pulses; and a reversed shear stress pulse with the movement of the wheel load (Lekarp et al. 2000a).

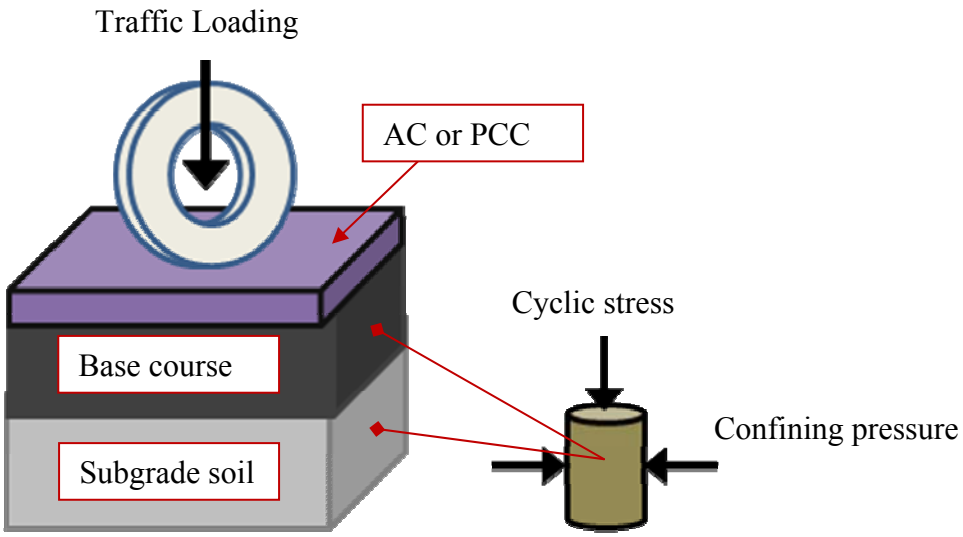

FIGURE 2.1: Typical Pavement Structure under Traffic Loading

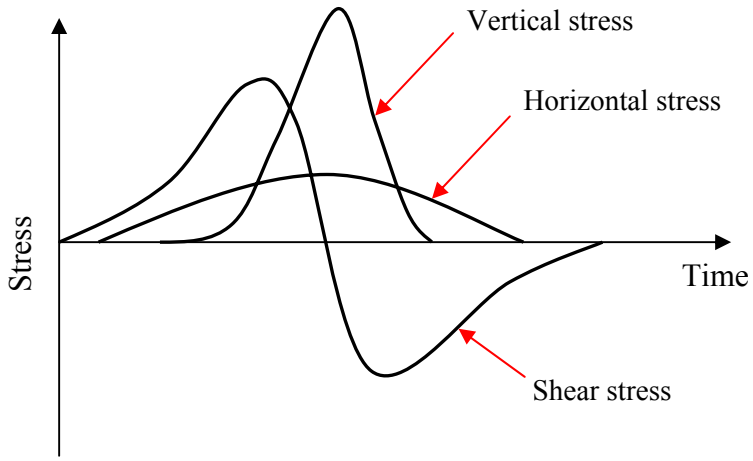

FIGURE 2.2: Stresses Induced in UGM layers and Subgrade Soil due to Moving Traffic Loading (Lekarp et al. 2000a)

UGM and subgrade soil are elastic-plastic materials. When subjected to a repeated traffic loading, UGM layer and subgrade soil undergo both resilient (elastic) strain and permanent (plastic) strain with each load repetition. Figure 2.3 shows a schematic diagram of stress-strain behaviour of UGM and subgrade soil under one repetition of traffic loading. The ratio of resilient strain and permanent strain to the total strain that UGM layer and subgrade soil undergo under traffic loading depends on:

- stiffness and quality of overlaying pavement layers,
- physical properties of UGM and subgrade soil,
- stress history of UGM and subgrade soil, and
- applied stress level.

Pavement materials are usually subjected to stress levels that exceed their elastic limits to accommodate the traffic loading with cost-effective design. Pavement structures fail due to gradual accumulation of permanent deformation, or degradation in materials during their service life, and not due to rapid collapse (Sharp 1985).

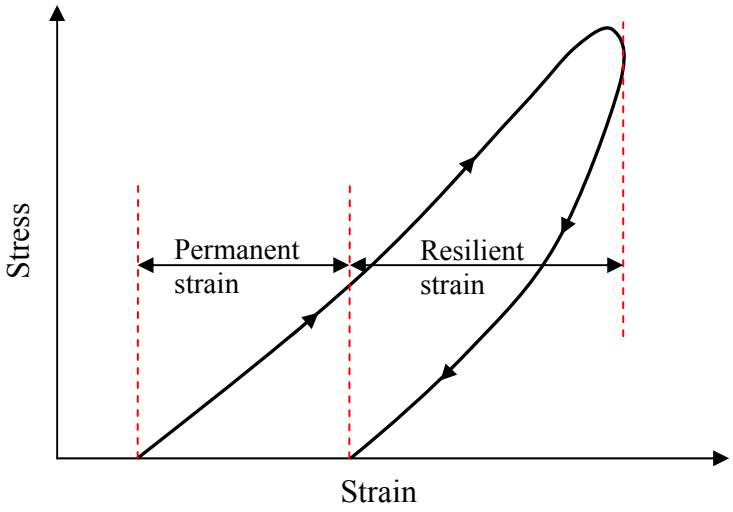

FIGURE 2.3: Stress-Strain Behaviour of UGM and Subgrade Soil under One Repetition of Traffic Loading

The M_R of UGM and subgrade soil is a measure of the elastic modulus of the material at a given stress state. It is mathematically defined as the applied deviator stress divided by the "recoverable" strain that occurs when the applied load is removed from the test specimen (Equation 2.1).

$$M_R = \frac{\sigma_d}{\varepsilon_r} \qquad \textbf{(2.1)}$$

Where:

σ_d = applied deviator stress in a repeated load triaxial test.

ε_r = recoverable or resilient strain.

Previous studies have shown that M_R test results can be affected by sampling technique, testing procedure, and errors that can occur during the testing program (Mohammad et al. 1994; Yau and Von Quintus 2001). Some of these errors include incorrect

conditioning/stress sequence, leaks in the membrane, incorrect stress levels, unstable Linear Variable Differential Transducer (LVDT) clamps attached to the specimen, exceeding the LVDT linear range limits, and specimen disturbance at the higher stress states.

2.2 Pavement ME Hierarchical Approach for Design Inputs

A reliable analytical design of pavement structures requires laboratory measured values for resilient modulus of subgrade soil and UGM (Frost et al. 2004). For analytical pavement design, it is necessary to consider the effect of climatic conditions which includes variations in moisture content of subgrade soil and UGM (Werkmeister et al. 2003). In addition to strength parameters, the drainability characteristics of UGM are required inputs to avoid premature failure of pavement structures (Richardson 1997).

The required design reliability and engineering effort shall be proportional to the significance of the project being designed, e.g., a low-volume secondary road doesn't require the same design reliability as a high-volume primary road (Christopher et al. 2006). Pavement ME has a hierarchical approach for determining the design input parameters based on the significance and the required design reliability for the project. According to this approach, three levels are available for the design input parameters (NCHRP 2004):

- Level 1: provide highest level of accuracy and reliability. Design input parameters are measured directly in the laboratory.

- Level 2: provide an intermediate level of accuracy and reliability. Basic material properties are measured in the laboratory (e.g. gradation, unconfined compressive strength, California bearing ratio,...). Design input parameters are estimated based on correlations between design inputs and the measured basic properties.
- Level 3: provide lowest level of accuracy and reliability. Design input parameters can be the default values provided by the design guide or typical values based on agency experience.

2.3 Laboratory Testing of Resilient Modulus

2.3.1 LTPP P46 Test Protocol for M_R

M_R test protocol P46 was developed in 1996, under the Long Term Pavement Performance (LTPP) test program, to provide a guideline for the laboratory testing of M_R of UGM and subgrade soils (LTPP 1996). According to protocol P46, UGM and subgrade soils are classified as either Type 1 or Type 2 based on their gradation. Type 1 class includes all materials with less than 70% passing the No. 10 (2.0 mm) sieve, less than 20% passing the No. 200 (75 μm) sieve, and have a plasticity index ≤10. Type 2 class includes all materials that do not meet the criteria for Type 1 class and the undisturbed samples of subgrade soils extracted from thin-walled tubes. Type 1 materials are molded in a 152 mm (6.0 in) diameter mold and Type 2 materials are molded in a 71 mm (2.8 in) diameter mold.

The required load pulse for the M_R test is Haversine shaped load pulse. The load pulse is of the form:

$$f(\theta) = \frac{1 - COS(\theta)}{2} \quad \textbf{(2.2)}$$

Where:

$\theta = 0$ to 2π

The load pulse has load duration of 0.1 sec followed by a rest period of 0.9 sec. During testing, the specimen is subjected to several loading combinations of dynamic cyclic stress and a static confining stress. Number of loading combinations and stress levels depend on whether the specimen is for a subgrade soil or a UGM material. Tables 2.1 and 2.2 show the loading sequences for subgrade soil and UGM, respectively. Axial deformation is measured by two Linear Variable Differential Transducers (LVDTs) fixed to opposite sides of the loading piston outside of the triaxial cell.

2.3.2 M_R Test Method Developed under NCHRP Project 1-28A

A test method for M_R of UGM and subgrade soils has been developed under NCHRP Project 1-28A: "Harmonized Test Methods for Laboratory Determination of Resilient Modulus for Flexible Pavement Design" to harmonize the procedures proposed by NCHRP Project 1-28 with the existing LTPP P46 test protocol, AASHTO T 292, and AASHTO T 294 methods (Harrigan and Witczak 2004). There are main differences in specimen preparation and testing procedures between this harmonized test method and P46 test protocol.

UGM and subgrade soils are classified into 4 categories, Type 1 to Type 4, based on their gradation and sampling method. Type 1 class includes all materials with maximum particle sizes greater than 9.5 mm (0.375 in). Type 2 class includes all materials with

maximum particle size less than 9.5 mm and less than 10% passing No. 200 (75 μm) sieve. Type 3 class includes all materials with maximum particle size less than 9.5 mm and more than 10% passing No. 200 sieve. Type 4 class includes undisturbed samples of subgrade soils extracted from thin-walled tubes. Type 1 samples can be molded in a 152 mm (6.0 in) diameter mold or a 102 mm (4 in) diameter mold. Type 2 and Type 3 samples shall be molded in a 102 (4.0 in) diameter mold. Type 4 is undisturbed samples and tested as 71 mm (2.8 in) diameter specimens.

TABLE 2.1: Loading Sequences for Subgrade Soils According to P46 Test Protocol

Sequence	Confining Pressure (kPa)	Contact Stress (kPa)	Cyclic Stress (kPa)	Total Stress (kPa)	No. of Cycles
Conditioning	41.4	2.8	24.8	27.6	500-1000
1	41.4	1.4	12.4	13.8	100
2	41.4	2.8	24.8	27.6	100
3	41.4	4.1	37.3	41.4	100
4	41.4	5.5	49.7	55.2	100
5	41.4	6.9	62.0	68.9	100
6	27.6	1.4	12.4	13.8	100
7	27.6	2.8	24.8	27.6	100
8	27.6	4.1	37.3	41.4	100
9	27.6	5.5	49.7	55.2	100
10	27.6	6.9	62.0	68.9	100
11	13.8	1.4	12.4	13.8	100
12	13.8	2.8	24.8	27.6	100
13	13.8	4.1	37.3	41.4	100
14*	13.8	5.5	49.7	55.2	100
15*	13.8	6.9	62.0	68.9	100

* Load sequences 14 and 15 are not to be used for Type 1 materials

TABLE 2.2: Loading Sequences for UGM According to P46 Test Protocol

Sequence	Confining Pressure (kPa)	Contact Stress (kPa)	Cyclic Stress (kPa)	Total Stress (kPa)	No. of Cycles
Conditioning	103.4	10.3	93.1	103.4	500-1000
1	20.7	2.1	18.6	20.7	100
2	20.7	4.1	37.3	41.4	100
3	20.7	6.2	55.9	62.1	100
4	34.5	3.5	31.0	34.5	100
5	34.5	6.9	62.0	68.9	100
6	34.5	10.3	93.1	103.4	100
7	68.9	6.9	62.0	68.9	100
8	68.9	13.8	124.1	137.9	100
9	68.9	20.7	186.1	206.8	100
10	103.4	6.9	62.0	68.9	100
11	103.4	10.3	93.1	103.4	100
12	103.4	20.7	186.1	206.8	100
13	137.9	10.3	93.1	103.4	100
14	137.9	13.8	124.1	137.9	100
15	137.9	27.6	248.2	275.8	100

The harmonized test method for M_R, developed under NCHRP project 1-28A, recommends the use of 2 different load durations for the load pulse according to the type of the tested sample. Subgrade soil is tested using a Haversine shaped load pulse, similar to P46 test protocol, with a load duration of 0.2 sec followed by a rest period of 0.8 sec. UGM is tested using a Haversine shaped load pulse with a load duration of 0.1 sec followed by a rest period of 0.9 sec. Three loading procedures are available in this test method. Each loading procedure has different number of loading combinations and stress levels. The selection of the loading procedure depends on whether the tested sample is fine-grained subgrade soil, coarse-grained subgrade soil, or UGM. Tables 2.3 to 2.5 show

the loading procedures for fine-grained subgrade soil, coarse-grained subgrade soil, and UGM respectively.

TABLE 2.3: Loading Sequences for Fine-Grained Subgrade Soils According to NCHRP 1-28A Test Method

Sequence	Confining Pressure (kPa)	Contact Stress (kPa)	Cyclic Stress (kPa)	Total Stress (kPa)	No. of Cycles
Conditioning	27.6	5.5	48.3	53.8	1000
1	55.2	11.0	27.6	38.6	100
2	41.4	8.3	27.6	35.9	100
3	27.6	5.5	27.6	33.1	100
4	13.8	2.8	27.6	30.4	100
5	55.2	11.0	48.3	59.3	100
6	41.4	8.3	48.3	56.6	100
7	27.6	5.5	48.3	53.8	100
8	13.8	2.8	48.3	51.1	100
9	55.2	11.0	69.0	80.0	100
10	41.4	8.3	69.0	77.3	100
11	27.6	5.5	69.0	74.5	100
12	13.8	2.8	69.0	71.8	100
13	55.2	11.0	96.6	107.6	100
14	41.4	8.3	96.6	104.9	100
15	27.6	5.5	96.6	102.1	100
16	13.8	2.8	96.6	99.4	100

Two measuring systems can be used to measure the axial deformation: on-sample LVDTs and end LVDTs. The on-sample LVDTs system consists of two LVDTs mounted directly on the specimen using two circular clamps to measure the deformation of the middle half of the specimen. The end LVDTs system consists of two LVDTS mounted on the top loading plate to measure the total vertical deformation of the specimen. The on-sample

LVDTs system is not recommended for soft specimens with undrained shear strength less than 37.9 kPa (Harrigan and Witczak 2004).

TABLE 2.4: Loading Sequences for Coarse-Grained Subgrade Soils According to NCHRP 1-28A Test Method

Sequence	Confining Pressure (kPa)	Contact Stress (kPa)	Cyclic Stress (kPa)	Total Stress (kPa)	No. of Cycles
Conditioning	27.6	5.5	55.2	60.7	1000
1	13.8	2.8	6.9	9.7	100
2	27.6	5.5	13.8	19.3	100
3	41.4	8.3	20.7	29.0	100
4	55.2	11.0	27.6	38.6	100
5	82.8	16.6	41.4	58.0	100
6	13.8	2.8	13.8	16.6	100
7	27.6	5.5	27.6	33.1	100
8	41.4	8.3	41.4	49.7	100
9	55.2	11.0	55.2	66.2	100
10	82.8	16.6	82.8	99.4	100
11	13.8	2.8	27.6	30.4	100
12	27.6	5.5	55.2	60.7	100
13	41.4	8.3	82.8	91.1	100
14	55.2	11.0	110.4	121.4	100
15	82.8	16.6	165.6	182.2	100
16	13.8	2.8	41.4	44.2	100
17	27.6	5.5	82.8	88.3	100
18	41.4	8.3	124.2	132.5	100
19	55.2	11.0	165.6	176.6	100
20	82.8	16.6	248.4	265.0	100

TABLE 2.5: Loading Sequences for UGM According to NCHRP 1-28A Test Method

Sequence	Confining Pressure (kPa)	Contact Stress (kPa)	Cyclic Stress (kPa)	Total Stress (kPa)	No. of Cycles
Conditioning	103.5	20.7	207.0	227.7	1000
1	20.7	4.1	10.4	14.5	100
2	41.4	8.3	20.7	29.0	100
3	69.0	13.8	34.5	48.3	100
4	103.5	20.7	51.8	72.5	100
5	138.0	27.6	69.0	96.6	100
6	20.7	4.1	20.7	24.8	100
7	41.4	8.3	41.4	49.7	100
8	69.0	13.8	69.0	82.8	100
9	103.5	20.7	103.5	124.2	100
10	138.0	27.6	138.0	165.6	100
11	20.7	4.1	41.4	45.5	100
12	41.4	8.3	82.8	91.1	100
13	69.0	13.8	138.0	151.8	100
14	103.5	20.7	207.0	227.7	100
15	138.0	27.6	276.0	303.6	100
16	20.7	4.1	62.1	66.2	100
17	41.4	8.3	124.2	132.5	100
18	69.0	13.8	207.0	220.8	100
19	103.5	20.7	310.5	331.2	100
20	138.0	27.6	414.0	441.6	100
21	20.7	4.1	103.5	107.6	100
22	41.4	8.3	207.0	215.3	100
23	69.0	13.8	345.0	358.8	100
24	103.5	20.7	517.5	538.2	100
25	138.0	27.6	690.0	717.6	100
26	20.7	4.1	144.9	149.0	100
27	41.4	8.3	289.8	298.1	100
28	69.0	13.8	483.0	496.8	100
29	103.5	20.7	724.5	745.2	100
30	138.0	27.6	966.0	993.6	100

2.3.3 Influence of LVDTs Location

Mohammad et al. (1994) studied the effect of changing the LVDTs location on the value of M_R. Two types of soil were evaluated: sand (coarse-grained soil) and silty clay (fine-grained soil). Two systems were used to measure the axial deformation of the specimens: external LVDTs placed outside the triaxial cell, and internal LVDTs mounted directly on the specimen at the middle third of the specimen. The influence of the two measuring systems on M_R values was addressed by the ratio of M_R measured by the internal LVDTs to M_R measured by the external LVDTs.

For the sand soil sample, the M_R values measured with the internal LVDTs were higher by 8.0% to 20.0% than the M_R values measured with the external LVDTs. The difference between the M_R values measured with the two LVDTs systems decreased with the increase of confining and deviatoric stresses. For the clay soil sample, the M_R values measured with the internal LVDTs were higher by 20.0% to 50.0% than the M_R values measured with the external LVDTs. The higher variation in the M_R values measured with the two LVDTs systems was due to the use of lower stresses in testing and the complex behaviour of clay specimens. The difference between the M_R values measured with the two LVDTs systems decreased at higher stresses due to the perfect contact between the end plates and the specimen ends. The difference between the two measuring systems for sand specimens was affected mainly by deviatoric stress, while for clay specimens it was affected by confining pressure.

Burczyk, et al. (1994) studied the influence of LVDTs location on M_R for cohesive soils. Re-compacted and undisturbed specimens were tested in this study. Axial deformation was measured with two systems: Two external LVDTs outside the triaxial cell and three internal LVDTs mounted directly on the specimen at the middle third. It was also found that the M_R values measured with the internal LVDTs was higher than the M_R values measured with the external LVDTs.

Konrad and Robert (2003) evaluated the M_R of UGM using two test setups: conventional triaxial setup and M_R test setup available at the Ministry of Transportation of Quebec (MTQ). The dimensions of the M_R specimens were 100 mm in diameter by 200 mm in height for the conventional triaxial setup, and 150 mm in diameter by 300 mm in height for the MTQ setup. For the conventional triaxial setup, two LVDTs mounted directly on the specimen at the middle third were used to measure the axial deformation. For the MTQ setup, two external LVDTs mounted outside the triaxial cell were used to measure the axial deformation. The M_R values measured with the conventional triaxial setup were 20.0% to 50.0% higher than the M_R values measured with the MTQ setup. LVDTs location was one of the factors that contributed to the difference between the M_R values measured with the two test setups.

2.3.4 Effect of Sampling Technique and Specimen Preparation on M_R

The M_R data collected for the LTPP test program was used to study the effect of sampling technique on M_R value (Yau and Von Quintus 2001). The M_R data was classified according to the sampling technique and soil/UGM type. Two sampling techniques were used for M_R specimens:

- Undisturbed specimens recovered from thin-walled Shelby tubes.
- Re-compacted specimens in the laboratory (disturbed specimens).

Undisturbed specimens are mainly available for cohesive soils. A statistical analysis was carried out to evaluate the effect of these two sampling techniques on M_R values. Results of statistical analysis showed that sampling technique (undisturbed versus disturbed test specimen) had an influence on M_R values for clay soils. The influence of sampling technique on M_R values can be due to the complex behaviour of clay soils and stress history of the specimen (Yau and Von Quintus 2001).

Mohammad et al. (1994) examined the influence of sample preparation on the target moisture content and density of re-compacted specimens. For sand and clay soils, no significant effect on specimens density was observed. Fine migration in sand specimens due to compaction and testing procedures was examined. After completing M_R test, sand specimens were carefully removed from the triaxial cell and cut into two slices. Each slice was dried for grain size distribution tests. Results of grain size distribution tests indicated that the compaction and testing procedures did not result in any fine migration, layering, or crushing of the aggregates.

For fine-grained cohesive soils, moisture migration during specimen compaction can result in variation in moisture content and partial saturation of the specimen (Mohammad et al. 1994). Partial saturation of the test specimen induces suction pressure that causes some confinement, which in turn increases the final M_R values. Moisture migration was checked by measuring the moisture content of different slices of re-compacted silty clay specimens before conducting M_R test (Mohammad et al. 1994). No significant variation

was observed in the moisture contents of these slices, which implies that moisture migration was not present in re-compacted specimens.

2.4 Regression Models of Resilient Modulus

The value of M_R depends on the stress state and the physical properties of UGM and subgrade soils. These physical properties can be dry density, moisture content, and gradation. Several relationships have been proposed for determining M_R for UGM and subgrade soils as a function of stress state and their physical properties. Some of these relationships are discussed in this section.

2.4.1 Stress Dependency and Nonlinear Elastic Behaviour of UGM and Subgrade Soil

The behaviour of UGM and subgrade soil depends on the stresses they incur when subjected to traffic loading. M_R test is conducted over a range of vertical stresses and confining pressures to evaluate the nonlinear elastic behaviour (stress dependency) of UGM and subgrade soil (Harrigan and Witczak 2004). Several relationships have been developed to represent M_R of UGM and subgrade soil as a function of their stress state. Von Quintus and Killingsworth (1998) found that the following constitutive equation provided a good fit to the LTPP test data for M_R (average multiple-correlation coefficient, R^2, exceeded 0.85):

$$M_R = K_1 P_a \left[\frac{\theta}{P_a}\right]^{K_2} \left[\frac{\sigma_d}{P_a}\right]^{K_3} \quad \textbf{(2.3)}$$

The NCHRP 1-28A test protocol recommends the use of the so-called "Universal Constitutive Equation" to fit the M_R test data (Harrigan and Witczak 2004). This constitutive equation, which is an expanded version of Equation 2.3, has the following form:

$$M_R = K_1 P_a \left[\frac{\theta - 3K_6}{P_a} \right]^{K_2} \left[\frac{\tau_{oct}}{P_a} + K_7 \right]^{K_3} \quad \textbf{(2.4)}$$

Where:

M_R= resilient modulus, kPa

θ = bulk stress, kPa

$$\theta = \sigma_1 + \sigma_2 + \sigma_3$$

τ_{oct} = octahedral shear stress, kPa

$$\tau_{oct} = \frac{1}{3}\sqrt{(\sigma_1 - \sigma_2)^2 + (\sigma_1 - \sigma_3)^2 + (\sigma_2 - \sigma_3)^2}$$

σ_d = deviator stress, kPa

$$\sigma_d = \sigma_1 - \sigma_3$$

σ_1, σ_2, and σ_3 = principal stresses, kPa (for triaxial test, $\sigma_2 = \sigma_3$ = confining pressure)

K_1, K_2, K_3, K_6, and K_7 = regression constants

P_a = atmospheric pressure at sea level = 101.35 kPa

Values of the regression constants shall be: K_1 and $K_2 \geq 0$; K_3 and $K_6 \leq 0$; and $K_7 \geq 1$. The value of K_2 is restrained to be greater than or equal to zero where K_2 is the exponent of the term that represent the cohesionless behaviour of the material (bulk stress). The value of K_3 is restrained to be less than or equal to zero where K_3 is the exponent of the term that represent the cohesive behaviour of the material (octahedral shear stress, or deviator stress). K_6 and K_7 can be assigned initial values of zero and one, respectively.

2.4.2 LTPP Regression Models for UGM and Subgrade Soil (Yau and Von Quintus 2001)

The LTPP test data for M_R was categorized according to UGM and subgrade soil type (Yau and Von Quintus 2001). Using Equation 2.4, nonlinear regression analysis was performed to find the values of K_1, K_2, and K_3. Values of K_6 and K_7 were assumed to be zero and one, respectively. Table 2.6 shows a summary of the regression analysis results for each UGM/soil group. The value of K_2 decreased as the gradation of UGM/soil became finer (moving from UGM to fine-grained soil). This means that the influence of the cohesionless term in Equation 2.4 on M_R value decreased when the gradation of UGM/soil became finer. Similarly, the absolute value of K_3 increased as the gradation of UGM/soil became finer which means that the influence of the cohesive term in Equation 2.4 on M_R value increased. The value of K_3 was zero for 25% of the M_R tests for the UGM and 10% of the tests for the coarse-grained subgrade soils.

The standard deviation of K_1, K_2, and K_3 ranged from 25% to more than 100% of their mean values which indicates a high variability within each UGM/soil group. The high variability of K_1, K_2, K_3 values is due to the existence of a wide range of UGM/soil types within each group. This variability can be reduced by dividing the M_R test data into more groups based on UGM/soil type and gradation.

2.4.3 Effect of UGM/Soil Physical Properties on M_R (Yau and Von Quintus 2001)

The seasonal variation in M_R is one of the required inputs for pavement analysis and design. Estimating M_R from the physical properties of UGM/soil is a good tool to capture the effect of seasonal variation on M_R, where seasonal changes in UGM/soil physical properties can be easily estimated. Yau and Von Quintus (2001) studied the effect of the physical properties of UGM/soils on M_R for LTPP test data. Table 2.7 shows the physical properties that were collected for UGM/soil samples and included in the statistical analysis.

TABLE 2.6: Median, Mean and Standard Deviation of K_1, K_2, K_3 for LTPP M_R Test Data (Yau and Von Quintus 2001)

Regression Coefficient		Material/Soil Group		
		UGM	Coarse-Grained Soils	Fine-Grained Soils
K_1	Median	0.8530	0.7640	0.8040
	Mean	0.8730	0.8020	0.8960
	Standard Deviation	0.2726	0.2661	0.3133
K_2	Median	0.6280	0.4460	0.2430
	Mean	0.6260	0.4520	0.2820
	Standard Deviation	0.1330	0.1927	0.1552
K_3	Median	-0.1290	-1.0520	-1.3990
	Mean	-0.1700	-1.1400	-1.5760
	Standard Deviation	0.2148	0.7365	1.1014
Number of Tests		423	257	105

TABLE 2.7: Physical Properties of UGM and Subgrade Soil (Yau and Von Quintus 2001)

UGM/ Soil Property	Measuring Units	Description
$P_{3/8''}$	%	Percentage passing sieve No. 3/8″ (9.51 mm)
$P_{No.\ 4}$	%	Percentage passing sieve No. 4 (4.76 mm)
$P_{No.\ 40}$	%	Percentage passing sieve No. 40 (0.420 mm)
$P_{No.\ 200}$	%	Percentage passing sieve No. 200 (0.074 mm)
% Silt	%	Amount of silt in the material/soil
% Clay	%	Amount of clay in the material/soil
LL	%	Liquid limit of material/soil
PI	%	Plasticity index of material/soil
W_{opt}	%	Optimum moisture content
γ_{opt}	Kg/m^3	Maximum dry density of material/soil
W_s	%	moisture content of the test specimen
γ_s	Kg/m^3	Dry density of the test specimen

UGM was divided to 7 groups according to LTPP material code (LTPP material code 302, 303, 304, 306, 307, 308, and 309). Subgrade soils were divided into 4 groups according to soil type (gravel, sand, silt, and clay). The undisturbed soil specimens were taken at various depths from Shelby Tubes, while the samples for physical properties were taken from the top 0.30 m of the subgrade soil. For this reason, the measured M_R for undisturbed clay specimens were not included in this analysis (Von Quintus and Killingsworth 1998). A statistical analysis was conducted to study the correlation between the measured M_R for each UGM/ soil group and the physical properties summarized in Table 2.7. Stepwise regression technique was used to identify the physical properties that have statistical influence on M_R values for each UGM/soil group. Table

2.8 shows the physical properties that had a significant correlation with M_R and found to be important for each UGM/soil group.

Table 2.8 shows the following observations:

- Maximum dry density had significant correlations with M_R for all UGM groups except LTPP material 309.
- Optimum moisture content and percentage passing sieve no. 3/8″ showed significant correlations with M_R for most coarse-grained UGM.
- Moisture content of the test specimen and percentage of clay had significant correlation with M_R for all subgrade soil groups.
- Percentage of silt had significant correlation with M_R for all subgrade soil groups but gravel.
- Liquid limit had significant correlations with M_R for all subgrade soil groups but silt.

A nonlinear optimization regression analysis was performed for each UGM/soil group to develop a model that incorporates the influence of physical properties and stress level on M_R. Using Equation 2.4 and M_R values for each UGM/soil group, coefficients K_1, K_2, and K_3 were regressed as function of the important physical properties for each group (Table 2.8). Coefficients K_6 and K_7 were assigned constant values of zero and one, respectively, where analysis showed that changing the values of K_6 and K_7 was not statistically significant. Equations 2.5 to 2.25 show the results of the regression analysis for crushed stone, crushed gravel, uncrushed gravel, and the four soil groups.

TABLE 2.8: Important Physical Properties for each UGM/Soil Group (Yau and Von Quintus 2001)

Physical Properties	Base/Subbase Materials							Soils			
	Crushed stone (303[a])	Crushed Gravel (304)	Uncrushed Gravel (302)	Sand (306)	Coarse-grained soil-Aggr. Mix (308)	Fine-grained soil-Aggr. Mix (307)	Fine-grained soil (309)	Gravel	Sand	Silt	Clay
$P_{3/8''}$	√	√		√	√	√		√	√		
$P_{No.\ 4}$					√	√			√		√
$P_{No.\ 40}$	√	√		√	√		√				√
$P_{No.\ 200}$			√		√	√			√		√
% Silt									√	√	√
% Clay								√	√	√	√
LL	√	√		√		√		√	√		√
PI		√		√	√		√	√		√	
W_{opt}	√	√	√		√	√			√		√
γ_{opt}	√	√	√	√	√	√			√		√
W_s		√	√		√			√	√	√	√
γ_s		√	√		√	√			√		√
No. of M_R tests	109	49	81	66	187	32	92	122	509	108	512

[a] LTPP material code

Crushed Stone UGM (LTPP Material Code 303)

$$K_1 = 0.7632 + 0.0084\left(P_{3/8}\right) + 0.0088\,LL - 0.0371 W_{opt} - 0.0001\,\gamma_{opt} \quad \textbf{(2.5)}$$

$$K_2 = 2.2159 - 0.0016\left(P_{3/8}\right) - 0.0008\,LL - 0.0380 W_{opt} - 0.0006\,\gamma_{opt} + 2.4\times10^{-7}\left(\frac{\gamma_{opt}^2}{P_{40}}\right) \quad \textbf{(2.6)}$$

$$K_3 = -1.1720 - 0.0082\,LL - 0.0014 W_{opt} + 0.0005\,\gamma_{opt} \quad \textbf{(2.7)}$$

Crushed Gravel UGM (LTPP Material Code 304)

$$K_1 = -0.8282 - 0.0065\left(P_{3/8}\right) + 0.0114\,LL + 0.0004\,PI - 0.0187\,W_{opt} + 0.0036\,W_s + 0.0013\,\gamma_s - 2.6\times10^{-6}\left(\frac{\gamma_{opt}^2}{P_{40}}\right) \quad \textbf{(2.8)}$$

$$K_2 = 4.9555 - 0.0057\,LL - 0.0075\,PI - 0.0470\,W_s - 0.0022\,\gamma_{opt} + 2.8\times10^{-6}\left(\frac{\gamma_{opt}^2}{P_{40}}\right) \quad \textbf{(2.9)}$$

$$K_3 = -3.5140 + 0.0016\,\gamma_s \quad \textbf{(2.10)}$$

Uncrushed Gravel UGM (LTPP Material Code 302)

$$K_1 = -1.8961 + 0.0014\,\gamma_s - 0.1184\left(\frac{W_s}{W_{opt}}\right) \quad \textbf{(2.11)}$$

$$K_2 = 0.4960 - 0.0074\,P_{200} - 0.0007\,\gamma_s + 1.6972\left(\frac{\gamma_s}{\gamma_{opt}}\right) + 0.1199\left(\frac{W_s}{W_{opt}}\right) \quad \textbf{(2.12)}$$

$$K_3 = -0.5957 + 0.0349\,W_{opt} + 0.0004\,\gamma_{opt} - 0.5166\left(\frac{W_s}{W_{opt}}\right) \quad \textbf{(2.13)}$$

Coarse-Grained Gravel Soils

$$K_1 = 1.3429 - 0.0051\left(P_{3/8}\right) + 0.0124\left(\%Clay\right) + 0.0053\ LL - 0.02311\ W_s \quad \textbf{(2.14)}$$

$$K_2 = 0.3311 + 0.0010\left(P_{3/8}\right) - 0.0019\left(\%Clay\right) - 0.0050\,LL - 0.0072\,PI + 0.0093\,W_s \quad \textbf{(2.15)}$$

$$K_3 = 1.5167 - 0.0302\left(P_{3/8}\right) + 0.0435\left(\%Clay\right) + 0.0626\,LL + 0.0377\,PI - 0.2353\,W_s \quad \textbf{(2.16)}$$

Coarse-Grained Sand Soils

$$K_1 = 3.2868 - 0.0412\left(P_{3/8}\right) + 0.0267\,P_4 + 0.0137\left(\%Clay\right) + 0.0083\,LL - 0.0379\,W_{opt} - 0.0004\,\gamma_s \quad \textbf{(2.17)}$$

$$K_2 = 0.5670 + 0.0045(P_{3/8}) - 2.98\times10^{-5}P_4 - 0.0043(\%Silt) - 0.0102(\%Clay) - 0.0041LL + 0.0014W_{opt} - 3.41\times10^{-5}\gamma_s - 0.4582\left(\frac{\gamma_s}{\gamma_{opt}}\right) + 0.1779\left(\frac{W_s}{W_{opt}}\right) \quad \textbf{(2.18)}$$

$$K_3 = -3.5677 + 0.1142(P_{3/8}) - 0.0839P_4 - 0.1249P_{200} + 0.103(\%Silt) + 0.1191(\%Clay) - 0.0069LL - 0.01034W_{opt} - 0.0017\gamma_s + 4.3177\left(\frac{\gamma_s}{\gamma_{opt}}\right) - 1.1095\left(\frac{W_s}{W_{opt}}\right) \quad \textbf{(2.19)}$$

Fine-Grained Silt Soils

$$K_1 = 1.0480 + 0.0177(\%Clay) + 0.0279\,PI - 0.0370W_s \quad \textbf{(2.20)}$$

$$K_2 = 0.5097 - 0.0286\,PI \quad \textbf{(2.21)}$$

$$K_3 = -0.2218 + 0.0047(\%Silt) + 0.0849\,PI - 0.1399W_s \quad \textbf{(2.22)}$$

Fine-Grained Clay Soils

$$K_1 = 1.3577 + 0.0106(\%Clay) - 0.0430W_s \quad \textbf{(2.23)}$$

$$K_2 = 0.5193 - 0.0073\,P_4 + 0.0095\,P_{40} - 0.0027P_{200} - 0.0030\,LL - 0.0049W_{opt} \quad \textbf{(2.24)}$$

$$K_3 = 1.4258 - 0.0288\,P_4 + 0.0303\,P_{40} - 0.0521\,P_{200} + 0.0251(\%Silt) + 0.0535\,LL - 0.0672\,W_{opt} - 0.0026\,\gamma_{opt} + 0.0025\,\gamma_s - 0.6055\left(\frac{W_s}{W_{opt}}\right) \quad \textbf{(2.25)}$$

It may not be feasible for some transportation agencies to include in the M_R regression models all the physical properties mentioned in Table 2.8, where the calibration of such models requires extensive testing program. For M_R regression models representing wide range of materials, including more physical properties in the regression model improves the prediction of M_R. For M_R regression models developed for a specific type of material, a limited number of physical properties is required to represent the variation within this

type of material. Transportation agencies can decide what physical properties to include in the M_R regression models based on the available testing budget and the types of UGM/soil available in their regions.

2.4.4 M_R Prediction Models for Louisiana Subgrade Soils

Nazzal et al. (2008) conducted a testing program to validate the use of the LTPP models to predict M_R for Louisiana subgrade soils. Undisturbed Shelby tube soil samples were collected from different pavement projects throughout Louisiana. The collected soil samples were classified as A-4, A-6, A-7-5, and A-7-6. These soil samples represent the typical soil types found in Louisiana. M_R test specimens were extracted from the Shelby tubes with dimensions of 71 mm (2.8 in) in diameter and 142 (5.6 in) in height. The soil specimens were taken from specific heights to represent the existing subgrade soil between 152 mm to 457 mm under the base coarse layer. M_R tests were performed according to AASHTO T307-99 test procedures (AASHTO 2003) with a loading pulse of 0.2 sec loading time and 0.8 sec rest period.

M_R specimens were categorized into four groups (Level 1 to Level 4) according to their moisture content. Level 1 group included all M_R samples that had a moisture content at the lower end of the dry side of the optimum moisture content (OMC). Level 2 group included all M_R samples that had a moisture content at the dry side of the OMC but higher than Level 1. Level 3 group included all M_R samples that had a moisture content at or close to the OMC. Level 4 group included all M_R samples that had a moisture content at the wet side of the OMC. Test results showed that M_R deceased by 50% to 70%,

depending on type of soil, due to the increase in moisture content from Level 2 to Level 4.

LTPP prediction models for fine-grained clay soils (Equations 2.23 to 2.25) were used to calculated M_R and the coefficients K_1, K_2, and K_3. The predicted values of K_1, K_2, and K_3 were comparable to the measured values for Louisiana soils. The highest difference between the predicted and the measured values was observed for coefficient K_3, where the LTPP model underestimated the measured values for K_3. The difference between the predicted and the measured M_R values was explain by the fact that the LTPP data used in the development of the prediction models did not include any M_R test data for Louisiana soils. It shall also be noted that M_R tests for this study were conducted on undisturbed specimens using a loading pulse of 0.2 sec loading time and 0.8 sec rest period. The LTPP prediction models were developed based on M_R tests of re-compacted specimens using a loading pulse of 0.1 sec loading time and 0.9 sec rest period.

Statistical analysis was performed on M_R test data to develop a prediction model for Louisiana subgrade soils. Compared to LTPP model, Louisiana prediction model incorporated variables that represent the combined influence of more than one physical property. An example of these variables is "MCCL" variable which represented the combined influence of specimen moisture content, OMC, and percentage of clay. In addition, Louisiana prediction model utilized the deviation of specimen moisture content from OMC instead of using the absolute value of the specimen moisture content. A catalog of M_R values for Louisiana subgrade soils was developed and compared to the

typical values recommended by the Mechanistic-Empirical Pavement Design Guide "Pavement ME" (NCHRP2004). For A-4 and A-6 soils, the values recommended by Pavement ME were higher than the average M_R values reported for Louisiana soils. For A-7-5 and A-7-6 soils, the Pavement ME M_R values and Louisiana M_R values were comparable. Table 2.9 shows the M_R values for Louisiana subgrade soils and the recommended values by the Pavement ME.

TABLE 2.9: M_R Values for Louisiana Subgrade Soils and Pavement ME Typical Values (Nazzal et al. 2008)

Soil Type	Moisture Content Level	Louisiana M_R Values (MPa)		Pavement ME Recommended M_R Values (MPa)[1]	
		Range	Mean	Range	Mean
A-4	2	73.4 - 80.4	76.3	148.1 – 199.8	165.4
	3	38.3 - 71.2	58.5		
	4	23.3 - 55.6	36.8		
A-6	1	44.1 – 68.8	57.3	93.0 – 165.4	117.1
	2	60.7 – 111.7	87.0		
	3	38.6 – 88.7	62.8		
	4	20.8 – 57.8	46.3		
A-7-5	2	70.4 – 167.3	97.0	55.1 – 120.6	82.7
	3	67.1 – 107.0	84.5		
	4	11.0 – 68.1	45.0		
A-7-6	2	37.1 – 97.1	80.4	34.5 – 93.0	55.1
	3	45.2 – 91.3	63.4		
	4	6.1 – 49.7	24.6		

[1] Pavement ME recommended values represent M_R values at optimum moisture content and maximum dry density

2.4.5 Feasibility of Using Existing Models in Prediction of M_R for Mississippi Soils

George (2004) evaluated the feasibility of using existing M_R models in predicting M_R of Mississippi subgrade soils. Seven M_R prediction models were included in this study. Three of these seven models were nonlinear models that incorporated soil physical properties and stress state (Von Quintus and Killingsworth 1998; Dai and Zollars 2002; Santha 1994). The remaining four prediction models were regression equations with different forms (i.e., linear, bilinear, etc.) based on soil properties and stress state (Carmichael and Stuart 1985; Drumm et al. 1990; Farrar and Turner 1991; Rahim and George 2004). The predicted M_R values with these seven models were validated by comparison to M_R values obtained from laboratory testing.

M_R tests were conducted on eight, fine-grained and coarse-grained, soil samples according to LTTP P46 test protocol. Soils were re-compacted and tested at OMC and maximum dry density. According to AASHTO soil classification system, the eight soil samples were classified as A-2-4, A-4, and A-6 soils. Table 2.10 shows the physical properties of the eight soil samples.

The physical properties in Table 2.10 were used to predict M_R values for each subgrade soil sample. For each soil sample, seven M_R values were calculated using the seven prediction models investigated in this study. Table 2.11 shows a comparison between the predicted values for M_R and the values measured in the laboratory. From Table 2.11, Santha (1994) and Dai and Zollars (2002) models did not provide reasonable predictions

for M_R of Mississippi soils. The remaining models either over predicted or under predicted M_R of Mississippi soils but the predicted values were comparable to the laboratory measured M_R. Based on deviations from the laboratory values for M_R, Rahim and George (2004) model provided the most reasonable prediction for M_R of Mississippi soils. Rahim and George (2004) model was calibrated using M_R test data of Mississippi soils which explains the better M_R predilection of this model than the other six models.

George (2004) performed sensitivity analysis to study the effect of changing soil properties on the prediction of M_R. Results of sensitivity analysis showed that moisture content, percentage passing No. 200 sieve, and plasticity index were the most significant soil properties in M_R prediction.

TABLE 2.10: Physical Properties of Mississippi Subgrade Soils (George 2004)

Sample No.	Soil Type	Liquid Limit (%)	Plasticity Index (%)	Passing No. 40 Sieve (%)	Passing No. 200 Sieve (%)	Clay (%)	Silt (%)
1	A-4	22.3	6.1	N/A[1]	55.0	10.6	44.5
2	A-4	27.0	8.0	N/A	56.0	14.2	41.8
3	A-4	25.0	7.0	N/A	56.0	10.8	45.2
4	A-6	28.1	12.4	90.0	60.0	12.3	48.1
5	A-6	37.2	13.1	99.0	96.0	19.3	78.7
6	A-2-4	20.5	1.0	N/A	28.0	3.2	25.4
7	A-4	24.4	4.9	N/A	42.0	9.0	33.1
8	A-6	35.8	13.3	99.0	98.0	18.9	79.1

[1] N/A: Not Available

TABLE 2.11: Comparison between Predicted M_R and Laboratory Measured M_R (George 2004)

Sample No.	Mean Value of M_R (MPa)							
	Laboratory Test	Von Quintus and Killingsworth (1998)	Santha (1994)	Dai and Zollars (2002)	Carmichael and Stuart (1985)	Drumm et al. (1990)	Farrar and Turner (1991)	Rahim and George (2004)
1	66.0	65.5	653.3	260.8	116.2	56.8	40.6	68.9
2	85.2	75.8	625.3	233.0	109.9	85.2	46.5	87.4
3	49.6	72.9	917.6	66.3	132.7	84.4	37.9	94.2
4	98.6	70.1	961.4	252.3	90.7	73.2	46.3	95.1
5	88.2	57.4	10693.9	-34878.0	37.1	75.1	75.5	93.6
6	81.5	64.8	N/A[1]	N/A[1]	75.8	N/A[1]	N/A[1]	62.9
7	103.5	75.9	428.8	35.4	145.0	76.2	37.1	100.2
8	77.3	51.9	7954.4	-28167.0	27.9	59.8	73.9	81.5

[1] N/A: Not Available

2.4.6 M_R Model for Quebec UGM and Moisture Sensitivity of M_R

Simplified nonlinear models that relate M_R to bulk stress were recommended by several studies in the literature for UGM. These models are applicable only for low strain values where they neglect the effect of shear strains on M_R (May and Witczak 1981; Uzan 1985). The Ministry of Transportation of Quebec (MTQ) proposed a linear relationship to describe the stress dependency of M_R in the first draft of the M_R standard LC22-400 (Bilodeau and Doré 2012b). The model expresses the relationship between M_R, in MPa, and bulk stress (θ), in kPa, as follows:

$$M_R = c_1\theta + c_2 \quad \textbf{(2.26)}$$

Where:

c_1 and c_2 = regression coefficients.

Bilodeau and Doré (2012a, 2012b) evaluated the M_R for three aggregate sources that are commonly used as UGM in Quebec: partially crushed gneiss (72% fractured particles), crushed limestone (100% fractured particles), and crushed basalt (100% fractured particles). For each aggregate source, six gradations were reconstituted and tested to represent the variation within and outside the MTQ grading envelope for UGM. The six gradations were:

- the fine limit of the grading envelope (F),
- the coarse limit of the grading envelope (C),
- middle of the grading envelope (M),
- uniform-graded within the grading envelope (U),
- well-graded within the grading envelope (WG), and
- a gradation finer than the fine limit of the grading envelope (FM).

Each gradation was tested at three states representing three moisture contents: at compaction moisture content, after vacuum saturation of compacted specimen, and after draining water from saturated specimen. Table 2.12 shows the regression coefficients of Equation 2.26, c_1 and c_2, and the degree of saturation, S_R, for the tested gradations (Bilodeau and Doré 2012b). The residuals mean square error (RMSE) ranged from 11 MPa to 32 MPa for gneiss gradations, 40 MPa to 76 MPa for limestone gradations, and 18 MPa to 34 MPa for basalt gradations.

TABLE 2.12: Laboratory Measured M_R for Quebec UGM (Bilodeau and Doré 2012b)

Gradation code	Gneiss			Limestone			Basalt		
	c_1 (−)	c_2 (MPa)	S_R (%)	c_1 (−)	c_2 (MPa)	S_R (%)	c_1 (−)	c_2 (MPa)	S_R (%)
F	0.951	90.3	21	1.465	132.9	22	0.986	83.3	19
	0.724	78.0	96	1.386	93.3	96	0.933	68.0	89
	0.713	78.1	72	1.381	107.9	54	0.932	66.0	38
M	0.824	108.9	13	1.555	137.1	26	1.024	95.3	17
	0.660	92.0	81	1.483	131.9	85	0.998	74.5	75
	0.676	92.9	35	1.534	124.9	43	1.008	70.7	28
C	0.791	109.3	22	1.746	169.6	20	1.070	100.5	17
	0.670	92.4	89	1.739	129.0	88	1.029	95.4	87
	0.692	92.7	42	1.726	149.0	27	1.036	87.4	33
U	0.735	84.5	18	1.401	125.7	17	0.941	86.5	13
	0.618	73.2	90	1.340	107.8	94	0.914	72.5	77
	0.653	77.9	28	1.346	103.8	36	0.922	70.3	26
WG	0.956	109.1	25	1.583	138.1	29	1.164	105.6	23
	0.747	96.1	89	1.489	123.4	93	1.094	89.3	83
	0.734	89.5	67	1.467	139.9	63	1.110	93.8	50
FM	1.134	102.1	18	1.144	137.8	15	0.802	111.2	9
	0.924	88.7	95	1.137	106.6	93	0.737	82.0	88
	0.915	96.6	67	1.143	122.6	57	0.748	86.9	26

The change in M_R with respect to M_R at saturation condition (ΔM_R) and the change in S_R (ΔS_R) was fitted using linear relationship. The slope of this linear relationship (S) was used to quantify the moisture sensitivity of M_R according to the following model:

$$S = \left(3.6233\times10^{-3}\theta + 0.4484\right)\left(\ln\left[0.01 n_f \%FR\right] + 6.5549\times10^{-3}\right) - 0.162 \quad \textbf{(2.27)}$$

Where:

S = slope of ΔM_R-ΔS_R relationship, MPa/%,

θ = bulk stress, kPa,

n_f = fine fraction porosity in decimal,

%FR = the percentage of fractured particles, %

Equation 2.27 provided adequate prediction to M_R variations with moisture for the tested aggregate sources compared to another model in the literature (Bilodeau and Doré 2012b).

2.5 Shakedown Behaviour of UGM

The quality and response of UGM layer are main factors that contribute to the service life of pavements (Pérez et al. 2006). Pavement materials are usually subjected to stress levels that exceed their elastic limits to accommodate the traffic loading with cost-effective design. Pavement structures fail due to gradual accumulation of permanent deformation, or degradation in materials during their service life, and not due to rapid collapse (Sharp 1985). The mode of failure of UGM layer is governed by the applied load and the shakedown behaviour of the material which is illustrated in Figure 2.4. The shakedown behaviour of an elastic-plastic material is assessed based on the shakedown theory which classify the deformation behaviour of the material according to its elastic and plastic deformation behaviour under repeated loading. Using the AASHTO road test data, and a case study conducted in Australia, Sharp (1985) found that pavements subjected to lighter traffic loading or with higher shakedown limit had longer service life.

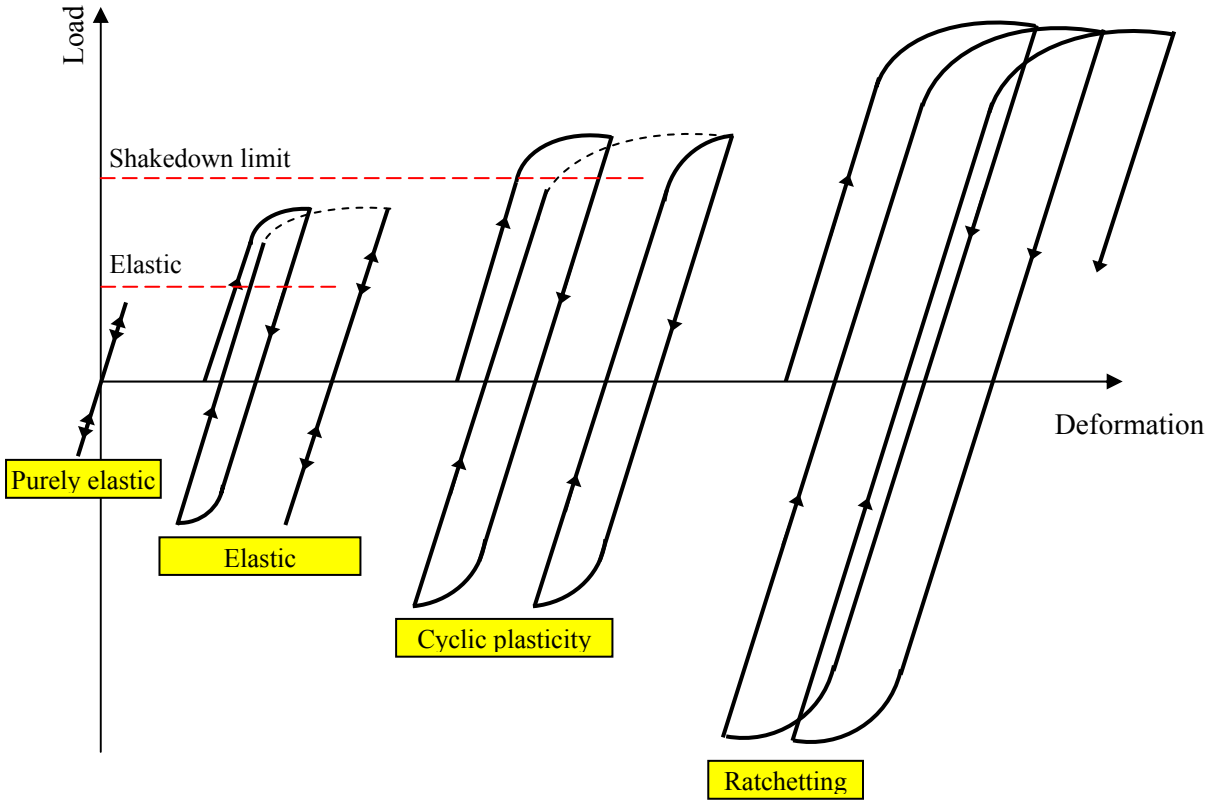

FIGURE 2.4: Shakedown Behaviour of Elastic-Plastic Material under Repeated Loading (Barber and Ciavarella 2000; Johnson 1985)

Johnson (1985) presented the shakedown process that elastic-plastic materials undergo when subjected to repeated loading, as shown in Figure 2.4. If the elastic limit is not exceeded, an elastic-plastic material undergoes purely elastic behaviour with no plastic deformation. When the elastic limit is initially exceeded, the material experiences initial plastic deformation which produces residual stresses. In subsequent load applications, the behaviour of the material is dependent on the combined action of the applied load and the residual stresses produced by previous load applications. After certain number of load repetitions, the residual stresses build up to a value that lead to a steady state with entirely

elastic deformation under subsequent load applications (shakedown limit). When the shakedown limit is exceeded, the material experiences incremental plastic deformation under repeated loading.

For repeated loads above the shakedown limit, an elastic-plastic material may undergo two deformation patterns: cyclic plasticity or progressive increase in plastic deformation (ratchetting), as shown in Figure 2.4 (Barber and Ciavarella 2000). It is important to determine which of these two patterns the material will undergo because the failure mode will be different. Failure is governed by low-cycle fatigue in the first deformation pattern and by exhaustion of ductility or static plastic collapse in the second pattern (Barber and Ciavarella 2000).

UGM response to loading is nonlinear and their behaviour is affected by stress history from previous loading. Results from laboratory tests and full-scale retaining wall tests support the existence of residual stresses in compacted UGM due to compaction load and/or repeated traffic loading. Therefore, a newly constructed granular base layer is not stress-free (Uzan 1985).

Barber and Ciavarella (2000) studied the influence of friction on contact problems. According to Coulomb friction condition, the state of any point in the contact area between two bodies must be:

- Stick: there is no relative motion at the interface between the two bodies, or
- Slip: there is relative motion at the interface between the two bodies.

The frictional slip depends on the material loading history where it is an incremental process (Barber and Ciavarella 2000). Sharp (1985) conducted shakedown analysis of different pavement structures using a reformulated Mohr-Coulomb model. Results showed that the first yield, shakedown, and static collapse loads increased with the increase of friction angle for a homogeneous half-space. The static collapse load showed more sensitivity to the increase of friction angle.

The shakedown approach was adopted in several studies to characterize the behaviour of UGM under repeated loading (Garcia-Rojo and Herrmann 2005; Nazzal et al. 2011; Tao et al. 2010; Werkmeister et al. 2001, 2005). The permanent deformation behaviour of UGM can be classified into three categories, as shown in Figure 2.5, according to the shakedown theory (Werkmeister et al. 2004):

- Plastic shakedown: UGM response is plastic for a finite number of cycles, with a rapid decrease in permanent strain rate; afterward the response becomes purely elastic.
- Plastic creep (intermediate response): UGM experiences high permanent strain rate in the early loading cycles which decreases later to low or constant strain rate. After a high number of loading cycles, UGM experiences progressive increase in permanent strain and advances toward an incremental collapse.
- Incremental collapse: UGM experiences progressive increment of permanent strain with each load cycle which leads to failure after a relatively low number of loading cycles.

The desirable behaviour of a well-designed UGM layer is to be within the plastic shakedown or the plastic creep categories with an acceptable total permanent deformation (Sharp 1985).

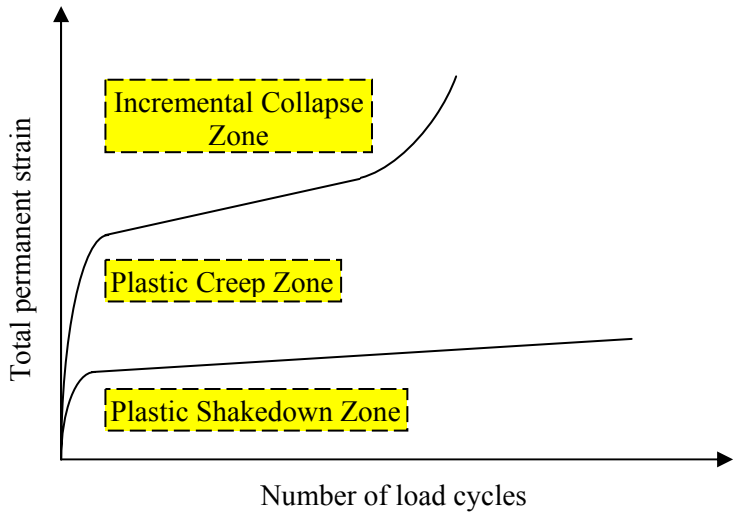

FIGURE 2.5: Permanent Deformation Behaviour of UGM According to Shakedown Approach (Werkmeister et al. 2004)

Gradation is one of the main factors that influence the elastic and plastic behaviour of UGM (Tian et al. 1998). Gradation has an influence on the permeability and frost susceptibility of UGM which affect the plastic behaviour of UMG layers (Bilodeau et al. 2008, 2011). Type, plastic or nonplastic, and amount of fines passing No. 200 sieve in UGM influence the elastic and plastic response of UGM layer under traffic loading (Tutumluer 2013).

Cerni et al. (2012) investigated the effect of the presence of plastic fines in UGM on permanent deformation behaviour. The permanent deformation of two crushed limestone aggregate mixtures was evaluated according to the European Standards: EN 13286-7 (European Committee for Standardization 2004). The two mixtures were identical except for the fines fraction. The first mixture (mixture A) contained calcareous (nonplastic) fines while the second mixtures (mixture B) contained silty clay fines with a plasticity index of 22. The two mixtures were tested at optimum moisture and saturation conditions. Mixture A showed more elastic response at higher stress levels and less sensitivity to moisture variation than mixture B. For the same stress ratio, the plastic shakedown limit for mixture A was almost 5 times the plastic shakedown limit for mixture B. Mixture B showed progressive loss of stiffness at saturation condition.

2.6 Specifications of UGM

Specifications for unbound granular base materials vary among transportation agencies based on the availability of materials, climatic conditions, and function. Specifications aim to provide durable materials that meet design requirements and achieve the target design life with cost effective materials. This section summarize the results of an environmental scan to compare UGM specifications employed by Manitoba Infrastructure and Transportation (MIT) to UGM specifications employed by neighbouring jurisdictions.

The specifications investigated were for UGM used for base layer construction. Specifications of the majority of Provinces across Canada and States located in the upper

Midwest and West regions of the United States were investigated due to the similar climatic condition to that of Manitoba as well as the availability of standard specifications from department of transportation. The regions investigated and the specification names are shown in Figure 2.6 and Table 2.13, respectively.

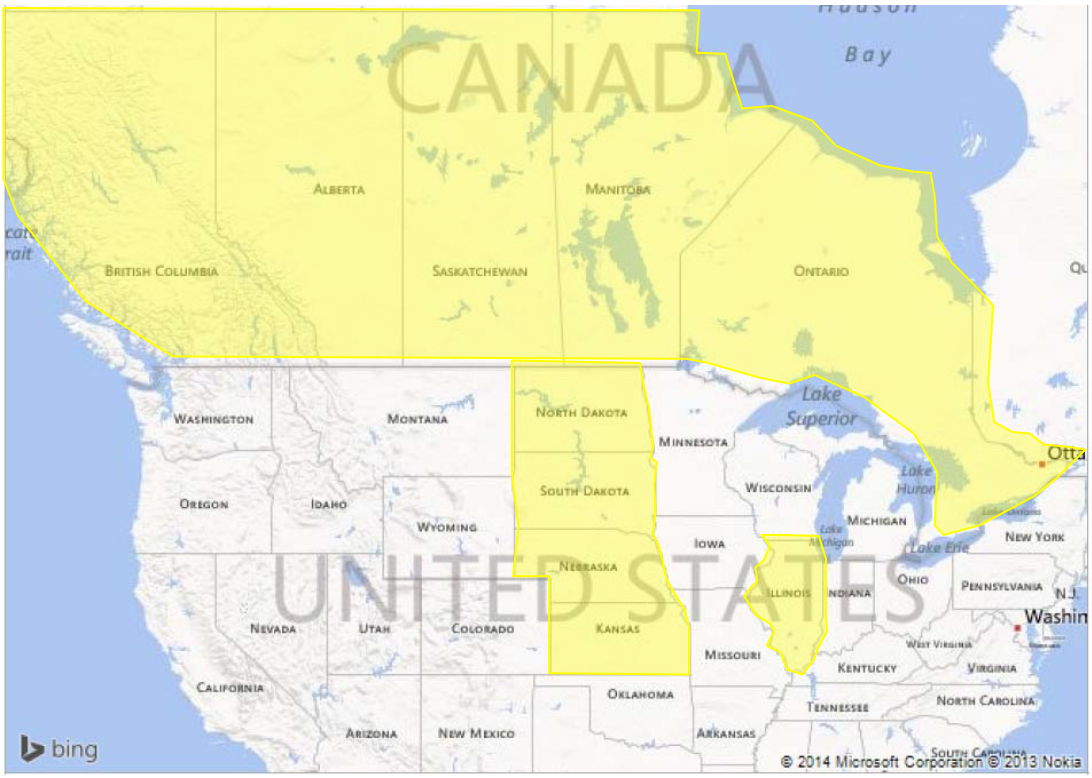

FIGURE 2.6: Map of Provinces and States Covered by the Environmental Scan

MIT specify two gradation limits for dense-graded base course materials: Class A gravel base and Class A limestone base. MIT gradation limits for Class A gravel base and Class A limestone base are listed in Table 2.14. Table 2.15 shows gradation limits for granular base materials according to the specifications of the jurisdictions covered by the environmental scan. Figure 2.7 compares MIT gradation limits to the gradation limits of other Canadian provinces. Figure 2.8 compares MIT gradation limits to the gradation limits of neighbouring States. The gradation limits employed by MIT allow finer

gradation than the average gradation limits of all other jurisdictions investigated. This is true for both the upper and lower gradation limits.

TABLE 2.13: The Regions Investigated and Specification Names

Province / State	Specification Name
Manitoba	Class A Granular Base Course (MIT 2002)
Ontario	Class A Granular Base Course (MTO 2003)
British Columbia	25mm (Top Layer) Well Graded Base Course (BCMOTI 2011)
Saskatchewan	Type 31 (Top Layer), Base Course (SKDHT 2004)
Alberta	Class 25 Granular Base Course (AT 2010)
Illinois	Aggregate Base Course CA 10 (IDOT 2012)
South Dakota	Aggregate Base Course (SDDOT 2004)
North Dakota	Aggregate Base (NDOT 2008)
Nebraska	Crushed Rock for Base Course (NDOR 2007)
Kansas	Aggregate Base AB-1 (KDOT 2007)

Figures 2.9 shows the maximum aggregate size based on the specifications of MIT and the jurisdictions investigated. The maximum particle size according to MIT specifications is 16.0 mm for Class A gravel base and 19.0 mm for Class A Limestone base, while the other jurisdictions have a maximum particle size ranging from 25.0 mm to 37.5 mm. Fines content (passing No. 200 sieve) is one of the factor that has a significant influence on the elastic and plastic response of granular base materials under traffic loading. Fines are required in dense-graded granular base material but to a certain limit to maintain higher resilient modulus and higher resistance to permanent deformation (Tutumluer 2013). Figures 2.10 shows the limits for the allowed fines content based on the specifications of MIT and the jurisdictions investigated. MIT specifications allow a higher fines content than any other jurisdiction investigated.

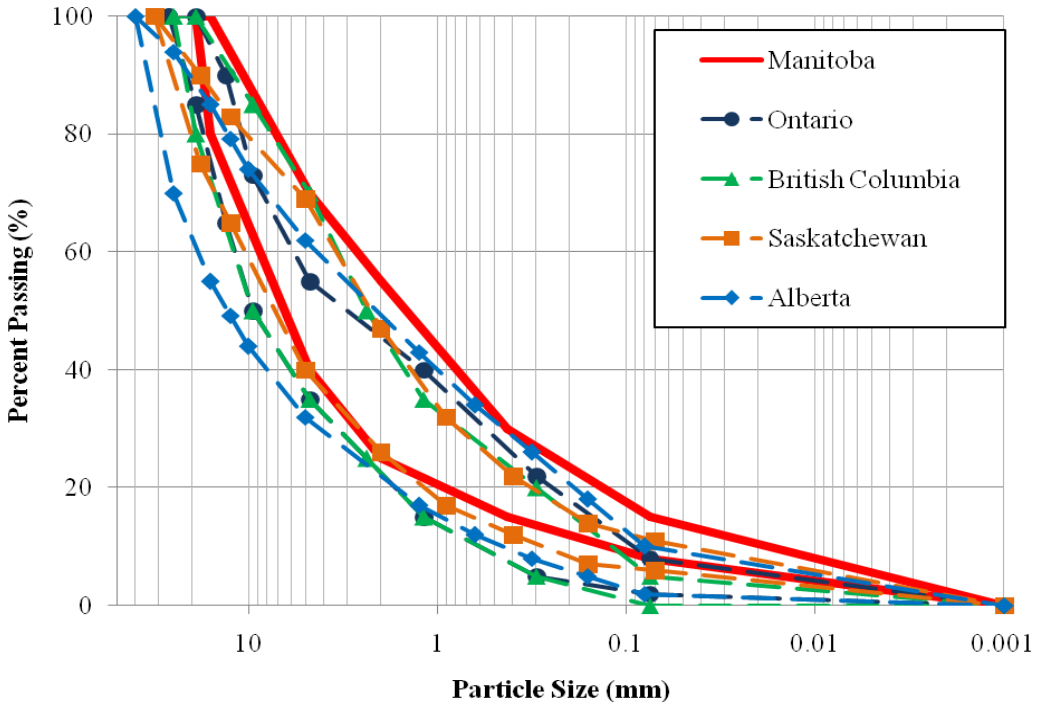

FIGURE 2.7: Gradation Limits for Aggregate Base Course: MIT vs. Surveyed Canadian Jurisdictions

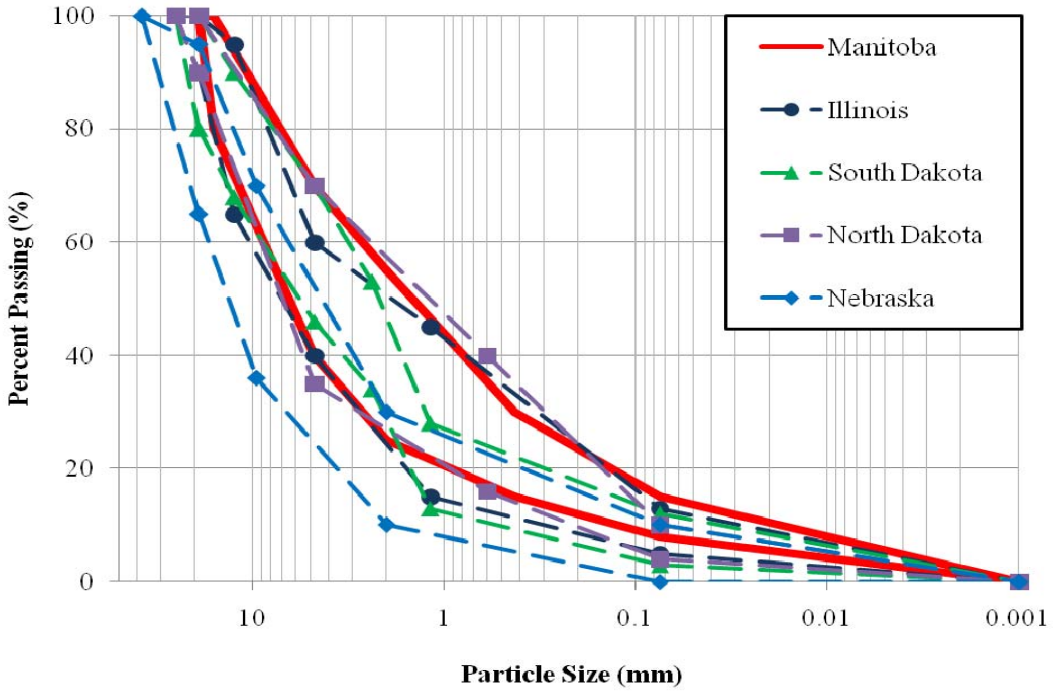

FIGURE 2.8: Gradation Limits for Aggregate Base Course: MIT vs. Surveyed US Jurisdictions

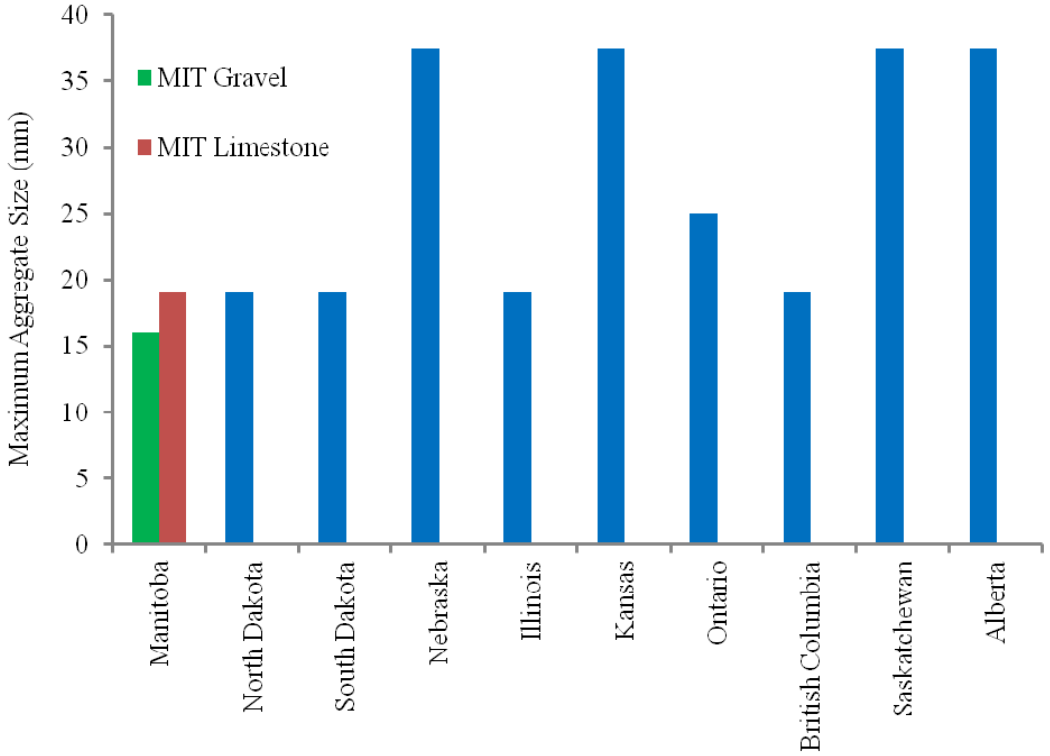

FIGURE 2.9: Maximum Aggregate Size by Jurisdiction

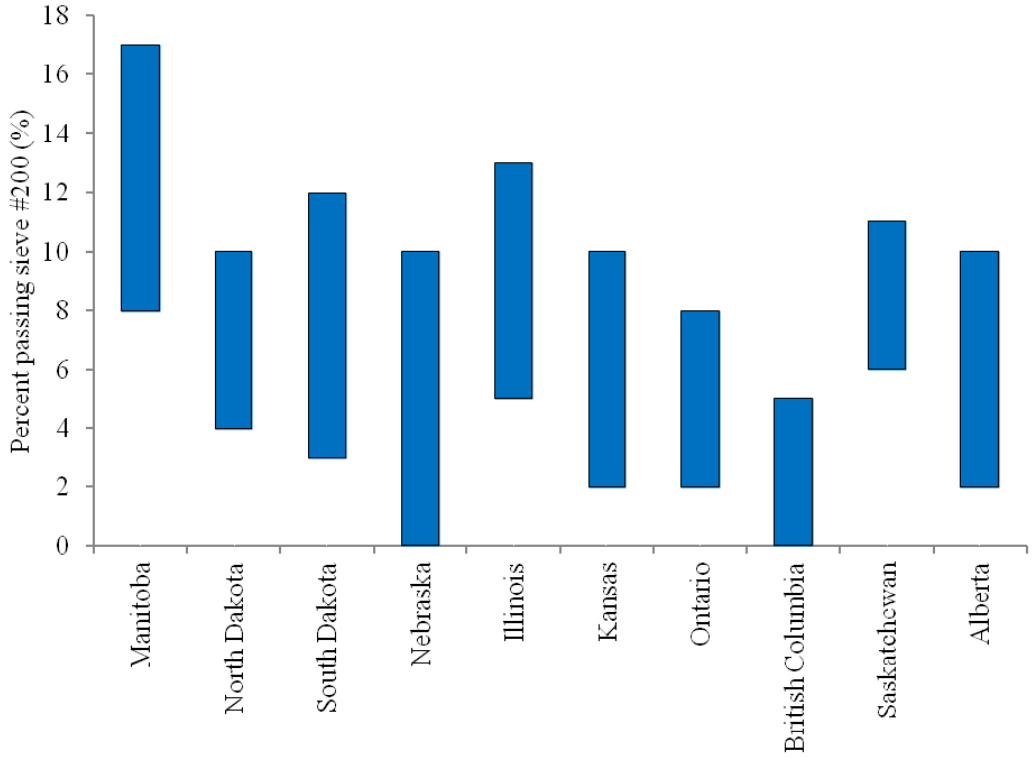

FIGURE 2.10: Limits for the Allowable Fines Content by Jurisdiction

TABLE 2.14: Gradation Limits for Aggregate Base Course in Manitoba

Particle Size (mm)	50	37.5	25	19	16	9.5	4.75	2.00	0.425	0.075
Gravel, Granite	100-100	100-100	100-100	100-100	80-100	63-87	40-70	25-55	15-30	8-15
Limestone	100-100	100-100	100-100	100-100	92-96	68-85	35-70	26-56	10-30	8-17

TABLE 2.15: Gradation Limits for Aggregate Base Course in the Surveyed Jurisdictions

Particle Size (mm)	50	37.5	25	19	16	9.5	4.75	2.00	0.425	0.075
Ontario	100-100	100-100	97-100	85-100	76-95	50-73	35-55	23-46	8-27	2-8
British Columbia	100-100	100-100	100-100	80-100	73-96	50-85	35-70	24-49	15-35	0-5
Saskatchewan	100-100	100-100	90-96	80-91	74-88	58-79	39-68	26-47	12-23	6-11
Alberta	100-100	96-99	70-94	61-88	55-85	43-73	31-61	22-49	10-29	2-10
Illinois	100-100	100-100	100-100	90-100	80-98	58-85	40-60	24-51	11-33	5-13
South Dakota	100-100	100-100	100-100	80-100	75-96	62-84	46-70	32-51	13-28	3-12
North Dakota	100-100	100-100	100-100	90-100	83-96	63-85	35-70	27-58	14-35	4-10
Nebraska	100-100	100-100	79-97	65-95	58-89	36-70	24-52	10-30	5-21	0-10
Kansas	100-100	90-100	72-97	60-95	56-92	43-80	25-65	14-44	5-22	2-10
Average	100-100	98-100	90-98	77-97	70-93	51-79	35-63	22-47	10-28	3-10

3 Experimental Program

3.1 Introduction

An experimental program was developed to evaluate the laboratory performance of fine-grains soils and UGM in Manitoba. For fine-grains soils, resilient modulus tests were conducted to evaluate the elastic behaviour of soils and the sensitivity of resilient modulus for moisture variation. For UGM, resilient modulus and permanent deformation tests were conducted to evaluate the elastic and plastic behaviour of the material. Permeability tests were also conducted on UGM to evaluate the drainability of the material. Results from laboratory testing were used to update values of design inputs and specifications of UGM. Table 3.1 summarize the laboratory tests conducted in the research and the use of each test.

TABLE 3.1: Laboratory Tests for Subgrade Soils and UGM

Material	Test Name	Measured Property	Application
Subgrade Soil	Resilient Modulus	Resilient modulus	• Update values of design inputs for Pavement ME • Develop local perdition models for resilient modulus
UGM	Resilient Modulus Permanent Deformation Permeability	Resilient modulus Permanent deformation versus loading cycles Drainability	• Update values of design inputs for Pavement ME • Develop local perdition models for resilient modulus • Update UGM specifications based on laboratory performance

3.2 Acquisition and Characterization of Materials

3.2.1 Subgrade Soils

Six soil samples were collected to represent three types of soil:

- High plastic clay (from Red River Valley),
- Silty sand/Sandy silt (from central & southern Manitoba), and
- Sandy clay (from western Manitoba).

The soil samples represent the typical soil types available in Manitoba. Grain size analysis, Atterberg limits, and Standard Proctor tests were conducted for the collected samples. Figure 3.1 shows the grain size distribution of the six soil samples. For each soil sample, four moisture contents were selected to evaluate the sensitivity of M_R to the variation in moisture content and dry density. The four moisture contents were selected to cover both the dry and wet sides of the Standard Proctor compaction curve. Table 3.2 shows AASHTO classification, maximum dry density (γ_{opt}), optimum moisture content (OMC), and M_R moisture contents for the tested soils.

Although AASHTO T307-12 is the latest test method for M_R, the NCHRP 1-28A test method was used in the research where part of the resilient modulus tests were conducted before the development of AASHTO T307-12. According to the NCHRP 1-28A M_R test protocol, subgrade soils are classified into two groups based on the percent passing No.200 (75 μm) sieve (Harrigan and Witczak 2004). Each soil group has a different testing procedure. The first group is coarse-grained subgrade soils for which the percent passing No. 200 sieve is less than 35%. The second group is cohesive subgrade soils for

which the percent passing No. 200 sieve is greater than 35%. The results of grain size analysis showed that the six soil samples belong to the second group (fine-grained subgrade soil).

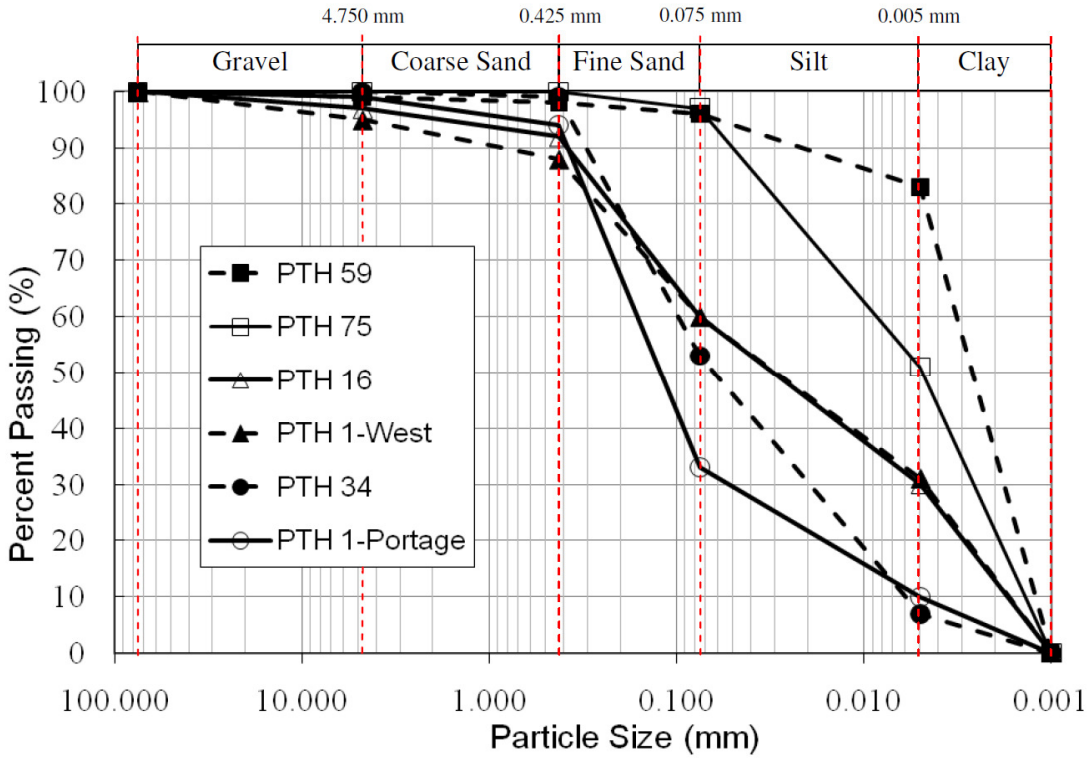

FIGURE 3.1: Grain Size Distribution of Soil Samples

3.2.2 Unbound Granular Materials

Three samples of UGM were collected by MIT from different sources in the Province to represent three types of UGM: uncrushed gravel, 100% crushed limestone, and 100% crushed granite. Figures 3.2 to 3.4 show the shape of the coarse portion (retained on No. 4 sieve) of gravel, limestone, and granite materials, respectively.

TABLE 3.2: Properties of Soil Samples and Moisture Contents for M_R Tests

Sample ID	Soil Type	AASHTO Classification	Plasticity Index (PI)	OMC (%)	γ_{opt} (kg/m^3)
PTH 59	High plastic clay	A-7-6	56	28.2	1473
PTH 75	High plastic clay	A-7-6	27	20.4	1631
PTH 16	Sandy clay	A-6	15	14.1	1856
PTH 1-West	Sandy clay	A-6	17	13.4	1877
PTH 34	Sandy silt	A-4	0	13.0	1865
PTH 1-Portage	Silty sand	A-2-4	0	10.8	1859

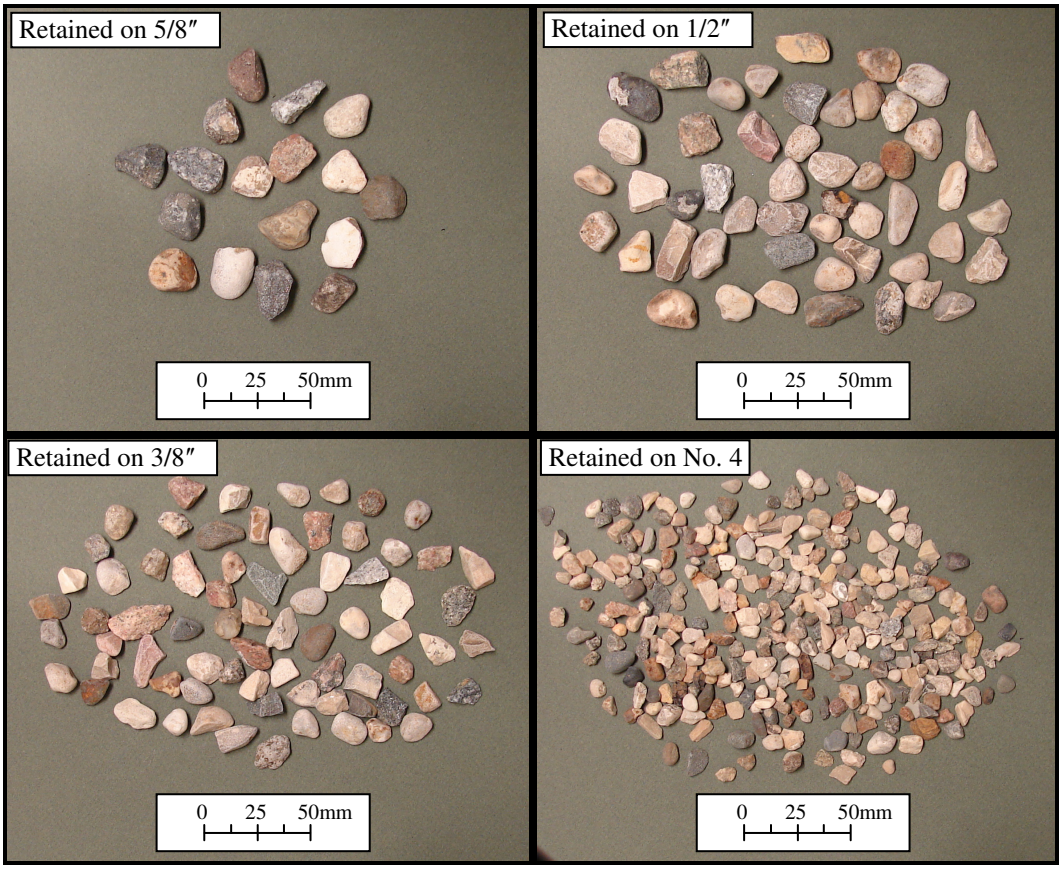

FIGURE 3.2: Shape of Coarse Portion (Retained on No. 4 Sieve) of Gravel UGM

The UGM samples were sieved into individual particle sizes. For gravel and limestone materials, the individual particle sizes were combined into three gradations with different fines content. Two gradations represent specification limits on allowable fines content and one gradation has less fines content than presently allowed by specifications. For Granite, the individual particle sizes were reconstituted into one gradation to represent the minimum allowable fines content, as per specifications.

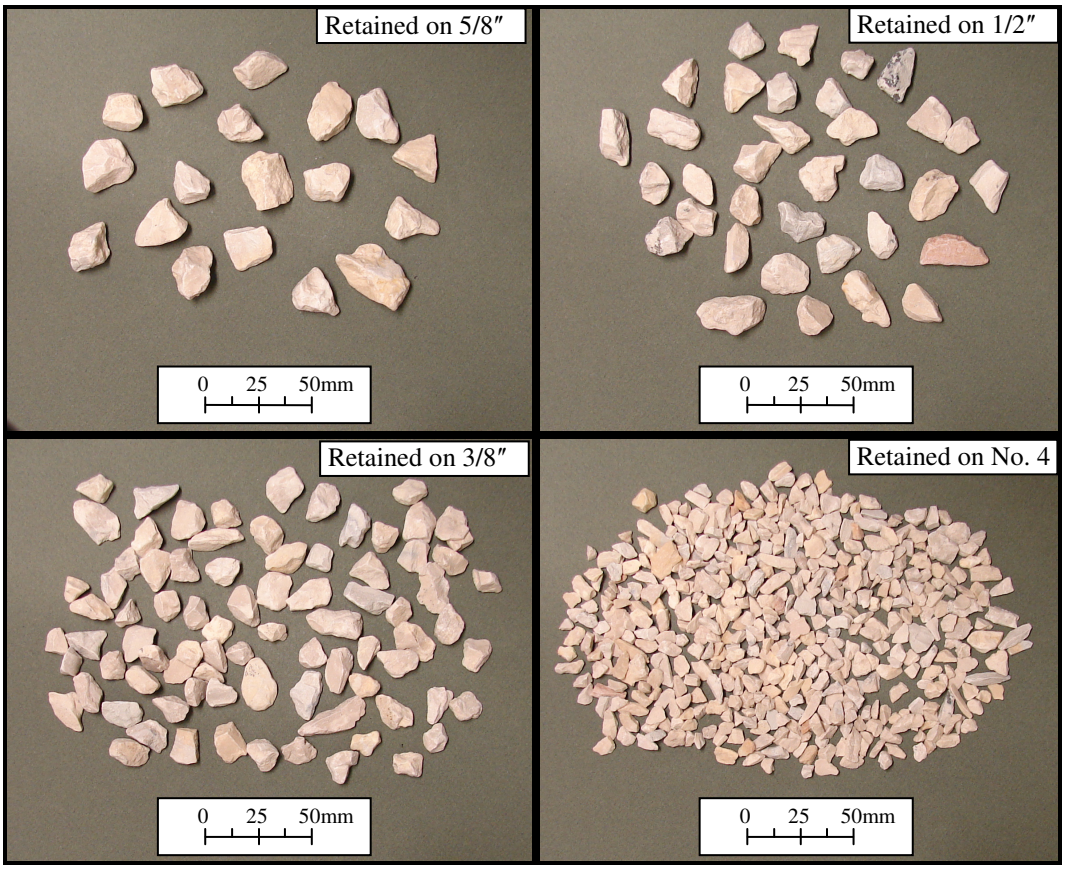

FIGURE 3.3: Shape of Coarse Portion (Retained on No. 4 Sieve) of Limestone UGM

For gravel, the fines contents for the three gradations were 4% (GA−4), 9% (GA−9), and 14.5% (GA−14.5). For limestone, the fines contents for the three gradations were 4.5% (LS−4.5), 10.5% (LS−10.5), and 16% (LS−16). For granite, the fines content for the

tested gradation was 9.0% (GR–9). The fines contents were selected based on the current specification of UGM in Manitoba to represent upper specification limit, lower specification limit, and a fines content below lower specification limit. The required material for each test specimen was mixed, bagged and stored separately to ensure a consistent gradation over all specimens. Figures 3.5 to 3.7 show the selected gradations of gravel, limestone, and granite materials, respectively.

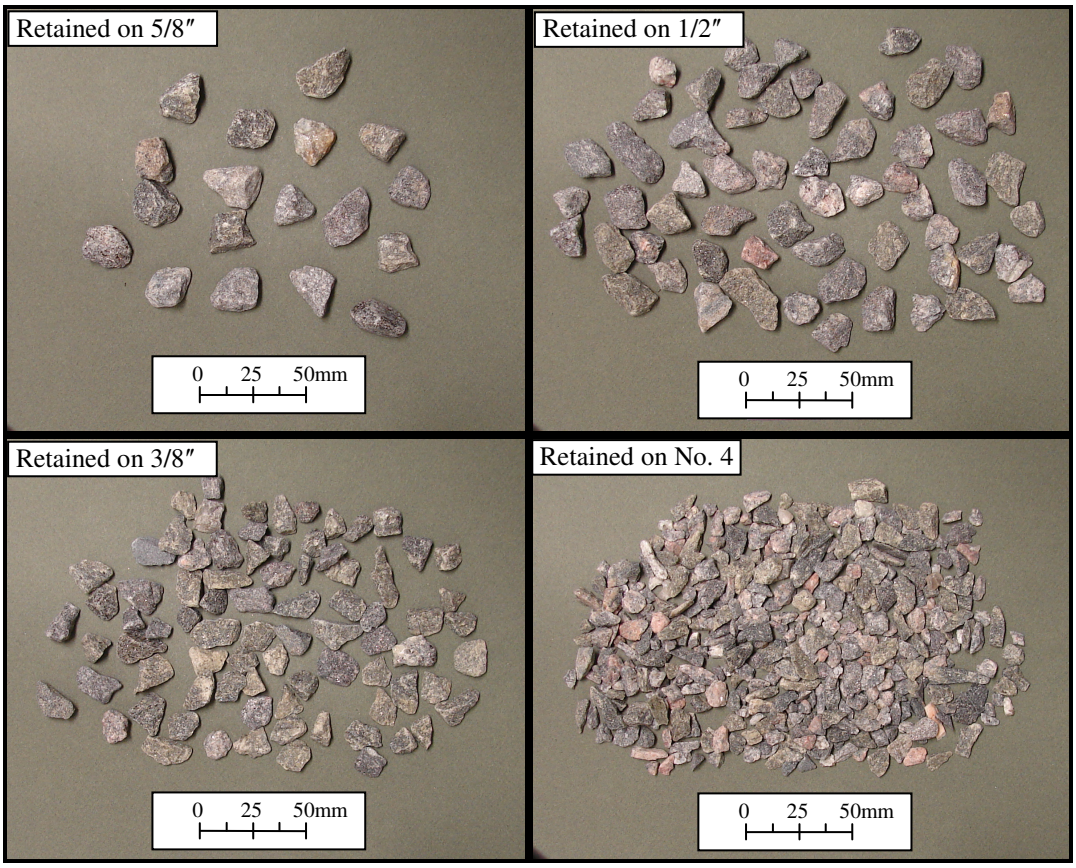

FIGURE 3.4: Shape of Coarse Portion (Retained on No. 4 Sieve) of Granite UGM

Standard Proctor and Atterberg Limits tests were conducted on all UGM gradations. Table 3.3 shows the maximum dry density and the OMC for all UGM gradations. All gradations had a plasticity index of zero. The fines portion (passing No. 200 sieve) was

calcareous fines for limestone, clayey silt for gravel with an average silt/clay ratio of 1.75, and clayey silt for granite with an average silt/clay ratio of 1.50.

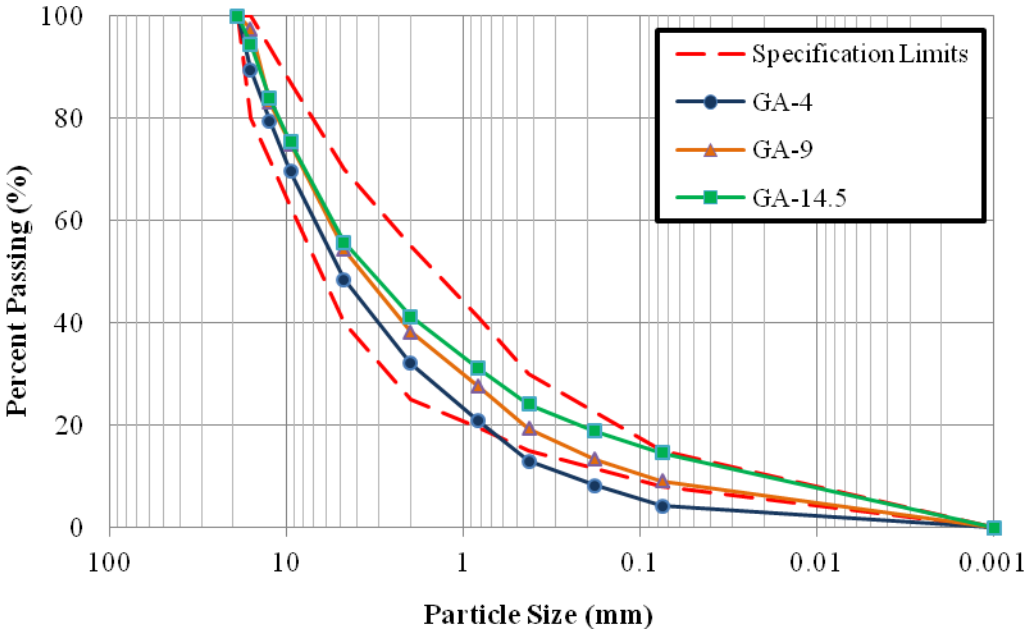

FIGURE 3.5: Particle Size Distribution for Gravel UGM Gradations

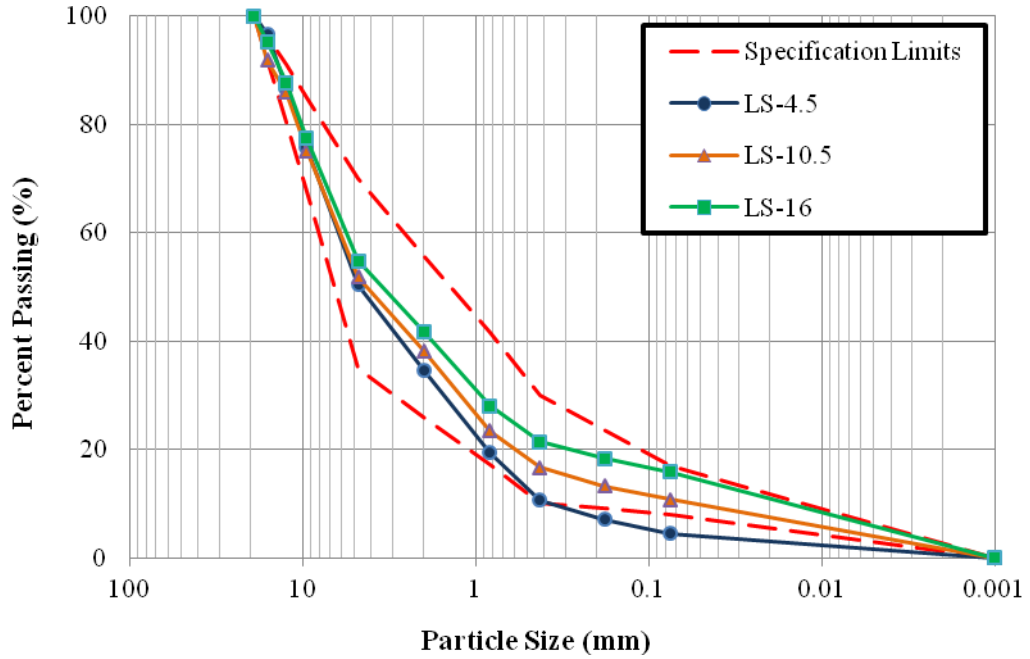

FIGURE 3.6: Particle Size Distribution for Limestone UGM Gradations

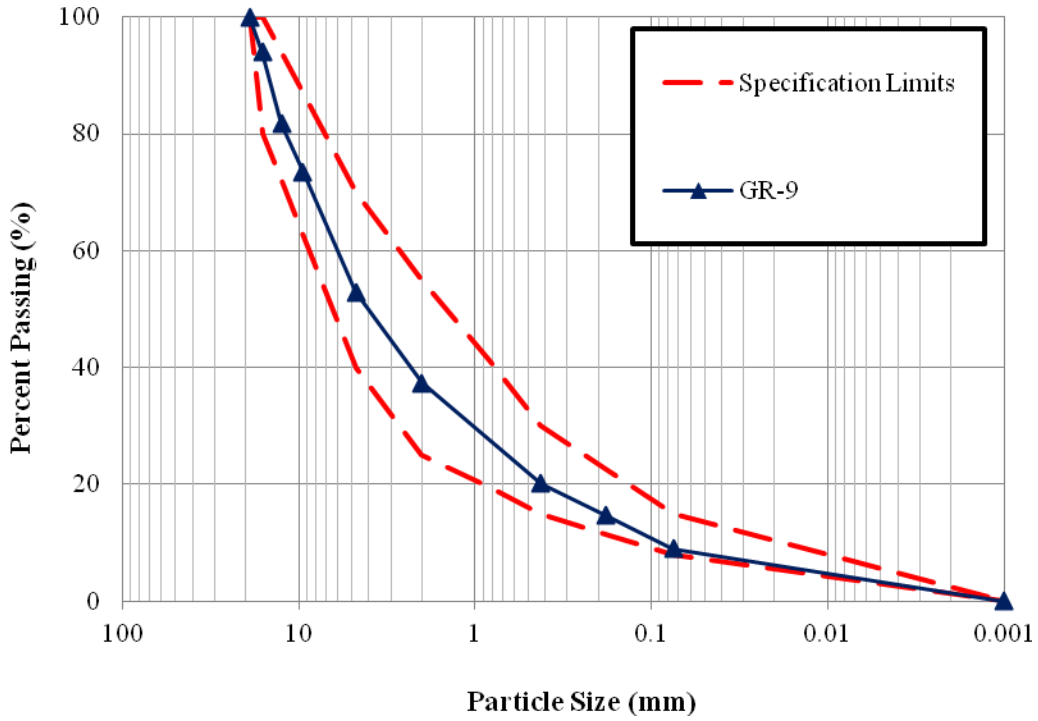

FIGURE 3.7: Particle Size Distribution for Granite UGM

TABLE 3.3: Properties of UGM Gradations

Material type	Gradation ID	Fines content (%)	OMC (%)	γ_{opt} (kg/m^3)	Plasticity index	Clay content (% of total)	Dust ratio
Gravel	GA–4	4.0	7.9	2170	NP*	1.7	0.33
	GA–9	9.0	7.0	2223	NP	3.5	0.47
	GA–14.5	14.5	8.3	2203	NP	4.7	0.61
Limestone	LS–4.5	4.5	7.5	2202	NP	-	0.42
	LS–10.5	10.5	7.0	2277	NP	-	0.65
	LS–16	16.0	6.5	2305	NP	-	0.74
Granite	GR–9	9.0	6.3	2308	NP	3.1	0.45

* NP: no plasticity

3.3 Resilient Modulus and Permanent Deformation Tests

3.3.1 Test Setup and Specimen Preparation

Specimens for M_R and permanent deformation tests were prepared according to the test protocol developed under NCHRP Project 1-28A (Harrigan and Witczak 2004). According to the grain size distribution of the soil and UGM samples, the test specimen measured 101.6 mm in diameter and 203.2 mm in height. Test specimens were compacted in eight layers, 25.4 mm each, to reach the target moisture content/dry density level according to Standard Proctor compaction curve. UGM samples were compacted using a vibration compactor, as shown in Figure 3.8. Soil samples were compacted using an automated impact compactor, as shown in Figure 3.9. A moisture content sample was taken from the soil/ UGM before preparing the specimen. After completing the test, the moisture content of the entire specimen was measured. Replicates with variation higher than 20% or with coefficient of determination lower than 0.9 after fitting test results to Equation 2.4 were excluded from the analysis.

FIGURE 3.8: Vibration Compactor for UGM Samples

FIGURE 3.9: Automated Impact Compactor for Soil Samples

The test setup consisted of a triaxial cell, 25 kN MTS loading frame with closed loop and servo hydraulic loading system, computer-controlled air pressure unit, and data acquisition system. Axial deformations were measured by two LVDTs mounted on the top loading plate. M_R and permanent deformation test setup and specimens were prepared according to the NCHRP 1-28A test protocol (Harrigan and Witczak, 2004). Figure 3.10 shows the setup for M_R and permanent deformation tests.

3.3.2 Testing Program and Procedures for Subgrade Soils

For each soil sample, the M_R tests were conducted at four moisture contents to cover both the dry and wet sides of the Standard Proctor compaction curve. The relative density for

all specimens ranged from 95% to 100%. Three replicates were tests at each moisture content. Table 3.4 shows the moisture contents and dry density for M_R tests.

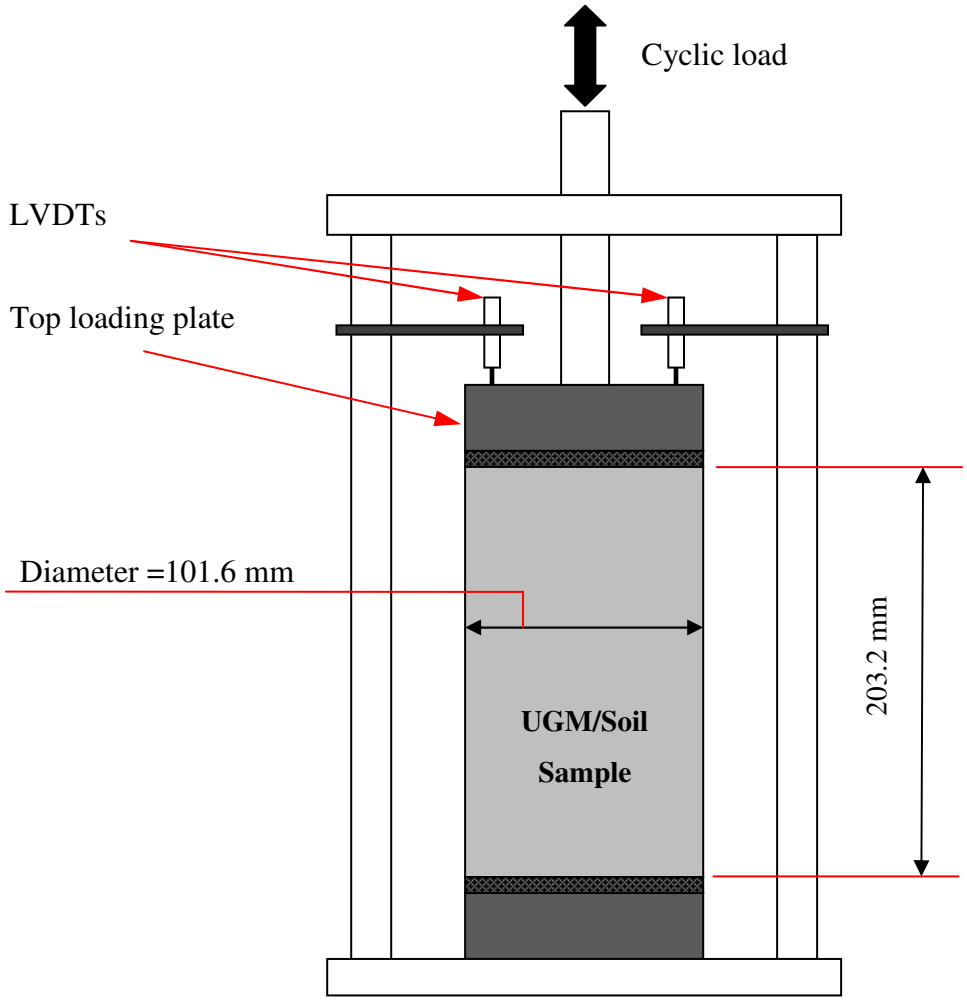

FIGURE 3.10: Setup for M_R and Permanent Deformation Tests

According to M_R test protocol, the load pulse was Haversine shaped load form (Equation 2.2). For subgrade soil testing, the load pulse had load duration of 0.2 sec and rest period of 0.8 sec (Harrigan and Witczak 2004). Test specimens were subjected to combinations of cyclic load and air confining pressure. First, soil specimen was subjected to 1000

conditioning cycles to obtain good contact between specimen ends and loading plates. Permanent deformation of the specimen was monitored during the test. The test shall be stopped when permanent deformation of the specimen exceeds 5%. After conditioning, the test specimen was subjected to 16 loading sequences according to NCHRP 1-28A test method for fine-grained subgrade soils, as shown in Table 2.3. Specimen was subjected to 100 cycles of each loading sequence. During each loading sequence, axial deformations, cyclic load, and confining pressure were recorded for the last 5 cycles. The recorded data was processed to calculate M_R. Analysis and results of M_R tests for subgrade soils are discussed in chapter 4.

TABLE 3.4: Moisture Contents and Dry Density for Soil M_R Tests

Soil Sample ID	Moisture Contents for M_R Tests (%) [Dry density (kg/m^3)]
PTH 59	26.0 [1418], 28.0 [1471], 30.0 [1449], 32.0 [1408]
PTH 75	18.0 [1600], 20.0 [1620], 22.0 [1620], 24.0 [1585]
PTH 16	12.0 [1792], 13.5 [1845], 15.5 [1835], 17.0 [1790]
PTH 1-West	10.0 [1800], 12.0 [1865], 14.0 [1875], 15.5 [1840]
PTH 34	8.0 [1764], 10.5 [1835], 13.0 [1865], 14.5 [1835]
PTH 1-Portage	7.0 [1780], 9.0 [1840], 12.5 [1845], 15.0 [1780]

3.3.3 Testing Program and Procedures for UGM

For each UGM gradation, two moisture contents were selected to evaluate the sensitivity of M_R and permanent deformation to the variation in moisture content. The two moisture

contents were 2.0% below the OMC and approximately at the OMC content according to the Standard Proctor curve for each gradation. All specimens were compacted at 99% of the maximum dry density according to Standard Proctor curve. Two replicate specimens were tested at each moisture content. A third replicate was tested when the variation between the two replicates was higher than 20%. Table 3.5 shows the moisture contents and dry density for M_R and permanent deformation tests.

TABLE 3.5: Moisture Contents and Dry Density for UGM M_R and Permanent Deformation Tests

Material type	Gradation ID	Moisture Contents for M_R and Permanent Deformation Tests (%)	Dry Density (kg/m^3)
Gravel	GA−4	5.9, 7.9	2148
	GA−9	5.0, 7.0	2201
	GA−14.5	6.3, 8.3	2181
Limestone	LS−4.5	5.5, 7.5	2180
	LS−10.5	5.0, 7.0	2254
	LS−16	4.5, 6.5	2282
Granite	GR−9	4.3, 6.3	2285

3.3..3.1 M_R Test for UGM

For M_R and permanent deformation testing of UGM, each loading cycle consisted of a load pulse, Equation 2.2, with a loading duration of 0.1 sec and a rest period of 0.9 sec (Harrigan and Witczak 2004). After 1000 conditioning cycles, the test specimen was

subjected to 30 combinations of cyclic load and air confining pressure according to NCHRP 1-28A test method for UGM, as shown in Table 2.5. The test was stopped when permanent deformation of the specimen exceeded 5%. During each loading sequence, axial deformations, cyclic load, and confining pressure were recorded for the last 5 cycles. The recorded data was processed to calculate M_R for UGM. Analysis and results of M_R tests for UGM are discussed in chapter 6.

3.3..3.2 Permanent Deformation Test for UGM

Permanent deformation tests have been conducted in the literature for 10,000 cycles, to capture the early plastic response of UGM, and up to 700,000 cycles to evaluate the long-term performance of UGM (Bilodeau et al., 2011; Cerni et al., 2012; Werkmeister et al., 2004). In this study, the test specimen was subjected to 13,000 loading cycles with a constant cyclic stress and confining pressure. The reason for selecting this number of loading cycles is to examine the early permanent deformation behaviour of UGM in a practical method compatible with laboratory testing constrains. The permanent deformation behaviour of UGM can be classified according to the shakedown concept based on this testing period (Bilodeau et al., 2011; Cerni et al., 2012; European Committee for Standardization, 2004; Werkmeister et al., 2004).

Each loading cycle consisted of a load pulse with a loading duration of 0.1 sec and a rest period of 0.9 sec. The cyclic stress for permanent deformation tests ranged from 106.5 kPa to 110.1 kPa; and the confining pressure ranged from 37.3 kPa to 40.0 kPa. These stresses represent the average stress levels in a base course layer in a typical pavement

structure (Bilodeau et al., 2011; Harrigan and Witczak, 2004). Analysis and results of permanent deformation tests for UGM are discussed in chapter 7.

3.4 Permeability Test for UGM

3.4.1 Test Setup and Specimen Preparation

A single ring rigid-wall permeameter was used to measure the hydraulic conductivity (permeability) of UGM. The procedures of ASTM D5856 "Standard Test Method for Measurement of Hydraulic Conductivity of Porous Material Using a Rigid-Wall, Compaction-Mold Permeameter" was followed (ASTM 2007). The dimensions of the permeameter are 101.6 mm in diameter and 115.9 mm in height. Test specimen was compacted in three layers using a vibration compactor, Figure 3.8, on the permeameter mold at the OMC and with a minimum relative density of 98%. The total length of the compacted specimen slightly exceeded the length of the permeameter ring to allow trimming of the top of the specimen to a height uniform with the top of the compaction ring.

Saturation of the specimen was accomplished initially by connecting the effluent port of the permeameter to a vacuum pump. After approximately 5 minutes, the effluent port was slowly closed and the influent valve was then slowly opened allowing the negative pressure within the cell to be replaced with water. This procedure was repeated with increasing vacuum pressures until no air was drawn from the permeameter. After vacuum saturation, the specimen was connected to a constant water head to saturate overnight before testing.

The test setup consisted of a constant water level tank, a single ring rigid-wall permeameter, and a beaker to measure the water flow. The hydraulic head is measured as the difference in elevation between the inlet water level (top of the constant head tank) to the outlet water level (end of effluent tube). Figure 3.11 shows the permeability test setup.

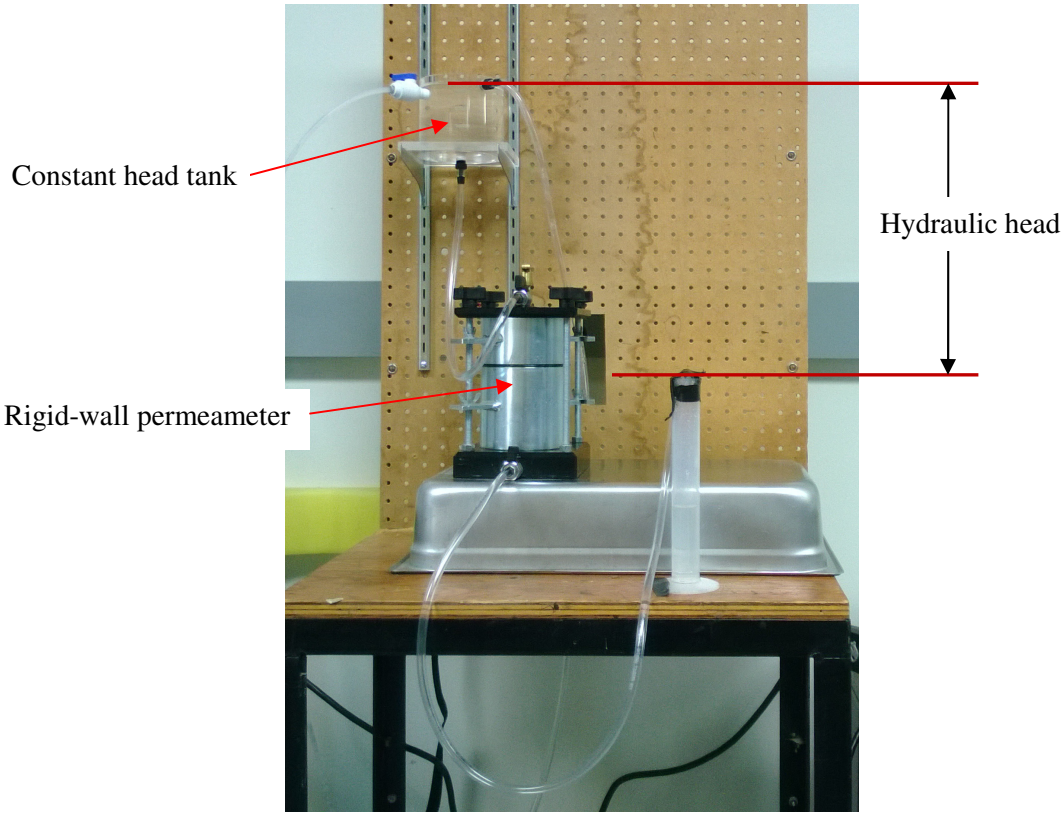

FIGURE 3.11: Permeability Test Setup

The permeameter was set up without a specimen, however all porous stones and filter papers used during the actual test were installed. The system was run at different hydraulic heads and the rate of flow was measured. The measured rate of flow for the empty permeameter, at different hydraulic heads, was more than 10 times the rate of flow

when a specimen is compacted inside the permeameter. Therefore, the head losses in the test setup did not cause a significant effect on the measured hydraulic conductivity (ASTM D5856, 2007).

3.4.2 Validation of Darcy's Law

The governing equation of the constant head permeability test is Darcy's Law. According to Darcy's Law, the velocity of water flow through the specimen is directly proportional to the hydraulic gradient (ASTM D5856, 2007). Darcy's law is valid when laminar flow condition exist which must be satisfied to ensure the validity of the test results. The validity of Darcy's law can be confirmed by measuring the hydraulic conductivity of UGM at various hydraulic gradients and observing whether a linear relationship exists between the hydraulic gradient and the velocity of water flow. Accordingly, the hydraulic conductivity of a specimen should not change with any change in the hydraulic head.

Hydraulic conductivity tests were conducted on a typical UGM specimen, representing an average gradation of the tested materials, over a range of hydraulic gradients to determine the validity of Darcy's Law. The hydraulic gradient ranged from 1.3 to 3.3. Figure 3.12 shows the relationship between hydraulic gradient and the velocity of water flow. A linear relationship existed between the tested range of hydraulic gradients and the velocity of water flow within the specimen with a coefficient of determination (R^2) equals 0.98, as shown in Figure 3.12 . Therefore, Darcy's Law was valid for UGM with hydraulic gradients ranging from 1.3 to 3.3. At the high end of the tested range of hydraulic gradients, there was no significant deviation of the velocity of flow from the

observed linear relationship, therefore the linear relationship can be valid at higher gradients than the tested range.

ASTM D5856 recommends different ranges of hydraulic gradient to be used for permeability test based on the observed hydraulic conductivity. Results of pilot tests indicated that the observed hydraulic conductivity for UGM should be ranging from 1×10^{-7} m/s to 1×10^{-5} m/s. According to ASTM D5856, a hydraulic gradient ranging from 2 to 5 shall be used for testing the permeability of UGM.

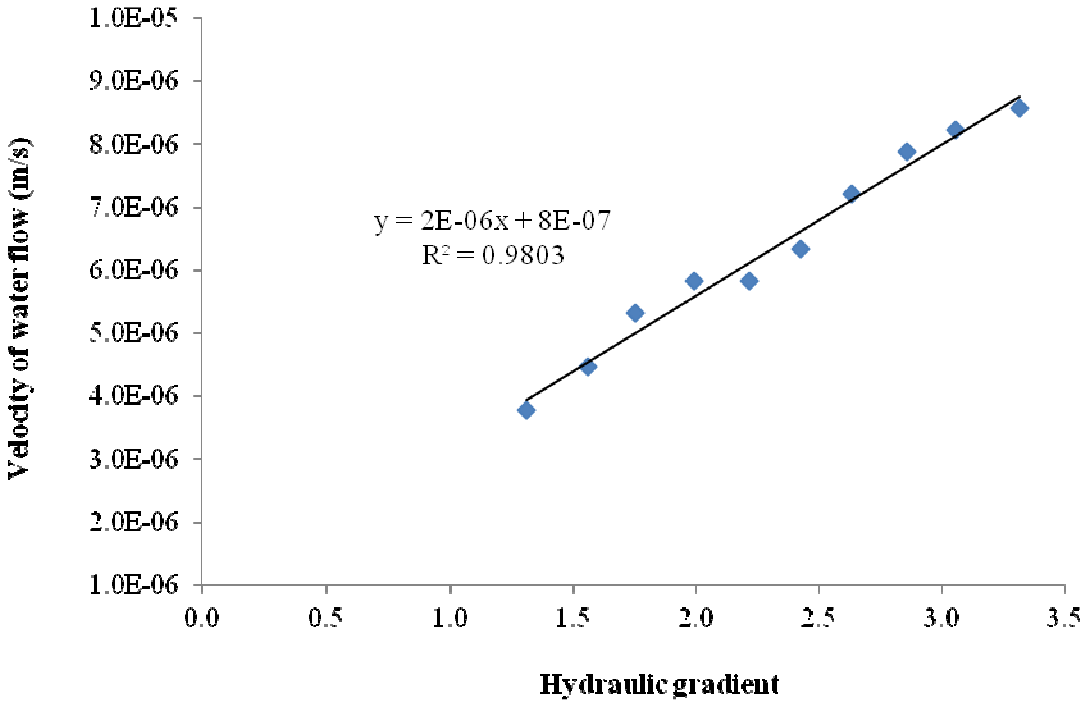

FIGURE 3.12: Relationship between Hydraulic Gradient and Velocity of Water Flow

4 Resilient Behaviour of Subgrade Soils

4.1 Analysis of Resilient Modulus Test Data

For each specimen, data from the 16 loading sequences were fitted to the "Universal Constitutive Model", Equation 2.4, according to NCHRP 1-28A test protocol (Harrigan and Witczak 2004). For the LTPP data, K_6 was found to be zero for more than 50% of the M_R tests and setting K_6 and K_7 equal to zero and one, respectively, did not have a significant effect on the regression statistics for fine-grained subgrade soils (Yau and Von Quintus 2002). For Pavement ME, Equation 2.4 is used in the design procedure with assigned values of zero for K_6 and one for K_7 (NCHRP 2004). Therefore, K_6 and K_7 were assigned values of zero and one, respectively, and Equation 2.4 became as follows:

$$M_R = K_1 P_a \left[\frac{\theta}{P_a}\right]^{K_2} \left[\frac{\tau_{oct}}{P_a} + 1\right]^{K_3} \quad \textbf{(4.1)}$$

Where:

M_R= resilient modulus, MPa

θ = bulk stress, kPa

$= \sigma_1 + \sigma_2 + \sigma_3$

τ_{oct} = octahedral shear stress, kPa

$$= \frac{1}{3}\sqrt{(\sigma_1 - \sigma_2)^2 + (\sigma_1 - \sigma_3)^2 + (\sigma_2 - \sigma_3)^2}$$

σ_1, σ_2, and σ_3 = principal stresses, kPa (for triaxial test, $\sigma_2 = \sigma_3$ = confining pressure)

K_1, K_2, and K_3 = regression constants

P_a = atmospheric pressure at sea level = 101.35 kPa

Nonlinear regression techniques were utilized to evaluate the values of the regression constants K_1, K_2, and K_3 for each specimen. The values of K_1, K_2, and K_3 of the three replicated were averaged. Replicates with variation higher than 20% were excluded from the analysis. Equation 4.1 and the evaluated regression constants (K_1, K_2, and K_3) can be used to calculate the subgrade resilient modulus at any stress state. M_R test protocol recommends the use of Equation 4.1 to calculate and report M_R of subgrade soils for confining pressure (σ_3) = 14 kPa and cyclic stress (σ_1- σ_3) = 41 kPa (Harrigan and Witczak 2004).

4.2 Resilient Modulus for High Plastic Clay Soil Samples

The collected soil samples from PTH 59 and PTH 75 were classified as high plastic clay soil. PTH 59 soil sample contained 83% clay and had a plasticity index (PI) of 56. PTH 75 soil sample contained 51% clay and had a plasticity index of 27. According to AASHTO classification system, PTH 59 and PTH 75 soil samples belonged to group A-7-6 with a group index (GI) of 20 and 17, respectively.

Tables 4.1 shows the values of M_R and the regression constants (K_1, K_2, and K_3) for PTH 59 and PTH 75 soil samples. Figure 4.2 shows the values of M_R for PTH 59 and PTH 75 soil samples versus specimen moisture content. Although it is known that the decline is likely not linear, a straight line trend is shown to illustrate the sensitivity of M_R

to moisture variation. M_R value for the two sample showed medium to high sensitivity to moisture content variation. For PTH 59 soil sample, M_R decreased from 63.9 MPa to 31.5 MPa (-50.7%) due to increasing the moisture content from 28.0% to 32.6%. For PTH 75 soil sample, M_R decreased from 108.0 MPa to 34.8 MPa (-67.8%) due to increasing the moisture content from 18.8% to 23.8%. The decrease in M_R with the increase of moisture content can be attributed to the reduction of suction pressure as the specimen approaches saturation level.

TABLE 4.1: Values of M_R and Regression Constants for High Plastic Clay Soil Samples

Sample ID	MC (%)	γ_{dry} (kg/m^3)	K_1	K_2	K_3	M_R (MPa)	STD (MPa)	CV (%)
PTH 59	28.0	1397	0.971	0.140	-2.313	63.9	0.2	0.3
	28.3	1452	1.014	0.091	-2.755	62.4	10.0	16.0
	31.2	1434	0.725	0.094	-3.415	39.7	3.1	7.9
	32.6	1409	0.588	0.094	-3.546	31.5	1.3	4.2
PTH 75	18.8	1593	1.558	0.250	-1.889	108.0	2.1	1.9
	20.4	1618	1.336	0.234	-2.842	78.7	6.4	8.1
	23.0	1584	0.788	0.271	-3.358	42.1	4.7	11.4
	23.8	1587	0.694	0.239	-3.760	34.8	2.5	7.3

4.3 Resilient Modulus for Sandy Clay Soil Samples

The collected soil samples from PTH 16 and PTH 1-West were classified as sandy clay soils. PTH 16 soil sample contained 30% clay and has a plasticity index of 15.

PTH 1-West soil sample contained 31% clay and has a plasticity index of 17. According to AASHTO classification system, PTH 16 and PTH 1-West soil samples belonged to group A-6 with a GI of 7 and 8, respectively.

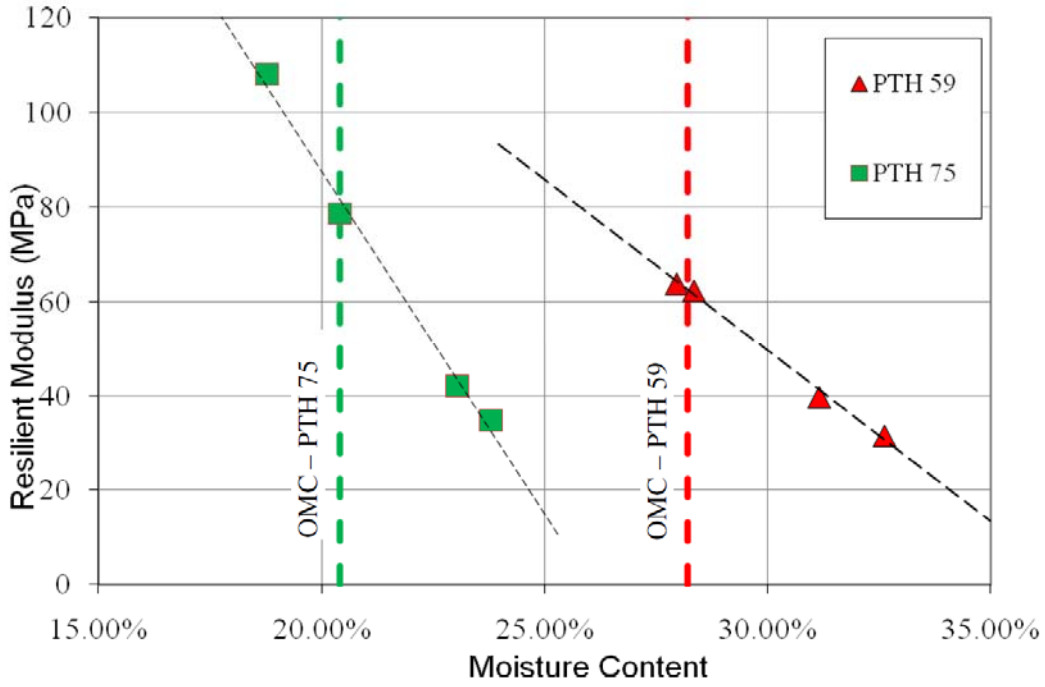

FIGURE 4.1: M_R versus Moisture Content for High Plastic Clay Soil Samples

Tables 4.2 shows the values of M_R and the regression constants (K_1, K_2, and K_3) for PTH 16 and PTH 1-West soil samples. The total permanent strain exceeded 5% for specimens with moisture contents of 16.9% for PTH 16 and 15.2% for PTH 1-West; and the test was stopped before completing the sixteen loading sequences.

Figure 4.2 shows the values of M_R for PTH 16 and PTH 1-West soil samples versus specimen moisture content. M_R value for the two sample showed high sensitivity to

moisture content variation. For PTH 16 soil sample, M_R decreased from 101.9 MPa to 15.4 MPa (-84.9%) due to increasing the moisture content from 12.4% to 16.9%. For PTH 1-West soil sample, M_R decreased from 105.4 MPa to 20.9 MPa (-80.2%) due to increasing the moisture content from 10.6% to 15.2%. The decrease in M_R with the increase of moisture content can be attributed to the reduction of suction pressure as the specimen approaches saturation level.

TABLE 4.2: Values of M_R and Regression Constants for Sandy Clay Soil Samples

Sample ID	MC (%)	γ_{dry} (kg/m^3)	K_1	K_2	K_3	M_R (MPa)	STD (MPa)	CV (%)
	12.4	1790	1.650	0.387	-2.396	101.9	0.5	0.5
PTH 16	13.6	1845	1.081	0.368	-2.730	63.2	3.9	6.1
	15.4	1819	0.581	0.635	-2.719	32.3	3.9	12.1
	16.9	1792	0.305	0.696	-3.187	15.4 [a]	1.0	6.3
PTH 1-West	10.6	1787	1.521	0.405	-1.712	105.4	15.2	14.4
	12.5	1859	1.315	0.426	-2.955	73.1	8.6	11.7
	14.0	1836	0.811	0.491	-3.086	43.5	4.9	11.2
	15.2	1849	0.466	0.670	-3.907	20.9 [a]	0.9	4.1

[a] Permanent strain exceeded 5%

4.4 Resilient Modulus for Sandy Silt/Silty Sand Soil Samples

The collected soil samples from PTH 34 and PTH 1-Portage were classified as sandy silt and silty sand soils, respectively. PTH 34 soil sample contained 46% silt and 47% sand. PTH1-Portage contained 23% silt and 66% sand. According to AASHTO classification

system, PTH 34 soil sample belonged to group A-4 with a GI of 4, while PTH1-Portage soil sample belonged to group A-2-4 with a GI of zero.

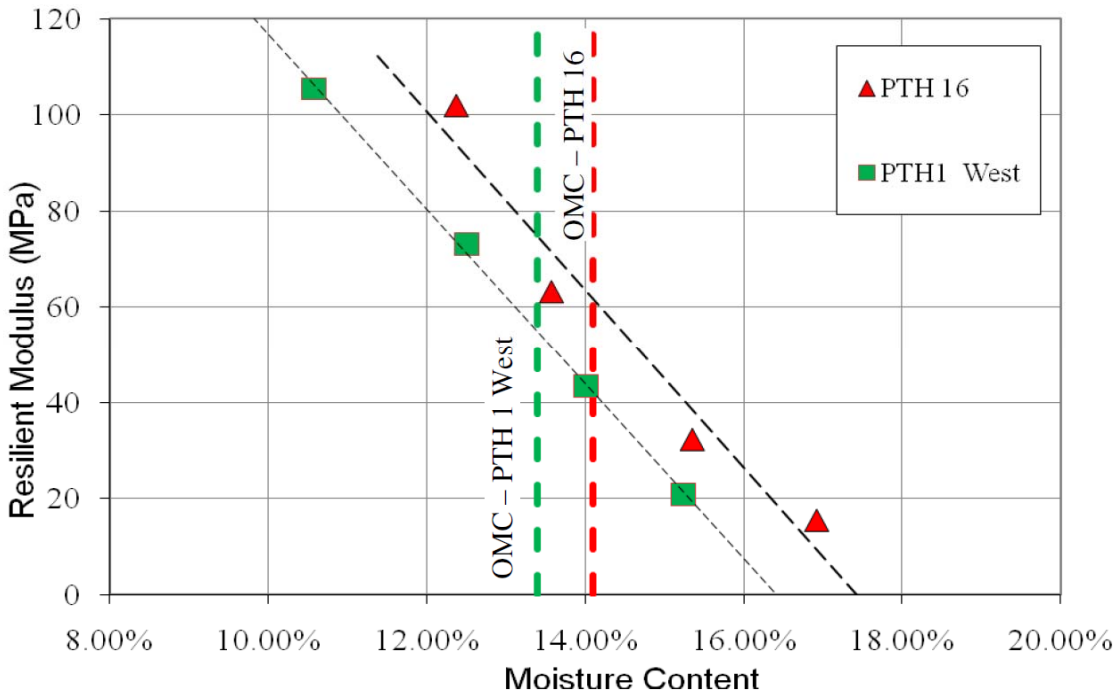

FIGURE 4.2: M_R versus Moisture Content for Sandy Clay Soil Samples

Tables 4.3 shows the values of M_R and the regression constants (K_1, K_2, and K_3) for PTH 34 and PTH 1-Portage soil samples. The total permanent strain exceeded 5% for specimens with moisture contents of 14.9% for PTH 34 and 14.0% for PTH 1- Portage; and the test was stopped before completing the sixteen loading sequences.

Figure 4.2 shows the values of M_R for PTH 34 and PTH 1-Portage soil samples versus specimen moisture content. M_R value for the two sample showed low sensitivity to moisture content variation. For PTH 34 soil sample, M_R decreased from 66.6 MPa to 56.9

MPa (-14.6%) due to increasing the moisture content from 8.5% to 14.9%. For PTH 1-Portage soil sample, M_R decreased from 58.4 MPa to 39.5 MPa (-32.4%) due to increasing the moisture content from 7.7% to 14.0%. The low sensitivity of M_R values to moisture variation can be attributed to the lower suction pressure in silty sand/sandy silty soils than high plastic clay/sandy clay soils at comparable saturation levels.

TABLE 4.3: Values of M_R and Regression Constants for Silty Sand/Sandy Silt Soil Samples

Sample ID	MC (%)	γ_{dry} (kg/m^3)	K_1	K_2	K_3	M_R (MPa)	STD (%)	CV (%)
PTH 34	8.5	1757	1.140	1.036	-1.965	66.6	2.0	2.9
	10.9	1825	1.0823	1.074	-1.970	62.8	4.9	7.8
	12.8	1851	1.122	0.942	-2.062	65.7	3.4	5.1
	14.9	1818	1.037	1.020	-2.346	56.9 [a]	7.7	13.4
PTH 1-Portage	7.7	1773	0.929	0.913	-1.689	58.4	2.0	3.4
	9.5	1834	0.834	0.997	-1.657	51.9	0.9	1.7
	12.4	1837	0.817	0.979	-1.800	49.7	1.7	3.5
	14.0	1799	0.672	1.048	-1.925	39.5 [a]	1.5	3.7

[a] Permanent strain exceeded 5%

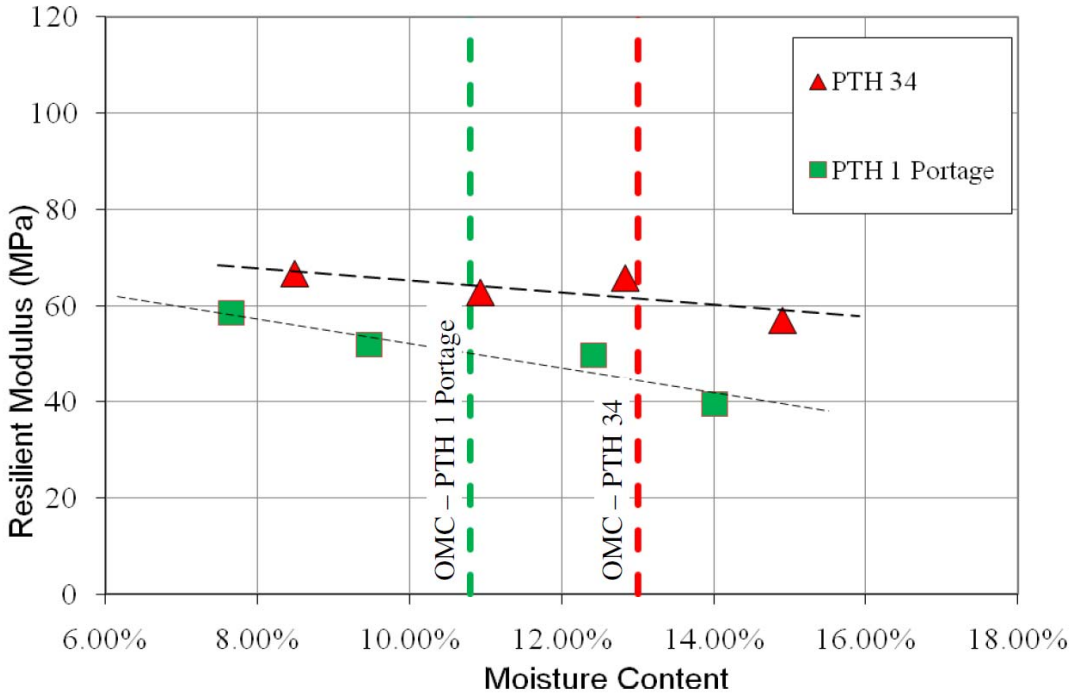

FIGURE 4.3: M_R versus Moisture Content for Silty Sand/Sandy Silt Soil Samples

4.5 Comparison between Resilient Modulus for Manitoba Soils and Values Reported in the Literature

Table 4.4 provides a comparison between M_R for Manitoba soils and M_R values reported in the literature for Louisiana and Mississippi soils (Nazzal et al. 2008, George 2004). M_R values for subgrade soils in Louisiana were measured at different moisture content levels (above, at, and below the optimum moisture content). M_R values for subgrade soils in Mississippi were measured at the optimum moisture content only. From Table 4.4, it is noted that M_R values for subgrade soils in Manitoba are comparable to M_R values for Louisiana and Mississippi soils. This agreement between M_R values in Manitoba and other values reported in the literature provides more confidence in the test results of this study.

TABLE 4.4: Comparison between M_R Values for Manitoba Soils and M_R Values Reported in the Literature for Louisiana and Mississippi Soils (Nazzal et al. 2008, George 2004)

Soil Type	Values and Ranges of Subgrade M_R (MPa)		
	Manitoba	Louisiana	Mississippi [a]
A-2-4	39.5 – 58.4	N/A [b]	81.5
A-4	56.9 – 66.6	36.8 – 76.3	49.6 – 103.5
A-6	15.4 – 105.4	46.3 – 87.0	77.3 – 98.6
A-7-6	31.5 – 108.0	24.6 – 80.4	N/A [b]

[a] M_R values for Mississippi soils were measured at the optimum moisture content only

[b] Data are not available

4.6 Database for Typical Values of Resilient Modulus for Manitoba Subgrade Soils

Subgrade M_R is the primary design input parameter for Pavement ME. For Level 3 design inputs, Pavement ME provides and recommends the use of default values for subgrade M_R based on AASHTO soil class. These default M_R values were developed based on testing a wide range of soil samples with different characteristics but still have the same AASHTO soil class. The reliability of Level 3 design inputs can be improved by transportation agencies through developing a database for M_R values for typical subgrade soils available in their regions. This database can be used to replace Pavement ME default values for Level 3 design inputs. This database shall be regularly updated to include the results of new M_R tests.

Results of the M_R tests conducted in this study can be used to establish a database for typical subgrade soils in Manitoba. Table 4.5 shows the typical M_R values for the fine-grained soil samples tested in this study. M_R values were calculated using equation 4.1 for confining pressure of 14 kPa and cyclic stress of 41 kPa which represent the stress state that subgrade soil encounters under traffic loading (Harrigan and Witczak 2004). Table 4.5 shows the range and mean of default values of M_R recommended by Pavement ME, for Level 3 design inputs, for each soil type (NCHRP 2004). It shall be noted that the default M_R values recommended by Pavement ME represent the M_R values at optimum moisture content and maximum dry density.

Table 4.5 shows that there is a large difference between M_R values obtained from laboratory testing in this study and the default values recommended by Pavement ME for A-2-4, A-4, and A-6 soils. The difference between laboratory M_R and the mean value of M_R recommend by Pavement ME ranges from 113% to 340%. For A-7-6 soils, the laboratory M_R values are comparable to the recommend values by Pavement ME. The difference between the laboratory M_R values for A-7-6 soils and the mean default value of M_R recommend by Pavement ME ranges from 12% to 30%. Similar findings were reported in the literature (Nazzal et al. 2008).

TABLE 4.5: Typical M_R Values for High Plastic Clay, Sandy Clay, Sandy Silt/Silty Sand Soils in Manitoba

Sample Location	AASHTO Classification	OMC (%)	MC (%)	Tested M_R (MPa)	Pavement ME M_R (MPa) [a]		Difference (%)
					Range	Mean	
PTH 1-Poratage	A-2-4, GI = 0 Silty Sand	10.8	7.7	58.4	192.9 - 258.4	220.5	340
			9.5	51.9			
			12.4	49.7			
			14.0	39.5 [b]			
PTH 34	A-4, GI = 4 Sandy Silt	13.0	8.5	66.6	148.1 – 199.8	165.4	145
			10.9	62.8			
			12.6	67.5			
			14.9	56.9 [b]			
PTH 16	A-6, GI = 7 Sandy Clay	14.1	12.4	101.9	93.0 – 165.4	117.1	115
			13.6	63.2			
			15.4	32.3			
			16.9	15.4 [b]			
PTH 1-West	A-6, GI = 8 Sandy Clay	13.4	10.6	105.4	93.0 – 165.4	117.1	113
			12.5	73.1			
			14.0	43.5			
			15.2	20.9 [b]			
PTH 75	A-7-6, GI = 17 High Plastic Clay	20.4	18.8	108.0	34.5 – 93.0	55.1	30
			20.4	78.7			
			23.0	42.1			
			23.8	34.8			
PTH 59	A-7-6, GI = 20 High Plastic Clay	28.2	28.0	63.9	34.5 – 93.0	55.1	12
			28.3	62.4			
			31.2	39.7			
			32.6	31.5			

[a] Pavement ME values represent M_R at optimum moisture content and maximum dry density

[b] Permanent strain exceeded 5%

5 Resilient Modulus Prediction Models for Fine-Grained Subgrade Soils

5.1 Introduction

The design thickness of a pavement structure and its predicted performance are highly dependent on subgrade modulus. Characterization of subgrade resilient modulus involves conducting advanced repeated loading triaxial testing that requires special equipment and technical experience that are not available in many soil laboratories. For Level 2 design inputs, Pavement ME recommends correlation models to estimate subgrade M_R from basic soil properties (e.g. gradation, unconfined compressive strength, California bearing ratio,...). These correlation models are developed based on data for a wide range of soil/material types which increases the associated error with M_R prediction.

The value of M_R depends on the stress state and the physical properties (gradation, moisture content, compaction characteristics, plasticity) of subgrade soil (Soliman and Shalaby 2010, 2014). These physical properties are dry density, moisture content, and gradation. Several relationships have been proposed for determining M_R for subgrade soils as a function of stress state and their physical properties (Dai and Zollars 2002; Santha 1994; Von Quintus and Killingsworth 1998; Yau and Von Quintus 2002). A potential benefit of estimating M_R for subgrade soil from its physical properties is that seasonal variations in resilient modulus can be estimated from seasonal changes in the

physical properties. Seasonal variations are critical for determining the design M_R for a particular project.

Research studies showed that current prediction models and default values in Pavement ME cannot be generalized to predict the response of any subgrade soil (Nazzal et al. 2008, George 2004). Therefore, transportation agencies should calibrate their own relationships based on soil types in their region. The selected value for resilient modulus of subgrade soil can significantly affect pavement design (Guan et al. 1998). Calibration of prediction models for subgrade M_R leads to more reliable information about the dynamic response of soil with less testing effort and expenses.

5.2 Comparing the Measured Resilient Modulus to the LTPP Prediction Models

Figures 5.1 to 5.3 compare the measured M_R to the predicted M_R using LTPP prediction models for the three types of soil evaluated in this study using all the test data (Yau and Von Quintus 2002). Equations 2.20 to 2.25 show the LTPP prediction models of K_1, K_2 and K_3 for silt and clay soils. Equations 2.20 to 2.22 were used to predict M_R for silty sand/sandy silt soils, while Equations 2.23 to 2.25 were used to predict M_R for high plastic clay and sandy clay soils.

Figure 5.3 shows that the LTPP model underestimated M_R for silty sand/sandy silt soils, while Figure 5.2 shows that LTTP model overestimated M_R for most of the data points. The Root Mean Square Error (RMSE) was 27.3 MPa for high plastic clay, 44.7 MPa for sandy clay, and 52.9 MPa for silty sand/sandy silt soils. The deviation of the predicted

M_R values from the measured values can be reduced by developing local prediction models. The local prediction models will improve the reliability of Level 2 design inputs.

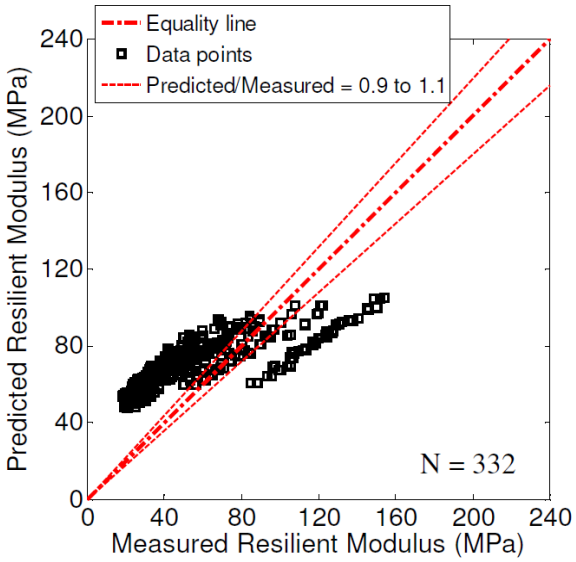

FIGURE 5.1: Measured and Predicted M_R Using LTPP Prediction Models for High Plastic Clay

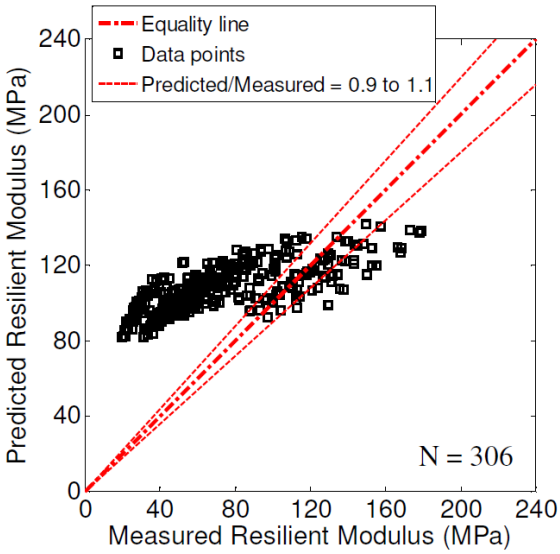

FIGURE 5.2: Measured and Predicted M_R Using LTPP Prediction Models for Sandy Clay

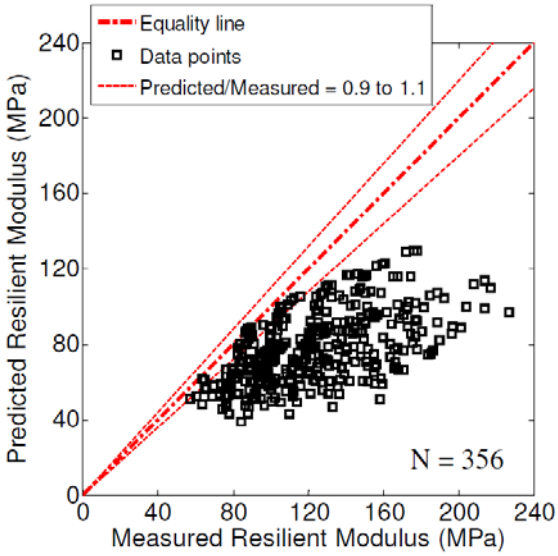

FIGURE 5.3: Measured and Predicted MR Using LTPP Prediction Models for Silty Sand/Sandy Silt

5.3 Effect of Physical Properties on Resilient Modulus

A statistical analysis was conducted to develop models that predict resilient modulus from soil physical properties. Before starting the statistical analysis, anomalies and outliers were identified and removed from M_R test data. An anomaly was identified to be the test data of any specimen that has a coefficient of determination less that 0.90 when fitted to the universal constitutive equation (Equation 4.1). A coefficient of determination less than 0.90 can be due to errors in the test and/or test specimen disturbance (NCHRP 2004). Three specimens were identified as anomalies and were excluded from the analysis.

Six fine-grained soil samples, representing three types of soil, were evaluated in this study. The variability of the gradation parameters (% passing sieve No. 200, % silt, and

% clay) in the M_R test data was not high enough to use these parameters individually as prediction variables. Several combined variables were developed to represent the combined effect of gradation parameters and the deviation of specimen moisture content from the optimum moisture content. The combined variables were developed based on the literature and the logical influence of the gradation and moisture content parameters on regression constants (K_1, K_2, K_3). Based on preliminary correlation analysis, only five variables were proposed as predictor variables that can be used in the prediction models. Liquidity index (LI) was included as a predictor variable for high plastic clay and sandy clay soils. Although its logical influence on sandy clay and silty sand/sandy silt soils, the % sand was found to be not a significant parameter for sandy clay and silty sand/sandy silt soils which can be due to its limited variability within the tested soils. Results of initial statistical analysis showed that developing three prediction models for the three soil types evaluated in this study is better than developing one model to fit M_R test data for all soil samples.

Tables 5.1 to 5.3 show the correlation coefficients between regression constants (K_1, K_2, K_3) and the proposed variables for the three soil types evaluated in this study. Tables 5.1 to 5.3 show also the probability associated with the t-test (p-value) which represents the significance of the calculated correlation coefficients. A p-value less than 0.05 indicates that the correlation coefficient is significant at a confidence level higher than 95%. For each regression constant, the predictor variable with the highest correlation coefficient and lowest p-values was selected to be a predictor variable for that regression constant. The selected predictor variables are shaded in Tables 5.1 to 5.3.

TABLE 5.1: Correlation between Regression Constants (K_1, K_2, K_3) and the Predictor Variables for High Plastic Clay Soils

Variable	K_1		K_2		K_3	
	Correlation Coefficient	p-value	Correlation Coefficient	p-value	Correlation Coefficient	p-value
$MC - OMC$	-0.911	$< 10^{-4}$	-0.220	0.338	-0.938	$< 10^{-4}$
$LI = \frac{MC - PL}{PI}$	-0.979	$< 10^{-4}$	-0.385	0.085	-0.882	$< 10^{-4}$
$\frac{MC \times \%\, Clay}{OMC}$	-0.617	0.003	-0.904	$< 10^{-4}$	-0.350	0.120
$\frac{MC \times \%\, P200}{OMC}$	-0.892	$< 10^{-4}$	-0.032	0.890	-0.950	$< 10^{-4}$
$\frac{MC}{\%\, Silt \times OMC}$	-0.472	0.031	-0.936	$< 10^{-4}$	-0.182	0.429

MC = specimen moisture content, OMC = optimum moisture content, PL = plastic limit, PI = plasticity index, % Clay = percentage of clay, % Silt = percentage of silt, and % P200 = percentage of passing sieve No. 200

5.4 Developing Local Resilient Modulus Prediction Models

Multiple regression analysis was performed on M_R test data for each type of soil. The regression analysis was performed using 84% of the test data. The remaining 16% of the test data was used to validate the prediction models. Equations 5.1 to 5.9 show the prediction models for K_1, K_2, and K_3 for each soil type. M_R for a given soil type can be estimated at any stress state by incorporating these prediction model into Equation 4.1. The overall coefficient of determination for the prediction models was 0.98 for high plastic clay and 0.94 for sandy clay and silty sand/sandy silt soils. Table 5.4 shows the 95% confidence intervals for regression constants of K_1, K_2, and K_3 prediction models.

The research provides adaptable guidelines for predicting the resilient modulus of subgrade soils. The prediction models were developed using limited data set. Ideally, the models should be validated using a wider data set according to the criteria presented in the study.

TABLE 5.2: Correlation between Regression Constants (K_1, K_2, K_3) and the Predictor Variables for Sandy Clay Soils

Variable	K_1		K_2		K_3	
	Correlation Coefficient	p-value	Correlation Coefficient	p-value	Correlation Coefficient	p-value
$MC - OMC$	-0.959	$< 10^{-4}$	0.873	$< 10^{-4}$	-0.730	$< 10^{-4}$
$LI = \frac{MC - PL}{PI}$	-0.960	$< 10^{-4}$	0.885	$< 10^{-4}$	-0.746	$< 10^{-4}$
$\frac{MC \times \%\, Clay}{OMC}$	-0.953	$< 10^{-4}$	0.866	$< 10^{-4}$	-0.785	$< 10^{-4}$
$\frac{MC \times \%\, P200}{OMC}$	-0.957	$< 10^{-4}$	0.868	$< 10^{-4}$	-0.740	$< 10^{-4}$
$\frac{MC}{\%\, Silt \times OMC}$	-0.952	$< 10^{-4}$	0.866	$< 10^{-4}$	-0.786	$< 10^{-4}$

MC = specimen moisture content, OMC = optimum moisture content, PL = plastic limit, PI = plasticity index, % Clay = percentage of clay, % Silt = percentage of silt, and % P200 = percentage of passing sieve No. 200

<u>High Plastic Clay Soils</u>

$$K_1 = 1.0039 - 4.9992\, LI \quad \textbf{(5.1)}$$

$$K_2 = 0.2885 - 2.2575 \frac{MC}{\%\, Silt \times OMC} \quad \textbf{(5.2)}$$

$$K_3 = 4.0740 - 0.0690 \frac{MC \times \%P200}{OMC} \quad \textbf{(5.3)}$$

TABLE 5.3: Correlation between Regression Constants (K_1, K_2, K_3) and the Predictor Variables for Silty Sand/Sandy Silt Soils

Variable	K_1		K_2		K_3	
	Correlation Coefficient	p-value	Correlation Coefficient	p-value	Correlation Coefficient	p-value
$MC - OMC$	-0.582	0.004	0.111	0.613	-0.307	0.154
$\frac{MC \times \%Clay}{OMC}$	-0.890	$< 10^{-4}$	-0.007	0.975	0.154	0.484
$\frac{MC \times \%P200}{OMC}$	0.297	0.169	0.317	0.141	-0.836	$< 10^{-4}$
$\frac{MC}{\%Silt \times OMC}$	-0.944	$< 10^{-4}$	-0.080	0.717	0.344	0.108

MC = specimen moisture content, OMC = optimum moisture content, PL = plastic limit, PI = plasticity index, % Clay = percentage of clay, % Silt = percentage of silt, and % P200 = percentage of passing sieve No. 200

Sandy Clay Soils

$$K_1 = 0.5364 - 4.2647\,LI \quad \textbf{(5.4)}$$

$$K_2 = 0.6059 + 1.1482\,LI \quad \textbf{(5.5)}$$

$$K_3 = 0.7567 - 105.35 \frac{MC}{\%Silt \times OMC} \quad \textbf{(5.6)}$$

Silty Sand/Sandy Silt Soils

$$K_1 = 1.2999 - 10.766 \frac{MC}{\%Silt \times OMC} \quad \textbf{(5.7)}$$

$$K_2 = 0.9184 + 0.0020 \frac{MC \times \%P200}{OMC} \quad \textbf{(5.8)}$$

$$K_3 = -1.2209 - 0.0176\frac{MC \times \%P200}{OMC} \quad \textbf{(5.9)}$$

Where:

LI = liquidity index,

MC = specimen moisture content, %

OMC = optimum moisture content, %

% Silt = percentage of silt in the soil sample, %

% Clay = percentage of clay in the soil sample, %

% P200 = percentage passing sieve No. 200, %

TABLE 5.4: Confidence Intervals for Regression Constants of K_1, K_2, and K_3 Prediction Models

Soil Type	95% Confidence Intervals for Regression Constants					
	K_1 Model		K_2 Model		K_3 Model	
	Interceptor*	predictor variable**	Interceptor	predictor variable	Interceptor	predictor variable
High plastic clay	0.9711 to 1.0368	-5.4858 to -4.5125	0.2643 to 0.3127	-2.6840 to -1.8309	2.9260 to 5.2220	-0.0802 to -0.0579
Sandy Clay	0.4516 to 0.6217	-4.8603 to -3.6692	0.5647 to 0.6471	0.8589 to 1.4375	-0.6363 to 2.1498	-145.62 to -65.09
Silty Sand/ Sandy Silt	1.2412 to 1.3586	-12.4270 to -9.1043	0.8178 to 1.0190	-0.0004 to 0.0044	-1.4245 to -1.0172	-0.0224 to -0.0126

* The constant component in Equations 5.1 to 5.9

** The multiplier for the independent variables in Equations 5.1 to 5.9

Figures 5.4 to 5.6 compare the measured M_R to the predicted M_R using Equations 5.1 to 5.9 for the three types of soil evaluated in this study using the validation data set. The RMSE was 4.3 MPa for high plastic clay, 9.3 MPa for sandy clay, and 8.2 MPa for silty sand/sandy silt soils. Figures 5.4 to 5.6 show that there was a good agreement between measured and predicted M_R values. For high plastic clay and sandy clay (Figures 5.4 and 5.5), the data points were less scattered around the equality line at low M_R values. This less scatter of the data points can be due to the better contact between ends of the test specimen and loading plates at higher cyclic stresses and moisture contents.

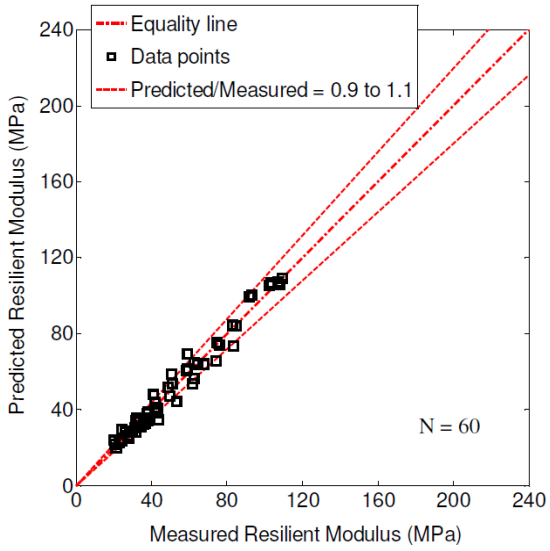

FIGURE 5.4: Measured and Predicted M_R Using the Proposed Models for High Plastic Clay

5.5 Effect of Degree of Saturation on Resilient Modulus

Figures 5.7 to 5.9 show the values of M_R versus specimen degree of saturation for high plastic clay, sandy clay, and silty sand/sandy silt soils. Although it is known that the decline is likely not linear, a straight line trend is shown to illustrate the sensitivity of M_R to degree of saturation. M_R values for High plastic clay and sandy clay soils showed medium to high sensitivity to degree of saturation variation, while M_R values for silty sand/sandy silt soils showed low sensitivity to degree of saturation variation.

For unsaturated soils, the soil-water characterization curve (SWCC) is used to define the relationship between degree of saturation (or water content) and matric suction for soil (Fredlund and Xing 1994). The effect of degree of saturation and matric suction on resilient modulus depends on the type of soil. For a given degree of saturation higher than zero, the matric suction for clayey soils is much higher than the matric suctions for silty and sandy soils (Fredlund 2002). The SWCC for the three soil types was not experimentally evaluated at this stage of the research. However, the effect of matric suction was incorporated implicitly by including moisture content, optimum moisture content, and liquidity index in the resilient modulus models.

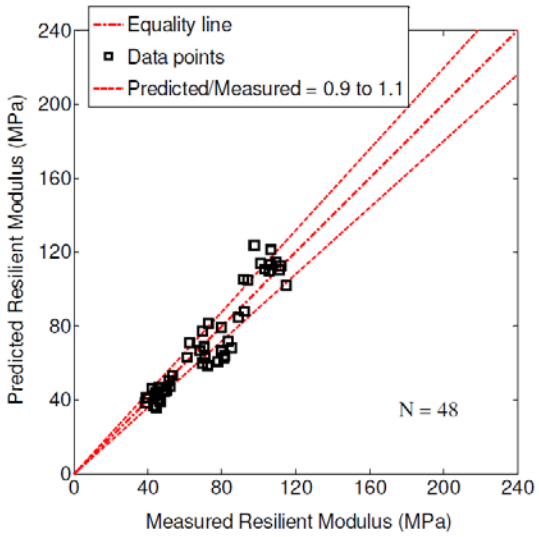

FIGURE 5.5: Measured and Predicted M_R Using the Proposed Models for Sandy Clay

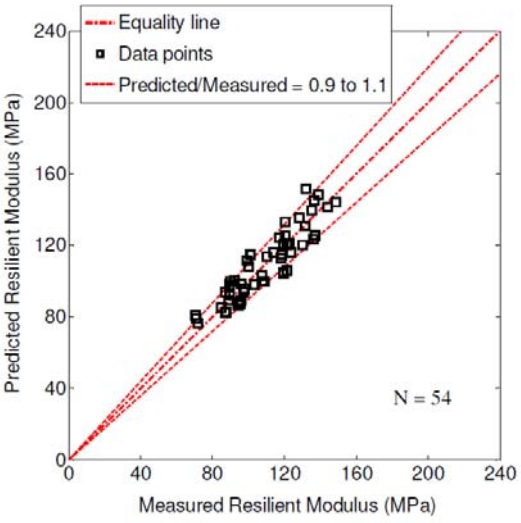

FIGURE 5.6: Measured and Predicted M_R Using the Proposed Models for Silty Sand/Sandy Silt

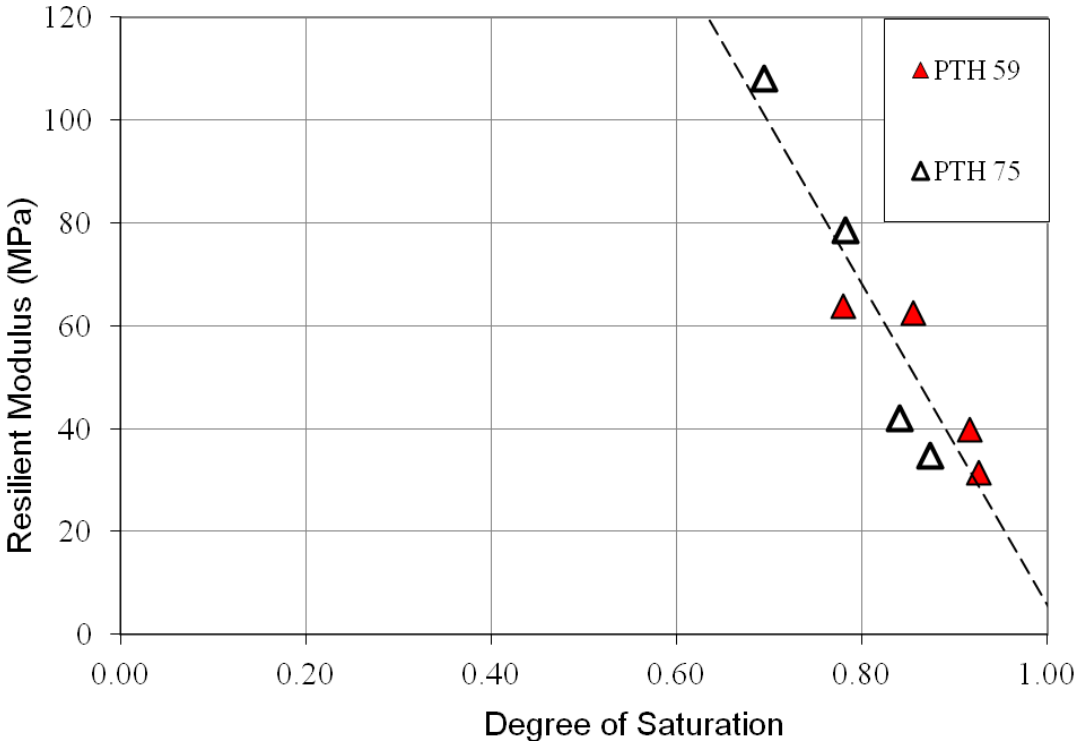

FIGURE 5.7: Measured M_R versus Specimen Degree of Saturation for High Plastic Clay

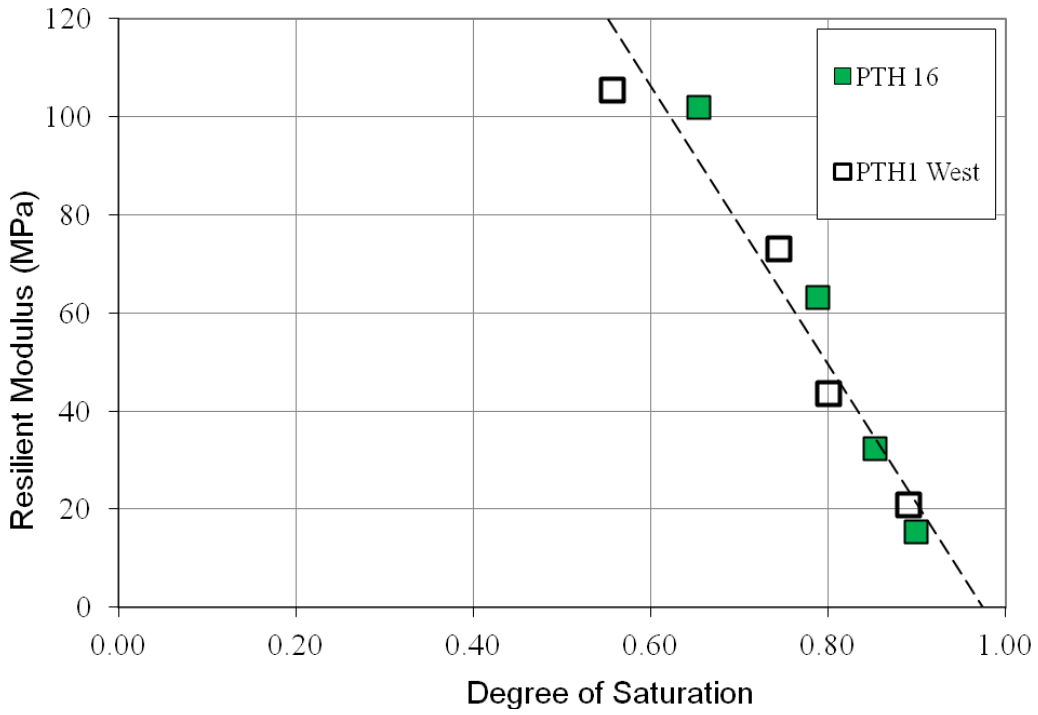

FIGURE 5.8: Measured M_R versus Specimen Degree of Saturation for Sandy Clay

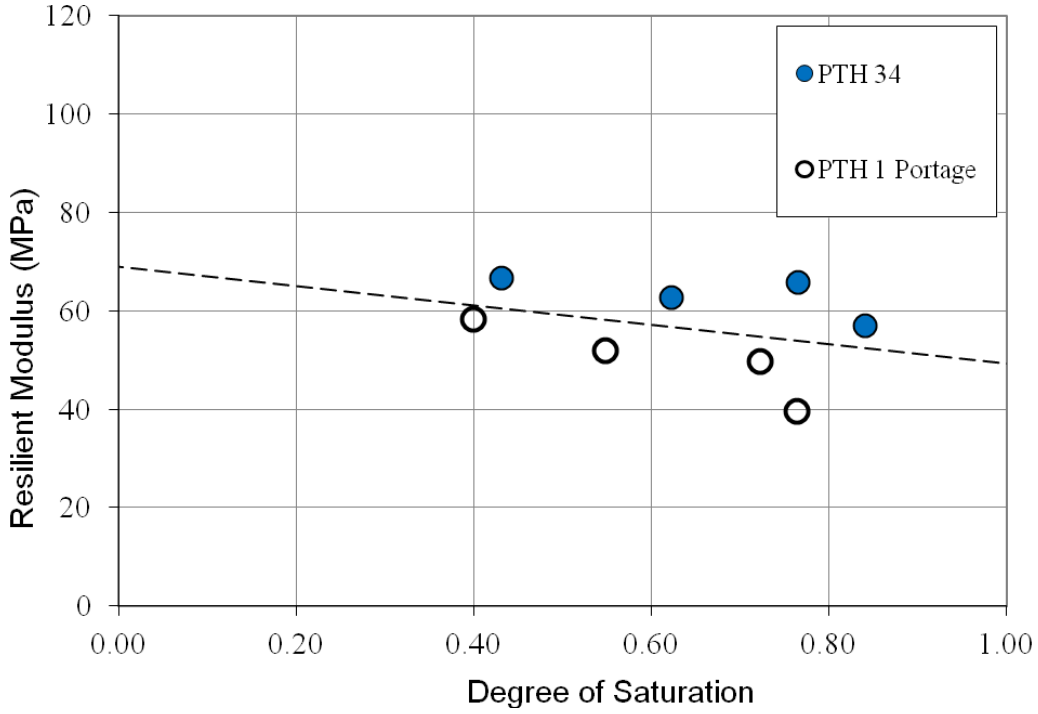

FIGURE 5.9: Measured MR versus Specimen Degree of Saturation for Silty Sand/Sandy Silt

5.6 Comments

When compared to Figures 5.4 to 5.6, data points in Figures 5.1 to 5.3 were more scattered around the equality line. Table 5.5 shows the difference between RMSE for the local prediction models and RMSE for the LTPP models. The RMSE for the LTPP models was higher than the RMSE for the local prediction model by 535%, 381% and 545% for high plastic clay, sandy clay, and silty sand/sandy silt soils, respectively. Accordingly, the local prediction models proposed in this study provide a better fit to M_R test data than LTPP prediction models.

TABLE 5.5: RMSE for the Local Prediction Models and the LTPP Models

Soil Type	RMSE (MPa)		Difference (%)
	Local prediction models	LTPP models	
High plastic clay	4.3	27.3	535
Sandy clay	9.3	44.7	381
Silty sand/sandy silt	8.2	52.9	545

6 Resilient Behaviour and Permeability of UGM

6.1 Introduction

Although UGM has a complex deformation behaviour under traffic loading, this behaviour can be described as the result of three main mechanism: densification/dilation, distortion, and attrition (Lekarp et al. 2000a). The densification/dilation mechanism is the change in shape of the particles assembly which affects the compressibility of the UGM. The distortion mechanism accounts for sliding and rolling of rounded particles, and bending of flat particles. Friction and cohesion between individual particles govern the resistance to sliding and rolling. The attrition mechanism, which is a progressive process, is the breakage and crushing of UGM particles when the applied stresses exceed the strength of individual particles. The crushing of UGM particles under loading is governed by particle shape and size, level of applied stress, aggregate mineralogy, and climatic conditions. Laboratory characterization of the locally available UGM is one of the requirements for reliable and sustainable design.

6.2 Effect of Fines Content on Compaction Characteristics

In addition to size, angularity and shape of coarse aggregate, fines content, affects the compaction characteristics of UGM. Figures 6.1 and 6.2 show the compaction curves for the gravel and limestone gradations, respectively. For gravel gradations, the maximum dry density increased from 2170 kg/m^3 to 2223 kg/m^3 due to increasing fines content from 4.0% to 9.0% and the optimum moisture content (OMC) decreased from 7.9% to

7.0%. A further increase of fines content to 14.5% resulted in the decrease of maximum dry density to 2203 kg/m^3 and the increase of OMC to 8.3%. For limestone gradations, the maximum dry density showed an increasing trend from 2202 kg/m^3 to 2305 kg/m^3 with the increase of fines content from 4.5% to 16.0%.

Mishra (2012) reported similar findings for uncrushed gravel and crushed limestone UGM with nonplastic fines. However, the higher fines content resulted in a higher sensitivity of unsoaked California Bearing Ratio (CBR) values to moisture content variation for both gravel and limestone UGM. Where, an increase of 2.0% in moisture content resulted in a decrease of 85% to 90% in unsoaked CBR values.

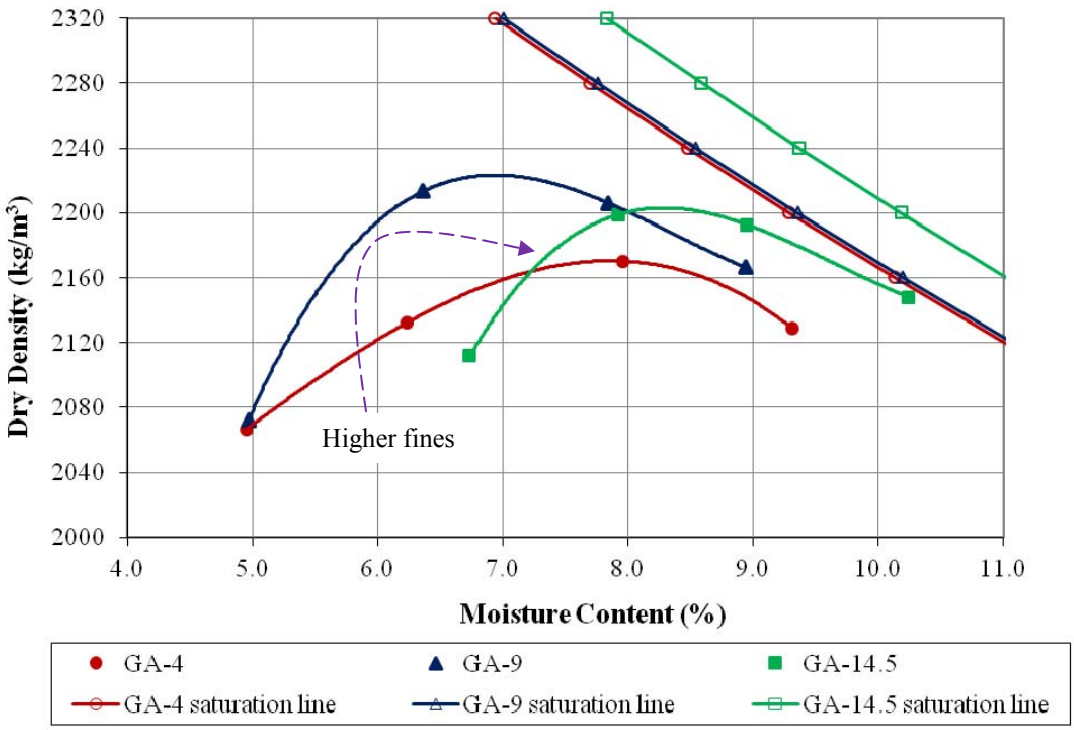

FIGURE 6.1: Effect of Fines Content on Compaction Characteristics of Gravel UGM

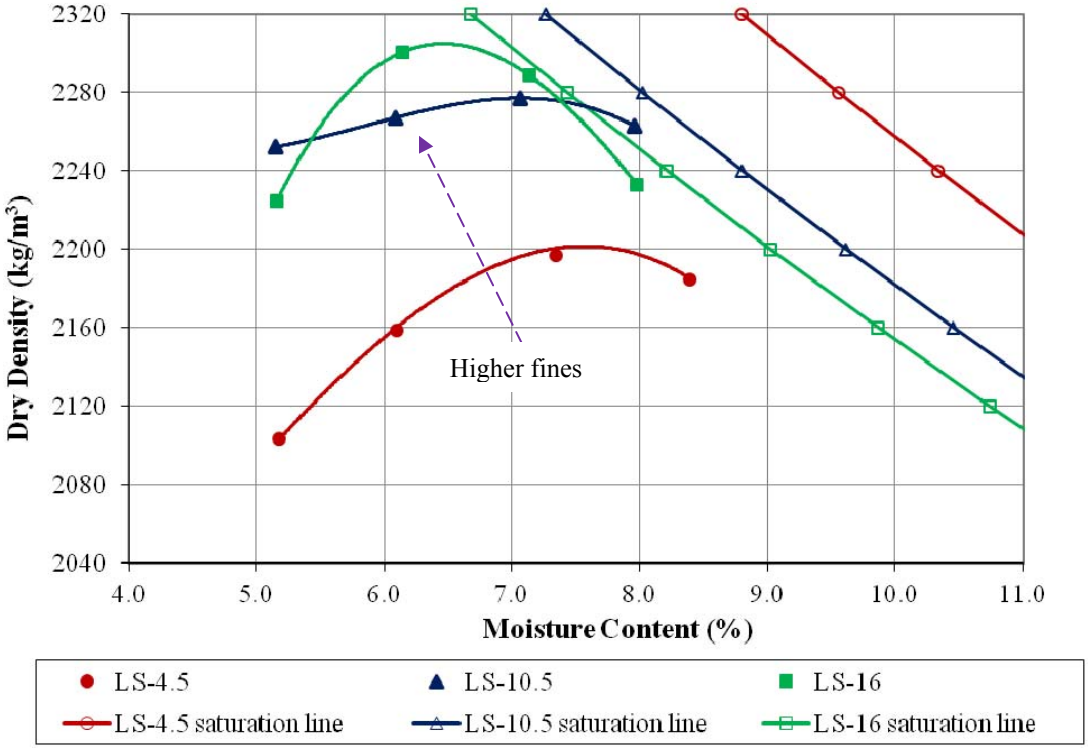

FIGURE 6.2: Effect of Fines Content on Compaction Characteristics of Limestone UGM

The different trends of the change in compaction characteristics, as shown in Figures 6.1 and 6.2, can be attributed to the difference in amount of total voids between uncrushed gravel and crushed limestone aggregate matrices. The aggregate matrix of uncrushed gravel has lower amount of total voids, due to the rounded aggregate particles, than that of crushed limestone UGM (Mishra 2012). For uncrushed gravel, the increase of fines content beyond the initial volume of total voids, at low fines content, changes the aggregate matrix structure and increases the gap between coarse aggregates as shown in Figure 6.3. The mechanism proposed by Mishra (2012) can be verified by imaging techniques. The increase in the gap between coarse aggregate particles changes the interlock and packing characteristic of the aggregate matrix. While the high volume of

total voids in crushed limestone aggregate matrix accommodates more amount of fines without change the aggregate matrix structure.

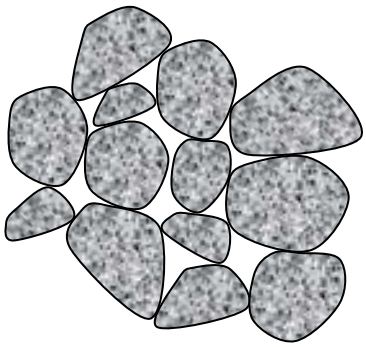

a) Initial total voids with no fines

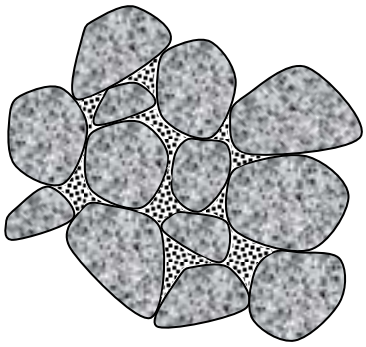

b) Fines ≤ the initial total voids

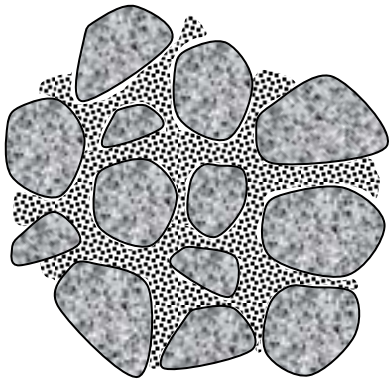

c) Fines > the initial total voids

FIGURE 6.3: Change in Aggregate Matrix and Voids Structure due to the Increase of Fines Content

6.3 Processing of Resilient Modulus Test Data

For each specimen, data from the 30 loading sequences were fitted to Equation 4.1, according to NCHRP 1-28A test protocol (Harrigan and Witczak 2004). Nonlinear regression techniques were utilized to evaluate the values of the regression constants K_1, K_2, and K_3 for each specimen. The values of K_1, K_2, and K_3 of the two replicated were

averaged. A third replicate when the variation between the two replicates was higher than 25%. Equation 4.1 and the evaluated regression constants (K_1, K_2, and K_3) can be used to calculate the UGM resilient modulus at any stress state. M_R test protocol recommends the use of Equation 4.1 to calculate and report M_R of UGM for confining pressure (σ_3) = 35 kPa and cyclic stress (σ_1- σ_3) = 103 kPa (Harrigan and Witczak 2004).

6.4 Resilient Modulus for Gravel Gradations

According to AASHTO classification system, the three gravel gradations belonged to group A-1-a with a GI of zero. The particle size at 60% passing (D_{60}, which is used as a predictor variable for material modulus in the literature) for the three gravel gradations GA-4, GA-9, and GA-14.5 was 7.3 mm, 6.0 mm, and 5.8 mm, respectively. Table 6.1 shows the values of M_R and the regression constants K_1, K_2, and K_3 for the gravel gradations. For GA-14.5, the total permanent strain exceeded 5% for specimens with a moisture content of 8.0% and the test was stopped without completing all loading sequences.

Figure 6.4 shows the M_R values for the three gravel gradations versus specimen moisture content. M_R values showed low to high sensitivity to moisture content variation according to the fines content in the UGM. The sensitivity of M_R to moisture content variation increased with the increase of fines content. For GA-4, M_R decreased from 150.1 MPa to 138.2 MPa (-7.9%) due to increasing the moisture content from 5.7% to 8.7%. For GA-14.5, M_R decreased from 226.0 MPa to 155.6 MPa (-31.2%) due to increasing the moisture content from 6.4% to 8.0%.

TABLE 6.1: Values of M_R and Regression Constants for Gravel UGM Gradations

Sample ID	MC (%)	γ_{dry} (kg/m^3)	K_1	K_2	K_3	M_R (MPa)	STD (MPa)	CV (%)
GA-4	5.7	2154	0.958	1.062	-0.838	150.1	5.7	3.8
	8.7	2165	0.866	1.045	-0.760	138.2	6.7	4.9
GA-9	5.3	2202	1.331	1.143	-0.952	211.3	14.2	6.7
	7.1	2213	1.085	1.088	-0.913	168.1	2.9	1.7
GA-14.5	6.4	2192	1.422	1.264	-1.172	226.0	26.0	11.5
	8.0	2189	0.917	1.382	-1.223	155.6 [a]	5.3	3.4

[a] Permanent strain exceeded 5%

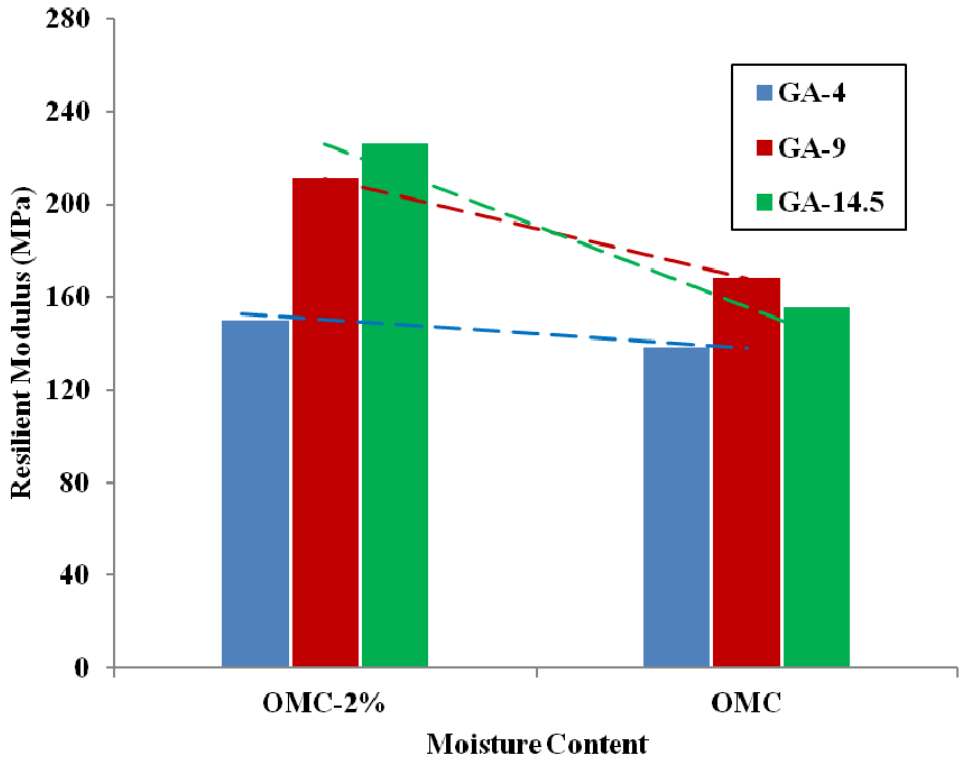

FIGURE 6.4: M_R versus Moisture Content for Gravel Gradations

Figure 6.5 shows the change in M_R versus the fines content in the sample. Samples with 9.0% fines content had the highest M_R value, 168.1 MPa, at OMC, while samples with 14.5% fines content had the highest M_R value, 226.0 MPa, at 2% below OMC. Samples with 4.0% fines content had the lowest M_R values, 150.1 MPa and 138.2 MPa, at 2% below OMC and at OMC, respectively.

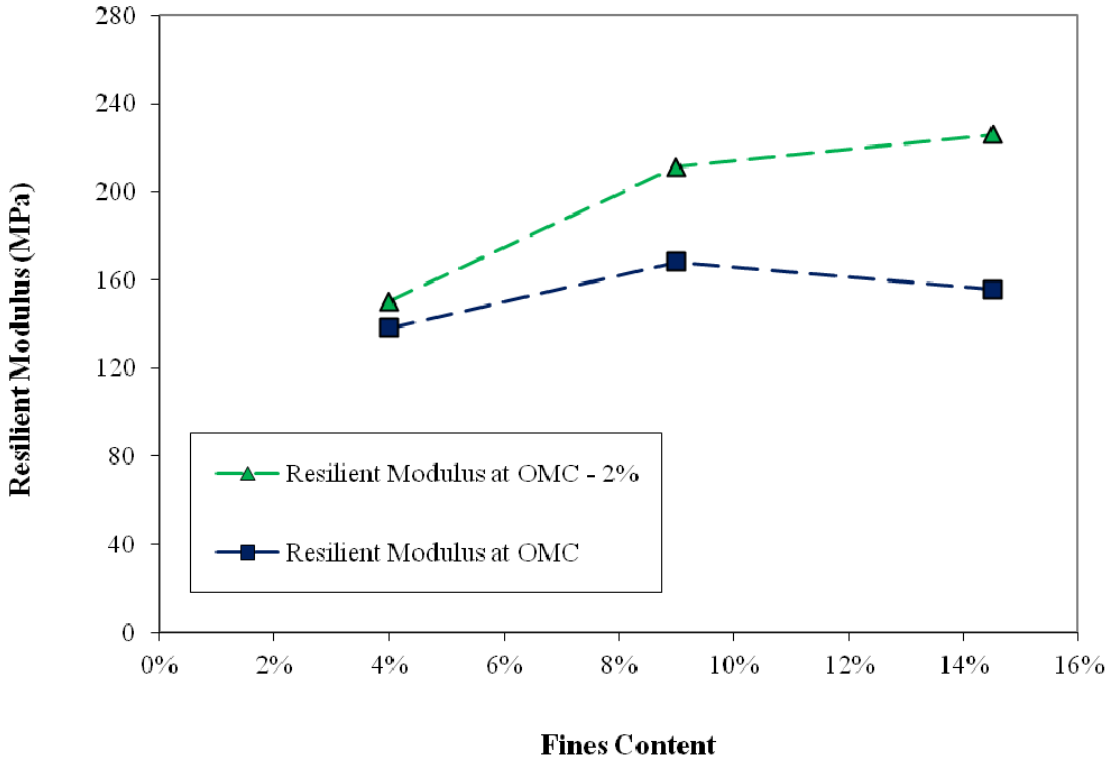

FIGURE 6.5: M_R versus Fines Content for Gravel UGM

6.5 Resilient Modulus for Limestone Gradations

According to AASHTO classification system, LS-4.5 and LS-10.5 gradations belonged to group A-1-a while LS-16 gradation belonged to group A-1-b with a GI of zero. The D_{60}

for the three limestone gradations LS-4.5, LS-10.5, and LS-16 was 6.6 mm, 6.4 mm, and 5.8 mm, respectively.

Table 6.2 shows the values of M_R and the regression constants K_1, K_2, and K_3 for the limestone gradations. Figure 6.6 shows the M_R values for the three limestone gradations versus specimen moisture content. M_R values showed low to high sensitivity to moisture content variation according to the fines content in the UGM. Similar to gravel UGM, the sensitivity of M_R to moisture content variation increased with the increase of fines content. For LS- 4.5, M_R decreased from 211.3 MPa to 195.7 MPa (-7.4%) due to increasing the moisture content from 5.3% to 7.6%. For LS-16, M_R decreased from 253.4 MPa to 149.3 MPa (-41.1%) due to increasing the moisture content from 4.0% to 6.0%.

TABLE 6.2: Values of M_R and Regression Constants for Limestone UGM Gradations

Sample ID	MC (%)	γ_{dry} (kg/m^3)	K_1	K_2	K_3	M_R (MPa)	STD (MPa)	CV (%)
LS-4.5	5.3	2182	1.410	1.016	-0.867	211.3	13.6	6.5
	7.6	2189	1.264	1.116	-0.968	195.7	10.3	5.3
LS-10.5	4.8	2261	1.289	1.110	-1.024	194.4	14.7	7.5
	7.6	2246	0.997	0.978	-0.698	155.4	6.0	3.9
LS-16	4.0	2293	1.581	1.165	-0.970	253.4	42.6	16.7
	6.0	2291	0.934	0.986	-0.645	149.3	5.4	3.6

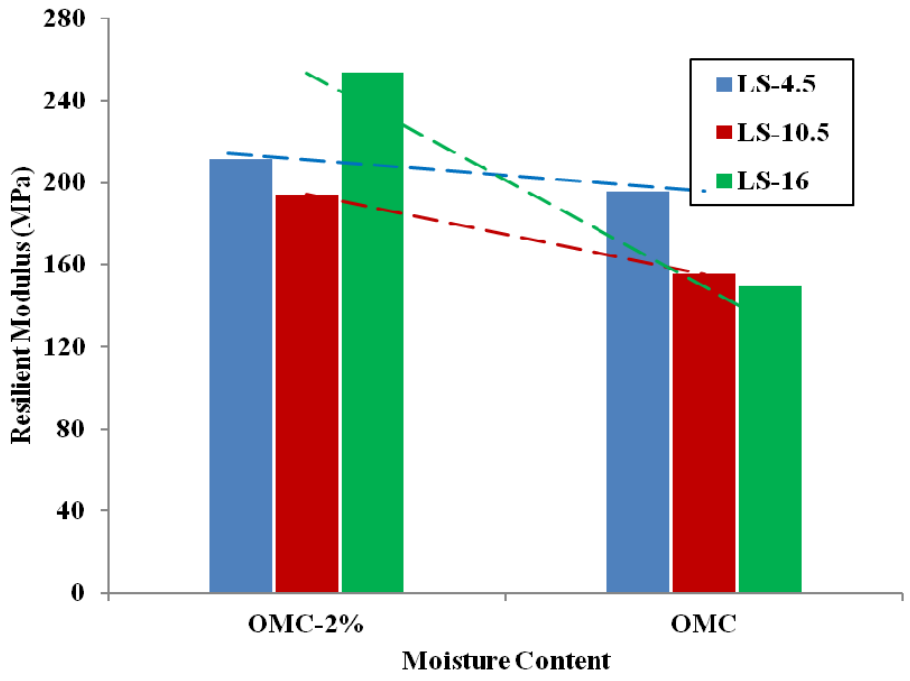

FIGURE 6.6: M_R versus Moisture Content for Limestone Gradations

Figure 6.7 shows the change in M_R versus the fines content in the sample. At OMC, M_R decreased from 195.7 MPa to 149.3 MPa (-23.7%) due to increasing the fines content from 4.5% to 16.0%. At 2% below OMC, M_R increased from 211.3 MPa to 253.4 MPa (+19.9%) due to increasing the fines content from 4.5% to 16.0%. At 2% below OMC, M_R increased with the increase of fines content due to the increase of specimen dry density. However, the increase of fines content increased the sensitivity of M_R to moisture variation where UGM experienced higher deformation.

6.6 Resilient Modulus for Granite UGM

Only one granite gradation with 9.0% fines content (GR-9) was tested. GR-9 belonged to group A-1-a with a GI of zero according to AASHTO classification system. The D_{60} for GR-9 was 6.4 mm.

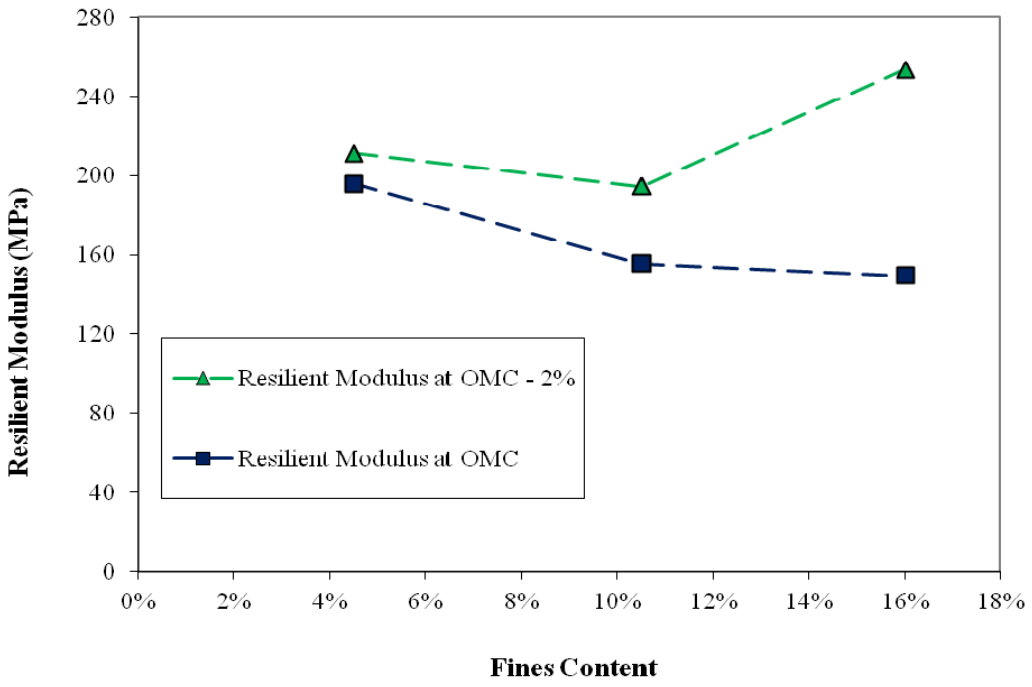

FIGURE 6.7: M_R versus Fines Content for Limestone UGM

Table 6.3 shows the values of M_R and the regression constants K_1, K_2, and K_3 for the granite UGM. Figure 6.8 shows the M_R values for the granite UGM versus specimen moisture content. M_R values for GR-9 showed sensitivity to moisture content variation, similar to gravel and limestone UGM. M_R decreased from 200.7 MPa to 166.3 MPa (-17.2%) due to increasing the moisture content from 4.6% to 7.2%.

TABLE 6.3: Values of M_R and Regression Constants for Granite UGM

Sample ID	MC (%)	γ_{dry} (kg/m^3)	K_1	K_2	K_3	M_R (MPa)	STD (MPa)	CV (%)
GR-9	4.6	2284	1.262	0.979	-0.646	200.7	26.0	13.1
	7.2	2289	0.946	1.301	-0.982	166.3	29.6	17.8

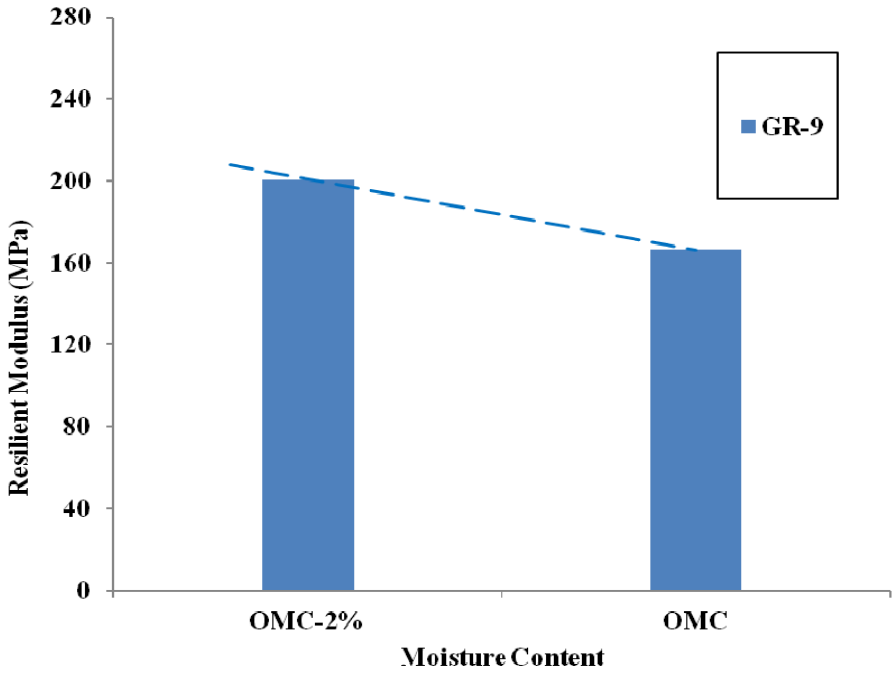

FIGURE 6.8: M_R versus Moisture Content for Granite UGM

6.7 Comparison between Resilient Modulus for Tested UGM and Values Reported in the Literature

Table 6.4 provides a comparison between the M_R values for the tested UGM and M_R values reported in the literature for materials with the same geological origin (Bilodeau and Doré 2012a, Gudishala 2004, Kancherla 2004, Mishra 2012). For gravel UGM, the M_R values were comparable to the values reported for Illinois uncrushed gravel. For limestone UGM, Illinois and Louisiana M_R values were higher than Manitoba $_{MR}$ values by 25% to 40%, while Quebec M_R values were higher by 50% to 125%. This difference can be attributed to the finer gradation of Manitoba UGM, smaller maximum nominal size and smaller D_{60}. Similarly, for granite UGM, the M_R value for Texas base material

was 100% higher than M_R value for Manitoba base material due to the finer gradation of Manitoba UGM.

6.8 Database for Typical Resilient Modulus Values for Manitoba UGM

For Level 3 design inputs, Pavement ME provides and recommends the use of default values for UGM resilient modulus based on AASHTO classification of UGM (Christopher et al. 2006). The reliability of Level 3 design inputs can be improved by transportation agencies through developing a database for M_R values for typical UGM available in their regions. This database can be used to replace Pavement ME default values for Level 3 design inputs. This database shall be regularly updated to include the results of new M_R tests.

Table 6.5 provides typical M_R values for the UGM samples tested in this study. M_R values were calculated using Equation 4.1 for confining pressure of 35 kPa and cyclic stress of 103 kPa. According to M_R test protocol, these confining pressure and cyclic stress represent the stress state that base materials encounters under traffic loading (Harrigan and Witczak 2004). For level 3 design, Pavement ME recommends values for M_R to be used by transportation agencies when laboratory values are not available. Table 6.5 shows the range of M_R values recommended in Pavement ME. The base materials tested in this project are classified as A-1-a, and A-1-b according to AASHTO classification system. It shall be noted that the M_R values recommended in Pavement ME represent the M_R values at optimum moisture content and maximum dry density.

TABLE 6.4: Comparison between M_R Values for Tested UGM and Values Reported in the Literature

Material Type	Location	Nominal Maximum Size (mm)	D_{60} (mm)	Fines Content (%)	OMC (%)	γ_{max} (kg/m^3)	M_R (MPa)
Gravel	Manitoba	16.0	7.3	4.0	7.9	2170	138.2
			6.0	9.0	7.0	2223	168.1
			5.8	14.5	8.3	2203	155.6
	Illinois	19.0	7.8	4.0	9.2	2080	157.1
			7.5	8.0	8.1	2110	139.7
			7.2	12.0	7.1	2160	114.7
Limestone	Manitoba	16.0	6.6	4.5	7.5	2202	195.7
			6.4	10.5	7.0	2277	155.4
			5.8	16.0	6.5	2305	149.4
	Quebec	20.0	11.5	2.0	4.7	2241	543.2 [a]
			8.2	4.5	5.7	2289	452.0 [a]
		14.0	5.0	7.0	5.0	2268	393.0 [a]
	Illinois	19.0	7.8	4.0	10.5	2080	228.5
			7.5	8.0	8.4	2140	215.5
			7.2	12.0	7.6	2200	208.5
			6.9	16.0	6.8	2230	190.7
	Louisiana	19.0	7.0	N/A [b]	5.9	2243	190.0
			7.0	N/A	3.2	2019	246.0
Granite	Manitoba	16.0	6.4	9.0	6.3	2308	166.3
	Texas	37.5	16.0	N/A	5.6	2353	334.0

[a] M_R values for Quebec UGM were measured at saturation condition

[b] Data are not available

TABLE 6.5: Typical M_R Values for UGM in Manitoba

Material Type	AASHTO Classification	Fines Content (%)	OMC (%)	MC (%)	Tested M_R (MPa)	Pavement ME M_R (MPa) [a]		Difference (%)
						Range	Mean	
Gravel	A-1-a, GI = 0	4.0	7.9	5.7	150.1	265.7 to 289.8	276.0	95
				8.7	138.2			
		9.0	7.0	5.3	211.3			62
				7.1	168.1			
		14.5	8.3	6.4	226.0			94
				8.0	155.6 [b]			
Limestone	A-1-a, GI = 0	4.5	7.5	5.3	211.3	265.7 to 289.8	276.0	41
				7.6	195.7			
		10.5	7.0	4.8	194.4			69
				7.6	155.4			
	A-1-b, GI = 0	16.0	6.5	4.0	253.4	245.0 to 276.0	262.2	113
				6.0	149.3			
Granite	A-1-a, GI = 0	9.0	6.3	4.6	200.7	265.7 to 289.8	276.0	55
				7.2	166.3			

[a] Pavement ME values for M_R at optimum moisture content and maximum dry density

[b] Permanent strain exceeded 5%

Table 6.5 shows that the M_R values recommended by Pavement ME were higher than the M_R values obtained from laboratory testing by 41% to 113%. Pavement ME default values were developed for material gradations having D_{60} ranging from 8.7 to 18.2 mm, while D_{60} for the tested base materials ranged from 5.8 to 7.3 mm (NCHRP 2001). The difference between Pavement ME recommended values and the laboratory values can be attributed to the finer gradation of the tested UGM in this study. This difference explains

the need to update the default M_R values recommended by Pavement ME to improve design reliability and avoid premature failure of pavement structures.

6.9 Permeability of UGM

Figure 6.9 and 6.10 show the measured hydraulic conductivity (k) for gravel and limestone materials, respectively, at different fines content. The reported hydraulic conductivity values are at a water temperature of 20^{o}C. For gravel gradations, the hydraulic conductivity decreased from 2.70×10^{-6} m/s to 0.85×10^{-6} m/s (-69%) due to increasing fines content from 4.0% to 9.0%. As the fines content increased further to 14.5%, the hydraulic conductivity decreased to 0.42×10^{-6} m/s (-84%). For Limestone gradations, the hydraulic conductivity decreased from 4.55×10^{-6} m/s to 1.75×10^{-6} m/s (-62%) due to increasing fines content from 4.5% to 10.5%. As the fines content increased further to 16.0%, the hydraulic conductivity decreased to 0.87×10^{-6} m/s (-81%).

The hydraulic conductivity for limestone gradations was higher than that for gravel gradations by 1.85×10^{-6} m/s at low fines content and by 0.45×10^{-6} m/s at high fines content. The difference in hydraulic conductivity can be due to the higher amount of total voids in the aggregate matrix of crushed limestone UGM than that of uncrushed gravel (Mishra 2012).

Table 6.6 provides a comparison between the hydraulic conductivity values for the tested UGM and the hydraulic conductivity values reported in the literature for limestone and sandstone UGM from different sources in Oklahoma (Ghabchi et al. 2013). The hydraulic

conductivity for Oklahoma UGM was measured using a falling headed flexible wall permeability setup at saturation condition. The Oklahoma UGM were compacted using Modified Proctor method with gradations representing the specification limits of Oklahoma Department of Transportation specifications for dense-graded base material. Although some Oklahoma samples had coarser gradation, the hydraulic conductivity values for Manitoba samples were higher than that for Oklahoma samples, by more than two orders of magnitude for some samples. The difference in hydraulic conductivity between Manitoba samples and Oklahoma samples is due to using different compaction energy where Manitoba samples were compacted using Standard Proctor energy. Using a compaction energy of 600 kN.m/m^3 (Standard Proctor energy) instead of 2700 kN.m/m^3 (Modified Proctor energy) can result in the increase of hydraulic conductivity by multiple orders of magnitude (Babic´ et al. 2000).

For Level 2 design inputs in Pavement ME, the saturated hydraulic conductivity can be determined from fines content (P_{200}), plasticity index (PI), and D_{60} (Christopher et al. 2006). The PI for all the test gradations was zero. The saturated hydraulic conductivity (k_{sat}), in ft/hr, can be determined from the following equation:

$$k_{sat} = 118.11 \times 10^{\left[-1.1275\left(\log D_{60}+2\right)^2 + 7.2816\left(\log D_{60}+2\right) - 11.2891\right]} \quad \textbf{(6.1)}$$

Equation 6.1 is valid for the following conditions:

$0 \leq P_{200} \times PI < 1$

$D_{60} < 0.75$ in

If $D_{60} > 0.75$ in, set $D_{60} = 0.75$ in

TABLE 6.6: Comparison between Hydraulic Conductivity Values for Tested UGM and Values Reported in the Literature

Location	Material Type	D_{60} (mm)	Fines Content (%)	OMC (%)	γ_{max} (kg/m^3)	k* ($\times 10^{-6}$ m/s)
Manitoba	Gravel	7.3	4.0	7.9	2170	2.700
		6.0	9.0	7.0	2223	0.850
		5.8	14.5	8.3	2203	0.420
	Limestone	6.6	4.5	7.5	2202	4.550
		6.4	10.5	7.0	2277	1.750
		5.8	16.0	6.5	2305	0.870
Oklahoma	Limestone 1	17.0	7.3	5.0	2264	1.550
		4.2	15.5	6.6	2447	0.004
	Limestone 2	19.6	4.9	5.0	2305	1.000
		4.8	12.9	6.2	2335	0.400
	Sandstone	17.5	6.6	6.0	2192	0.700
		3.8	13.9	6.4	2182	0.004

* Hydraulic conductivity values are at saturation condition and a water temperature of 20°C. Manitoba samples were compacted using Standard Proctor energy and Oklahoma samples were compacted using Modified Proctor energy.

Table 6.7 shows the hydraulic conductivity values for the gravel and limestone gradations determined using Equation 6.1. For gravel gradations, the calculated hydraulic conductivity was higher than the laboratory measured value by 217%, 352% and 693% for GA-4, GA-9, and GA-14.5, respectively. For limestone gradations, the calculated hydraulic conductivity was higher than the laboratory measured value by 25%, 187% and 283% for LS-4.5, LS-10.5, and LS-16, respectively.

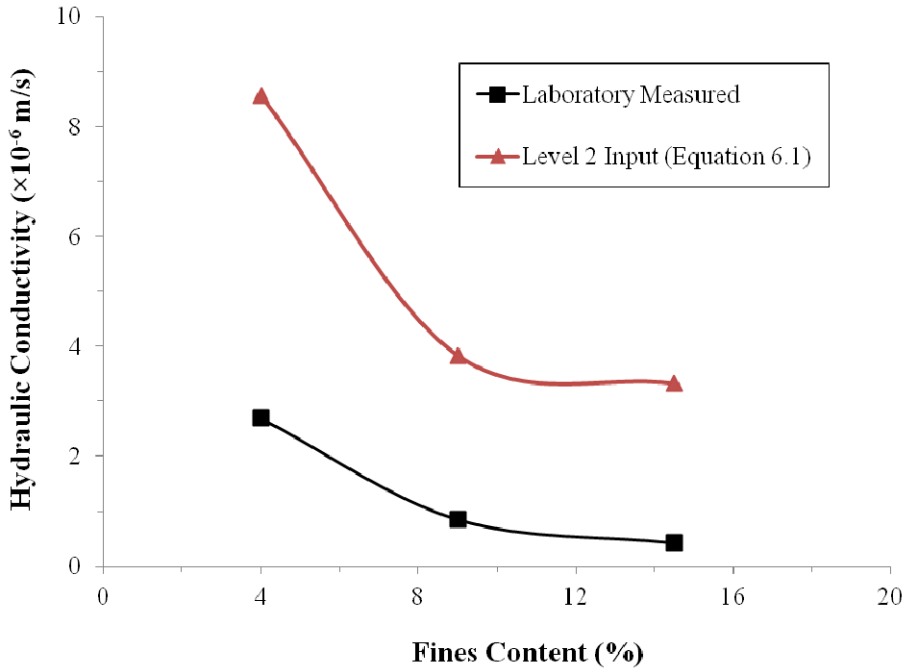

FIGURE 6.9: Measured Hydraulic Conductivity for Gravel UGM

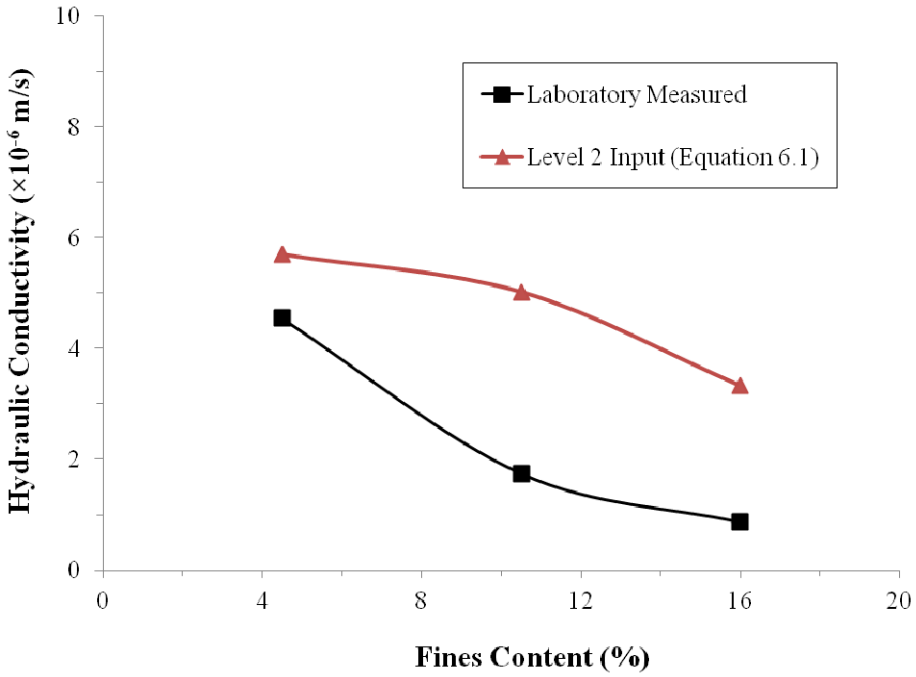

FIGURE 6.10: Measured Hydraulic Conductivity for Limestone UGM

The deviation between the calculated hydraulic conductivity and the laboratory measured value increased as the fines content increase where Equation 6.1 depends on D_{60} and does not account for the change in fines content. Overestimating the hydraulic conductivity of base layer results in under designing the pavement structure and reducing the pavement service life.

TABLE 6.7: Hydraulic Conductivity of the Tested UGM Determined Using Equation 6.1, Level 2 Design Input

Gradation ID	D_{60} (mm)	Fines Content (%)	Laboratory Measured k ($\times 10^{-6}$ m/s)	k_{sat} using Equation 6.1 ($\times 10^{-6}$ m/s)	Difference (%)
GA-4	7.3	4.0	2.700	8.563	217
GA-9	6.0	9.0	0.850	3.840	352
GA-14.5	5.8	14.5	0.420	3.331	693
LS-4.5	6.6	4.5	4.550	5.697	25
LS-10.5	6.4	10.5	1.750	5.021	187
LS-16	5.8	16.0	0.870	3.331	283

AASHTO 1986 design guide was utilized to determine the effect of changing the hydraulic conductivity of UGM on the quality of drainage of base layer (AASHTO 1986). Assuming a two-lane road section with a slope of 2%, the time required to drain a base layer of 0.3 m thickness to 50% saturation and the quality of drainage were determined. Table 6.8 shows the time to drain the base layer and the quality of drainage using the laboratory measured hydraulic conductivity, Level 1 input, and the values obtained from Equation 6.1 for Level 2 input. For both gravel and limestone gradations,

the time to drain the base layer decreased as the fines content decreased and the quality of drainage improved one category up. The improvement in quality of drainage extends the service life of pavement and reduces the required thickness of pavement layers. Table 6.8 shows that using Level 2 design input for hydraulic conductivity will over estimates the quality of drainage for GA-9, GA-14.5, and LS-16. Overestimating the quality of drainage can contribute to premature failure of a pavement structure due to under designing the required layer thicknesses.

TABLE 6.8: Time to Drain and Quality of Drainage Based on the Hydraulic Conductivity Values for the Tested UGM

Gradation ID	Level 1 Design Input (Laboratory Measured)		Level 2 Design Input (Equation 6.1)	
	Time to drain base (day)	Quality of drainage	Time to drain base (day)	Quality of drainage
GA-4	4	Good to Fair	2	Good to Fair
GA-9	8	Fair to Poor	2	Good to Fair
GA-14.5	9	Fair to Poor	2	Good to Fair
LS-4.5	2	Good to Fair	2	Good to Fair
LS-10.5	5	Good to Fair	2	Good to Fair
LS-16	8	Fair to Poor	2	Good to Fair

7 Resilient Modulus Prediction Models for UGM

7.1 Introduction

Similar to subgrade soils, for Level 2 design inputs, Pavement ME recommends correlation models to estimate M_R from basic UGM properties (e.g. gradation, California bearing ratio, compaction characteristics,...). Stress level is the most significant factor that impacts M_R for UGM (Lekarp et al. 2000a). The stress level can be represented by bulk stress only at low strain levels or bulk stress and octahedral shear stress to account for the effect of shear strains of M_R (May and Witczak 1981; Uzan 1985). In addition to stress level, gradation and moisture content affects the resilient response of UGM (Lekarp et al. 2000a, Tutumluer 2013).

Several models have been proposed to determining M_R for UGM as a function of stress state and physical properties (Bilodeau and Doré, 2012b; Tian et al. 1998; Yau and Von Quintus 2002). Research studies showed that current prediction models and default values in Pavement ME cannot be generalized to predict the response of any UGM. This chapter introduces correlation models to estimate M_R for the UGM evaluated in this study as function of stress state and basic properties. These models can be used for Level 2 design in Pavement ME and to evaluate the effect of seasonal variation on M_R.

7.2 Comparing the Measured Resilient Modulus to the LTPP Prediction Models

Figures 7.1 and 7.2 compare the laboratory measured M_R to the predicted M_R using LTPP prediction models for the gravel and limestone UGM evaluated in this study (Yau and Von Quintus 2002). Equations 2.11 to 2.13, the LTPP prediction models of K_1, K_2 and K_3 for uncrushed gravel UGM, were used to predict M_R for the gravel material. Equations 2.5 to 2.7, the LTPP prediction models of K_1, K_2 and K_3 for crushed stone UGM, were used to predict M_R for the limestone material.

Figure 7.2 shows that the LTPP model underestimated M_R for the limestone material. The RMSE was 157.1 MPa for gravel UGM and 188.9 MPa for limestone UGM. The coefficient of variation of the RMSE was 50.3% for gravel material and 55.6% for limestone material. The high residuals associated with evaluating M_R using the LTPP models provide a need to develop local prediction models to improve the reliability of Level 2 design inputs.

7.3 Effect of Gradation and Compaction Characteristics on Resilient Modulus

Six UGM gradations representing two material types, crushed limestone and uncrushed gravel, were evaluated in this study. Data for each material type was analyzed separately. Comparable M_R test data from the literature was utilized to increase the size of the data set (Mishra 2012). Preliminary statistical analysis was conducted to study the correlation

between the regression constants of Equation 4.1 (K_1, K_2, K_3) and the gradation and compaction parameters for each material type.

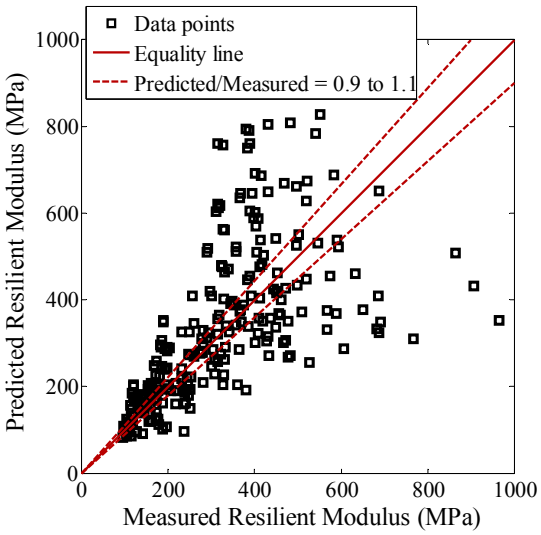

FIGURE 7.1: Measured and Predicted M_R Using LTPP Prediction Models for Gravel Base Material

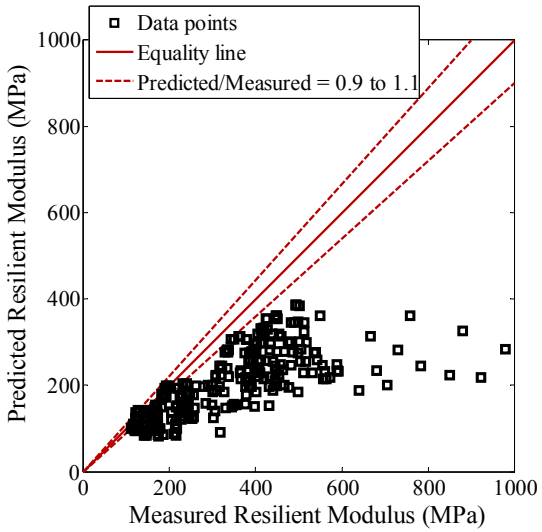

FIGURE 7.2: Measured and Predicted M_R Using LTPP Prediction Models for Limestone Base Material

Tables 7.1 and 7.2 show the correlation coefficients, and their significance (p-value), between regression constants and the gradation and compaction parameters for gravel and limestone, respectively. Tables 7.1 and 7.2 show only the parameters that had an absolute correlation coefficient greater than 0.5 for any of the three regression constants.

TABLE 7.1: Correlation between Regression Constants (K_1, K_2, K_3) and Gradation & Compaction Parameters for Gravel UGM (p-value < 0.05 is significant at a confidence level > 95%)

Variable	K_1		K_2		K_3	
	Correlation Coefficient	p-value	Correlation Coefficient	p-value	Correlation Coefficient	p-value
P3/8	0.513	0.025	0.642	0.007	-0.684	0.004
P4	0.560	0.024	0.817	$< 10^{-4}$	-0.862	$< 10^{-4}$
P40	0.443	0.086	0.764	0.001	-0.790	$< 10^{-4}$
P200	0.256	0.339	0.589	0.016	-0.586	0.017
γ_{opt}	0.464	0.070	0.747	0.001	-0.769	$< 10^{-4}$
MC	-0.551	0.027	-0.252	0.346	0.299	0.260

P3/8 = percentage of passing sieve No. 3/8″, P4 = percentage of passing sieve No. 4, P40 = percentage of passing sieve No. 40, P200 = percentage of passing sieve No. 200, γ_{opt} = maximum dry density, and MC = specimen moisture content.

Combined variables were developed to represent the combined effect of gradation and compaction parameters, and the deviation of specimen moisture content from the OMC. The combined variables were developed based on the literature and the logical influence of the gradation and compaction parameters on regression constants (K_1, K_2, K_3). Based on preliminary correlation analysis, five variables for gravel UGM, and four for limestone, were proposed as predictor variables that can be used in the regression models.

The deviation of specimen moisture content from OMC was incorporated to account for the effect, if any, of degree of saturation variation on resilient modulus. The fines content (% passing sieve No.200) was found to be not a significant parameter despite its influence on the measured resilient modulus. However, the effect of fines content was incorporated implicitly in the maximum dry density, and optimum moisture content in the regression model.

TABLE 7.2: Correlation between Regression Constants (K_1, K_2, K_3) and Gradation & Compaction Parameters for Limestone UGM (p-value < 0.05 is significant at a confidence level > 95%)

Variable	K_1		K_2		K_3	
	Correlation Coefficient	p-value	Correlation Coefficient	p-value	Correlation Coefficient	p-value
P3/8	-0.194	0.474	0.811	$< 10^{-4}$	-0.696	0.014
P4	-0.251	0.349	0.746	0.001	-0.602	0.014
γ_{opt}	-0.334	0.206	0.596	0.014	-0.461	0.072
OMC	0.295	0.268	-0.531	0.034	0.425	0.101
MC	-0.225	0.401	-0.634	0.008	-0.642	0.007

P3/8 = percentage of passing sieve No. 3/8″, P4 = percentage of passing sieve No. 4, OMC = optimum moisture content, γ_{opt} = maximum dry density, and MC = specimen moisture content.

Tables 7.3 and 7.4 show the correlation coefficients between regression constants (K_1, K_2, K_3) and the proposed variables for gravel and limestone, respectively. Tables 7.3 and 7.4 show also the significance (p-value) of the calculated correlation coefficients. A p-value less than 0.05 indicates that the correlation coefficient is significant at a confidence level higher than 95%. For each regression constant, the predictor variable with the

highest correlation coefficient and lowest p-values was selected to be a predictor variable for that regression constant. The selected predictor variables are shaded in Tables 7.3 and 7.4. Although the same predictor variables were found significant for both materials, two prediction models were developed for uncrushed gravel and crushed limestone due to the different characteristics and behaviour of each material (Yau and Von Quintus 2002).

TABLE 7.3: Correlation between Regression Constants (K_1, K_2, K_3) and the Predictor Variables for Gravel UGM (p-value < 0.05 is significant at a confidence level > 95%)

Variable	K_1		K_2		K_3	
	Correlation Coefficient	p-value	Correlation Coefficient	p-value	Correlation Coefficient	p-value
$MC-OMC$	-0.608	0.012	-0.270	0.312	0.339	0.199
$\frac{\gamma_{opt}}{P40}$	-0.418	0.107	-0.748	0.001	0.767	0.001
$\frac{\gamma_{opt}}{P4}$	-0.564	0.023	-0.818	$< 10^{-4}$	0.867	$< 10^{-4}$
$\frac{\gamma_{opt}}{MC}$	0.586	0.017	0.258	0.334	-0.304	0.252
$\frac{P200}{MC}$	0.497	0.050	0.595	0.015	-0.612	0.012

P4 = percentage of passing sieve No. 4, P40 = percentage of passing sieve No. 40, P200 = percentage of passing sieve No. 200, γ_{opt} = maximum dry density, MC = specimen moisture content, and OMC = optimum moisture content

7.4 Developing Local Resilient Modulus Prediction Models for UGM

After identifying and removing outliers, multiple regression analysis was performed on M_R test data for each material type. The regression analysis was performed using 83% of

the test data. The remaining 17% of the test data was used to validate the prediction models. Equations 7.1 to 7.6 show the prediction models for K_1, K_2, and K_3 for each material type. M_R for each material type can be estimated at any stress state by incorporating these prediction model into Equation 4.1. The overall coefficient of determination for the prediction models was 0.82 for uncrushed gravel and 0.74 for crushed limestone.

TABLE 7.4: Correlation between Regression Constants (K_1, K_2, K_3) and the Predictor Variables for Limestone UGM (p-value < 0.05 is significant at a confidence level > 95%)

Variable	K_1		K_2		K_3	
	Correlation Coefficient	p-value	Correlation Coefficient	p-value	Correlation Coefficient	p-value
$MC-OMC$	-0.568	0.022	-0.493	0.052	0.591	0.016
$\frac{\gamma_{opt}}{P4}$	0.180	0.506	-0.811	$< 10^{-4}$	0.680	0.004
$\frac{\gamma_{opt}}{OMC}$	-0.302	0.255	0.545	0.029	-0.409	0.115
$\frac{\gamma_{opt}}{MC}$	0.353	0.179	0.610	0.012	-0.622	0.010

P4 = percentage of passing sieve No. 4, γ_{opt} = maximum dry density, MC = specimen moisture content, and OMC = optimum moisture content

Table 7.5 shows the 95% confidence intervals for regression constants of K_1, K_2, and K_3 prediction models. Figures 7.3 and 7.4 show the regression residuals and the 95% confidence intervals for the residuals represented by an error bar. Figures 7.3 and 7.4

indicate that no outliers in the data sets for gravel and limestone materials where all the error bars cross the zero reference line. The presented analysis provides adaptable guidelines for predicting the resilient modulus of UGM. The prediction models were developed using limited data set. Ideally, the models should be validated, and calibrated if required, using a wider data set according to the criteria presented in the study.

Uncrushed Gravel

$$K_1 = 0.9804 - 0.1349(MC - OMC) \quad \textbf{(7.1)}$$

$$K_2 = 3.4675 - 0.0571\frac{\gamma_{opt}}{P4} \quad \textbf{(7.2)}$$

$$K_3 = -4.4656 + 0.0860\frac{\gamma_{opt}}{P4} \quad \textbf{(7.3)}$$

100% Crushed Limestone

$$K_1 = 1.2087 - 0.1067(MC - OMC) \quad \textbf{(7.4)}$$

$$K_2 = 5.1153 - 0.0949\frac{\gamma_{opt}}{P4} \quad \textbf{(7.5)}$$

$$K_3 = -5.0141 + 0.0975\frac{\gamma_{opt}}{P4} \quad \textbf{(7.6)}$$

Where:

MC = specimen moisture content, %

OMC = optimum moisture content, %

γ_{opt} = maximum dry density, kg/m^3

P4 = percentage passing sieve No. 4, %

TABLE 7.5: Confidence Intervals for Regression Constants of K_1, K_2, and K_3 Prediction Models

Soil Type	95% Confidence Intervals for Regression Constants					
	K_1 Model		K_2 Model		K_3 Model	
	Interceptor*	predictor variable**	Interceptor	predictor variable	Interceptor	predictor variable
Gravel	0.8353 to 1.1256	-0.2459 to -0.0239	2.4476 to 4.4874	-0.0808 to -0.0334	-5.7382 to -3.1930	0.0564 to 0.1155
Limestone	1.0888 to 1.3287	-0.1892 to -0.0241	3.3138 to 6.9167	-0.1357 to -0.0541	-7.8067 to -2.2214	0.0343 to 0.1608

* The constant component in Equations 7.1 to 7.6

** The multiplier for the independent variables in Equations 7.1 to 7.6

Figures 7.5 and 7.6 compare the measured M_R to the predicted M_R using Equations 7.1 to 7.6 for gravel and limestone materials, respectively, using the validation data set. The RMSE was 49.3 MPa for gravel and 67.8 MPa for limestone base materials. The coefficient of variation of the RMSE was 17.8% for gravel and 21.7% for limestone base materials. Figures 7.5 and 7.6 show that there was a good agreement between measured and predicted M_R values. The data points for gravel material, Figure 7.5, were less scattered around the equality line than the data points for limestone material, Figure 7.6.

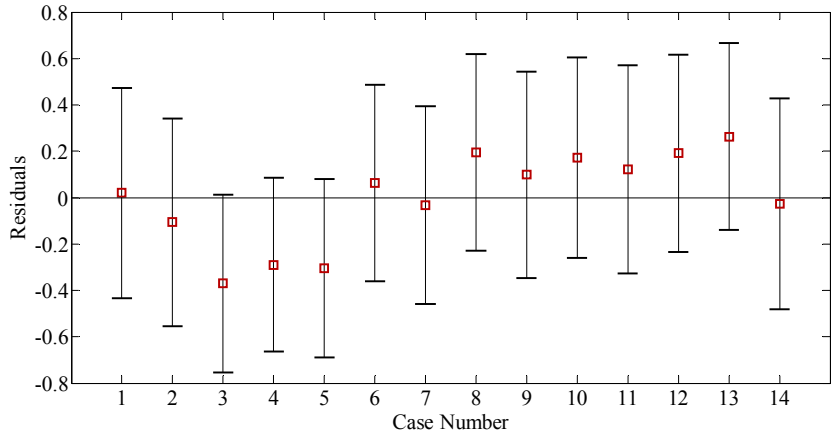

a) K_1 model

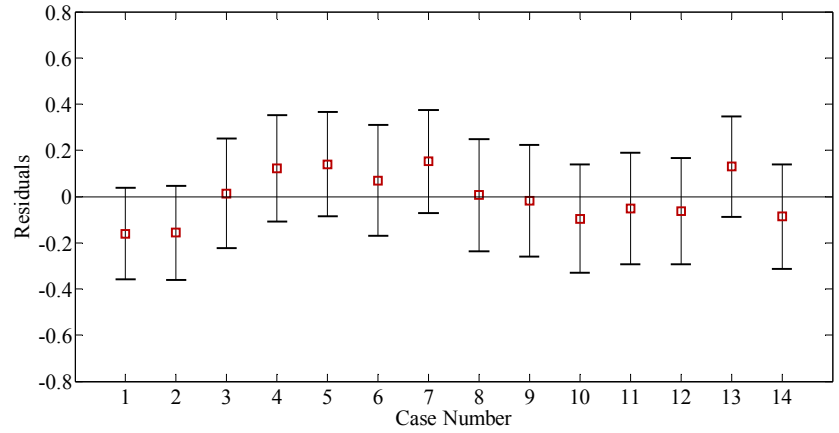

b) K_2 model

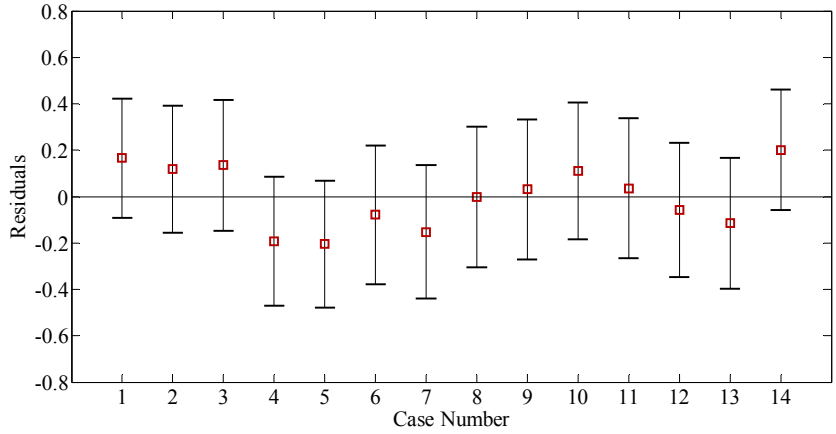

c) K_3 model

FIGURE 7.3: Residuals and 95% Confidence Intervals of Gravel Regression Models

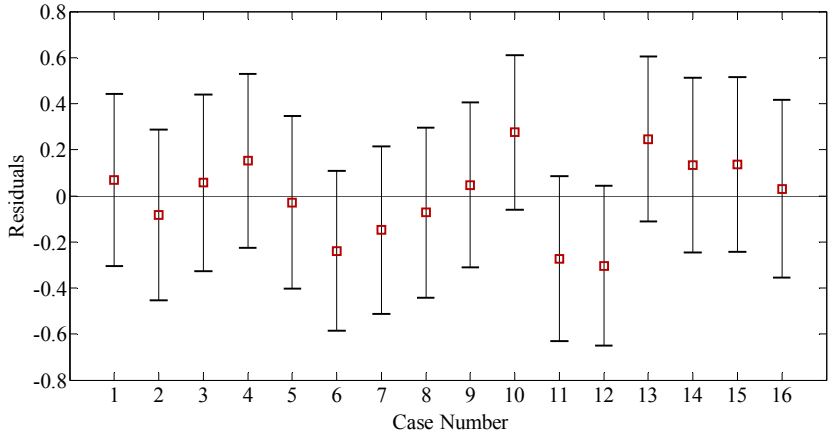

a) K_1 model

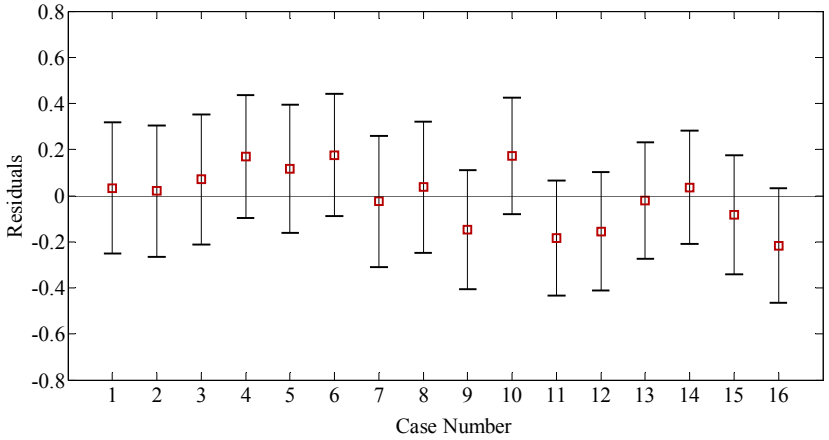

b) K_2 model

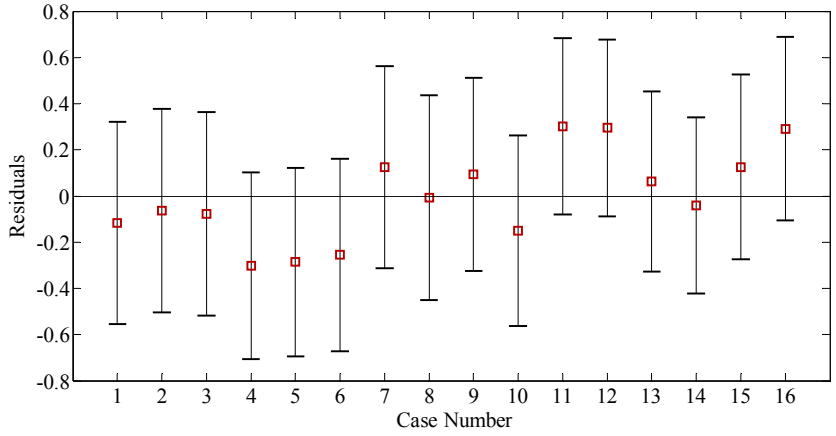

c) K_3 model

FIGURE 7.4: Residuals and 95% Confidence Intervals of Limestone Regression Models

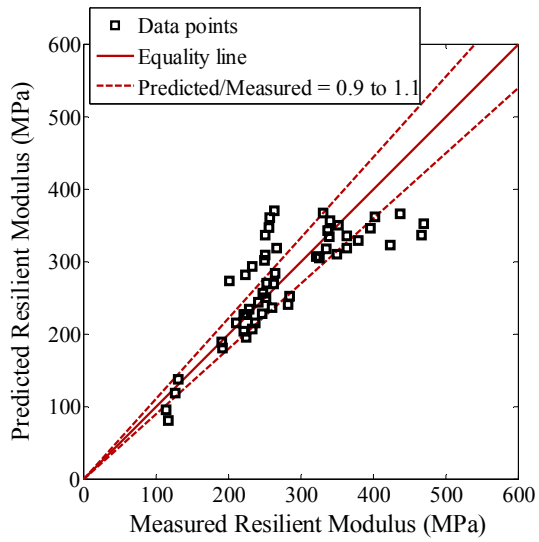

FIGURE 7.5: Measured and Predicted M_R Using the Proposed Models for Gravel Base Material

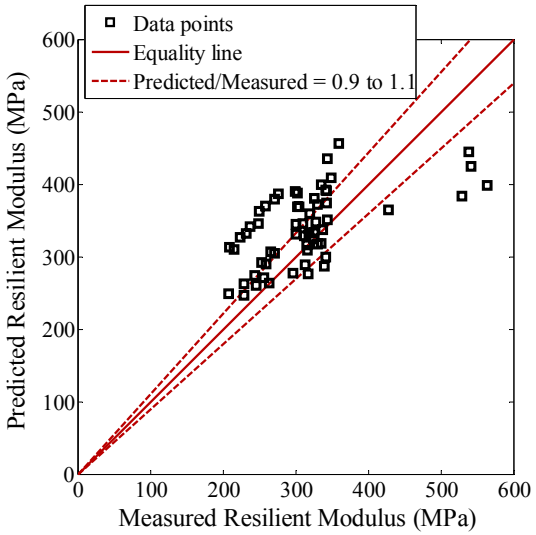

FIGURE 7.6: Measured and Predicted M_R Using the Proposed Models for Limestone Base Material

7.5 Comments

When compared to Figures 7.5 and 7.6, data points in Figures 7.1 and 7.2 were more scattered around the equality line. Table 7.6 shows the RMSE and its coefficient of variation for the local prediction models and the LTPP models. The RMSE for the LTPP models was higher than the RMSE for the local prediction model by 219% and 179% for gravel and limestone UGM, respectively. The coefficient of variation of the RMSE for the LTPP models was higher than the coefficient of variation of the RMSE for the local prediction models by 183% and 156% for gravel and limestone UGM, respectively. Accordingly, the prediction models proposed in this study provide a better fit to the UGM M_R test data than LTPP prediction models.

TABLE 7.6: RMSE for the Local Prediction Models and the LTPP Models

UGM Type	RMSE (MPa)			Coefficient of variation of the RMSE (%)		
	Local models	LTPP models	Difference (%)	Local models	LTPP models	Difference (%)
Gravel	49.3	157.1	219	17.8	50.3	183
Limestone	67.8	188.9	179	21.7	55.6	156

8 Permanent Deformation and Shakedown Behaviour of UGM

8.1 Introduction

The stresses that pavement materials experience in-service are usually beyond their elastic limits to accommodate the traffic loading with cost-effective design. The behaviour of UGM after exceeding the elastic limit has a substantial influence on the performance and service life of pavements (Boulbibane et al. 2005). The mode of failure of an UGM layer is governed by the applied load and the shakedown behaviour of the material. Pavements subjected to lighter traffic loading or with higher shakedown limit are expected to have longer service life (Sharp 1985).

This chapter presents the effect of fines content on the permanent deformation behaviour of the gravel, limestone, and granite UGM evaluated in this study. The permanent deformation behaviour was evaluated based on the changes in permanent strain, permanent strain rate, and shakedown behaviour.

8.2 Test Results and Modeling of Permanent Deformation Behaviour

Figures 8.1 to 8.3 show the permanent deformation of gravel, limestone, and granite UGM gradations, respectively. Two replicates were tested at each moisture content. The permanent deformation of the gravel and limestone gradations was evaluated at 2%

below OMC and at OMC; while the permanent deformation of the granite gradation was evaluated at OMC only.

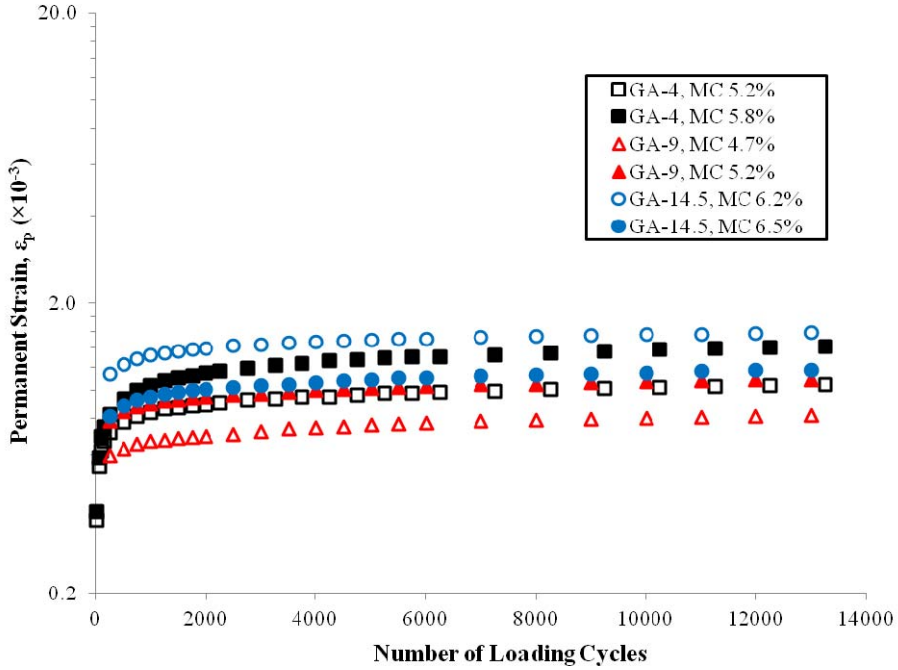

a) at 2% below OMC

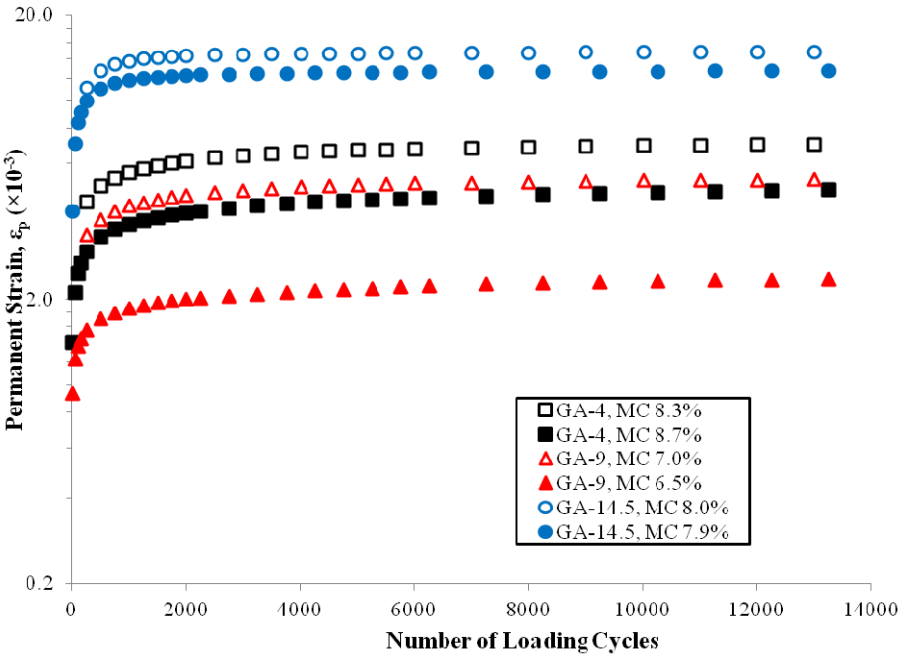

b) at OMC

FIGURE 8.1: Permanent Strain versus Number of Loading Cycles for Gravel UGM Gradations

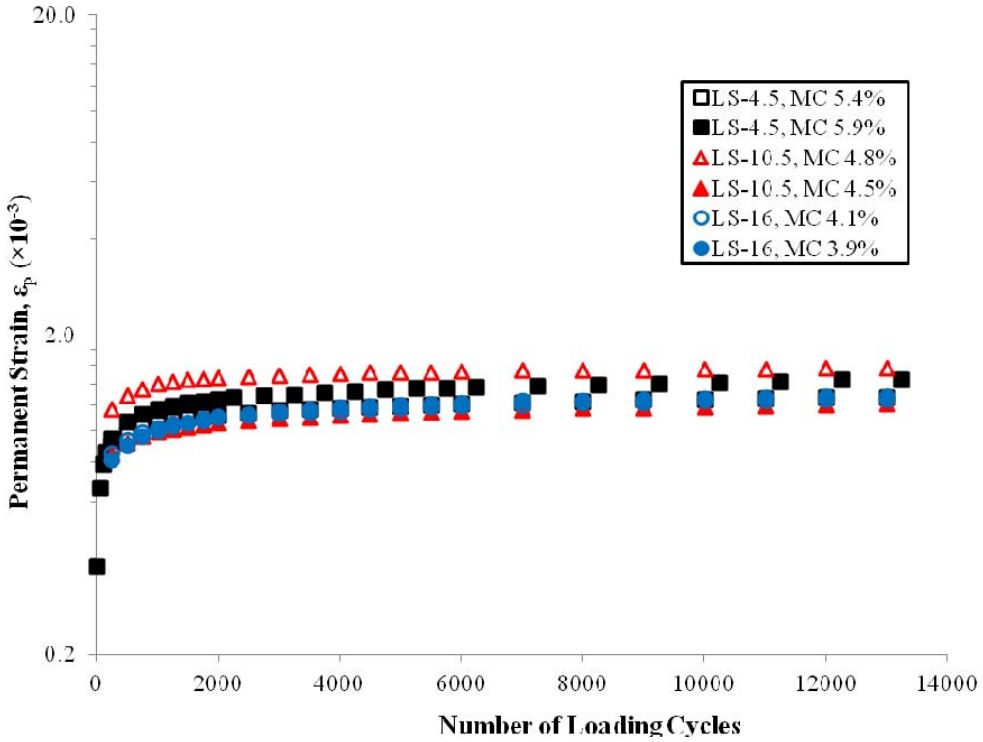

a) at 2% below OMC

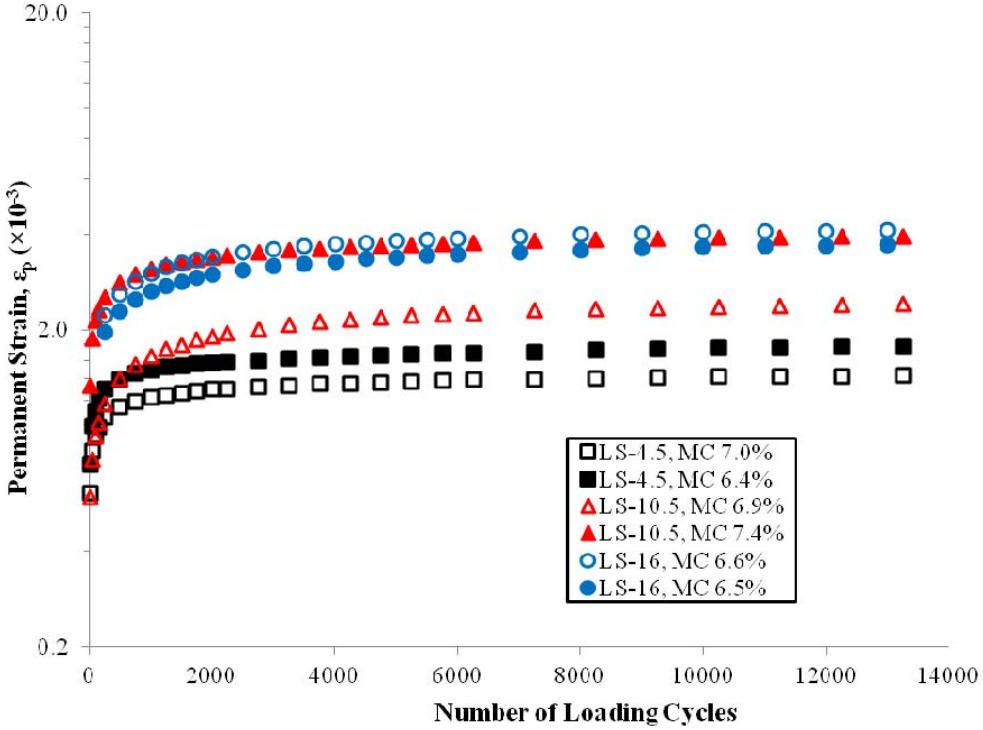

b) at OMC

FIGURE 8.2: Permanent Strain versus Number of Loading Cycles for Limestone UGM Gradations

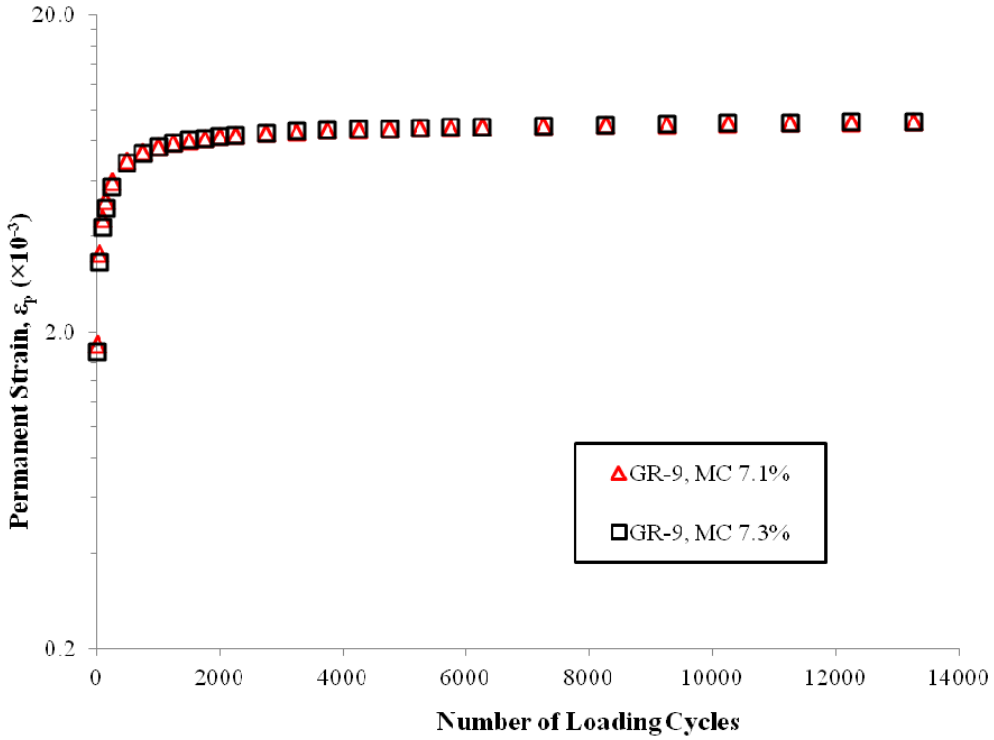

FIGURE 8.3: Permanent Strain versus Number of Loading Cycles for Granite UGM Gradation at OMC

For gravel UGM gradations, GA−9 showed an average permanent strain, at OMC and 2% below OMC, lower than the average permanent strain for GA−4 and GA−14.5. For limestone UGM gradations, the permanent strain for the three gradations at 2% below OMC were comparable; while LS−4.5 showed an average permanent strain lower than LS−10.5 and LS−16 at OMC. When comparing the permanent strain behaviour of the three material types, limestone showed lower permanent strains than gravel and granite at OMC.

Data from each permanent deformation test was fitted to the following three parameter model:

$$\varepsilon_p = \varepsilon_o e^{-\left(\frac{\rho}{N}\right)^{\beta}} \quad \textbf{(8.1)}$$

Where:

ε_p = permanent strain,

ε_o, ρ, and β = material parameters,

N = number of load cycles,

Equation 8.1 provides a good fit of permanent deformation test data for granular base and subgrade soils, and has been applied by Pavement ME to predict permanent deformation of flexible pavement layers (NCHRP, 2004; Tseng and Lytton, 1989).

Nonlinear regression techniques were used to obtain the values of the material parameters ε_o, ρ, and β for each specimen. Tables 8.1 to 8.3 show the values of the material parameters ε_o, ρ, and β for gravel, limestone, and granite specimens, respectively. Tables 8.1 to 8.3 show the total permanent strain after 13,000 loading cycles, $\varepsilon_{p,\ 13000}$, and the permanent strain rate at 13,000 cycles. The permanent strain rate and total permanent strain after 13,000 cycles represent the material performance at the end of the laboratory testing. The permanent strain rate at 13,000 cycles is the slope of the tangent to permanent strain curve (Equation 8.1) at N = 13,000. For all gravel and limestone gradations except LS−4.5, the permanent strain rate at 13,000 cycles increases with the increase of moisture content.

Figures 8.4 and 8.5 show the effect of fines content and moisture content variations, respectively, on the total permanent strain after 13,000 loading cycles for gravel and limestone materials. From Figure 8.4, GA−9 and LS−4.5 showed lower permanent strain after 13,000 cycles than the remaining gravel and limestone gradations, respectively. For gravel UGM, the permanent strain of GA−14.5 showed higher sensitivity to moisture variation than the permanent strain of GA−4 and GA−9, as shown in Figure 8.5. For limestone UGM, the permanent strain of LS−4.5 showed lower sensitivity to moisture variation than the permanent strain of LS−10.5 and LS−16.

TABLE 8.1: Permanent Deformation Regression Parameters for Gravel Gradations

Gradation ID	MC (%)	ε_o ($\times 10^{-3}$)	ρ	β	ε_p rate @ N = 13,000 ($\times 10^{-9}$/cycle)	$\varepsilon_{p,\ 13000}$ ($\times 10^{-3}$)
GA−4	5.2	1.368	35.139	0.2179	4.797	1.0452
	5.8	2.548	501.350	0.1637	10.473	1.4169
	8.3	8.028	72.784	0.3981	27.481	7.0253
	8.7	7.860	214.040	0.1808	32.322	4.8652
GA−9	4.7	2.049	4362.300	0.0788	4.553	0.8224
	5.2	2.386	750.840	0.0856	5.619	1.0883
	6.5	4.479	363.770	0.1266	14.686	2.3639
	7.0	6.026	66.220	0.3965	20.029	5.2986
GA−14.5	6.2	2.025	19.534	0.2161	6.463	1.5855
	6.5	2.518	782.340	0.0968	6.670	1.1755
	7.9	13.031	29.880	0.6537	12.119	12.7430
	8.0	14.978	71.114	0.9498	7.721	14.8860

TABLE 8.2: Permanent Deformation Regression Parameters for Limestone Gradations

Gradation ID	MC (%)	ε_o ($\times 10^{-3}$)	ρ	β	ε_p rate @ N = 13,000 ($\times 10^{-9}$/cycle)	$\varepsilon_{p,\ 13000}$ ($\times 10^{-3}$)
LS−4.5	5.4	1.617	23.770	0.2276	5.313	1.2751
	5.9	1.741	43.621	0.2919	6.130	1.4508
	6.4	2.219	15.635	0.2217	6.806	1.7762
	7.0	1.764	13.745	0.2354	5.215	1.4372
LS−10.5	4.5	1.674	34.902	0.1916	5.752	1.2147
	4.8	1.636	34.521	0.5468	2.853	1.5771
	6.9	5.369	2647.100	0.1619	23.853	2.4219
	7.4	5.940	98.219	0.1899	23.104	3.9587
LS−16	3.9	1.567	70.047	0.3129	6.054	1.2819
	4.1	1.566	36.385	0.2577	5.477	1.2508
	6.5	5.264	242.450	0.2708	26.546	3.7234
	6.6	5.150	162.130	0.3519	24.067	4.1361

TABLE 8.3: Permanent Deformation Regression Parameters for Granite Gradation

Gradation ID	MC (%)	ε_o ($\times 10^{-3}$)	ρ	β	ε_p rate @ N = 13,000 ($\times 10^{-9}$/cycle)	$\varepsilon_{p,\ 13000}$ ($\times 10^{-3}$)
GR−9	7.1	10.328	52.539	0.4006	31.351	9.1886
	7.3	10.452	62.926	0.4049	33.503	9.2228

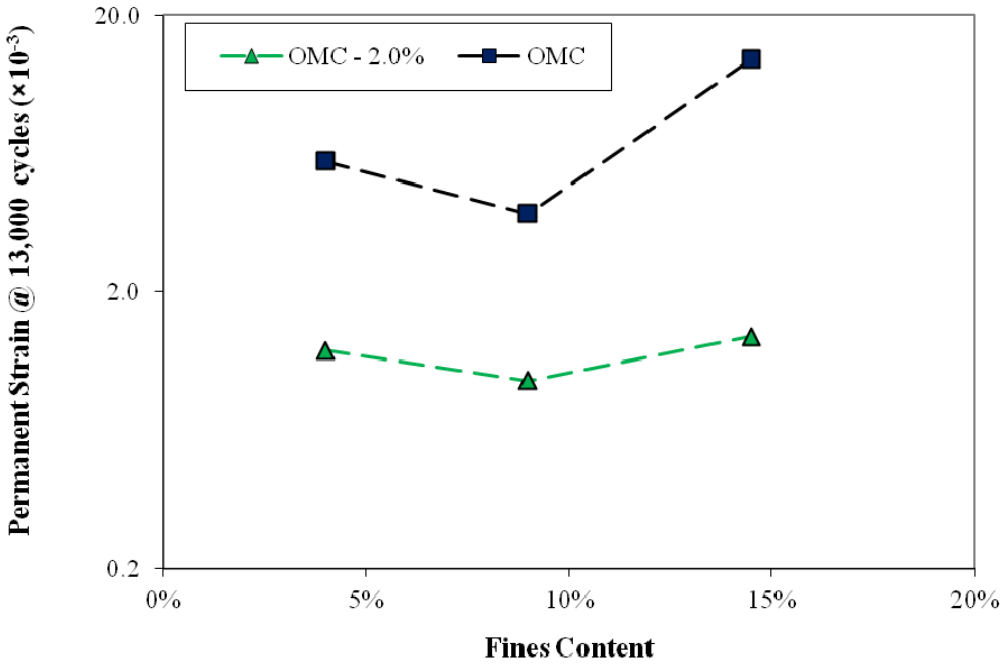

a) Gravel UGM

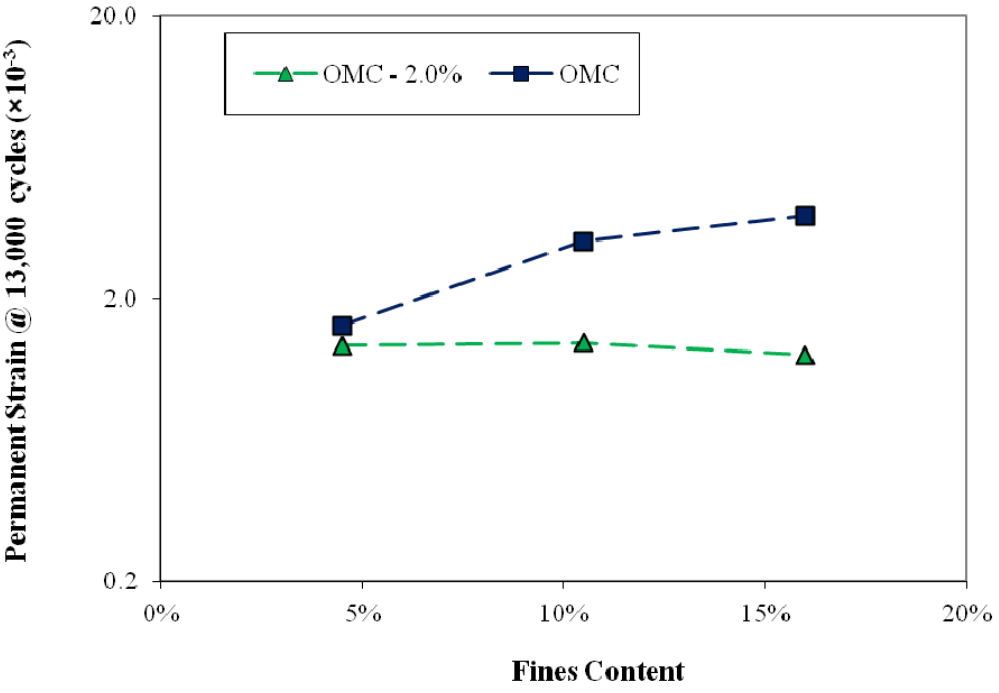

b) Limestone UGM

FIGURE 8.4: Effect of Fines Content Variation on Permanent Strain after 13,000 Cycles

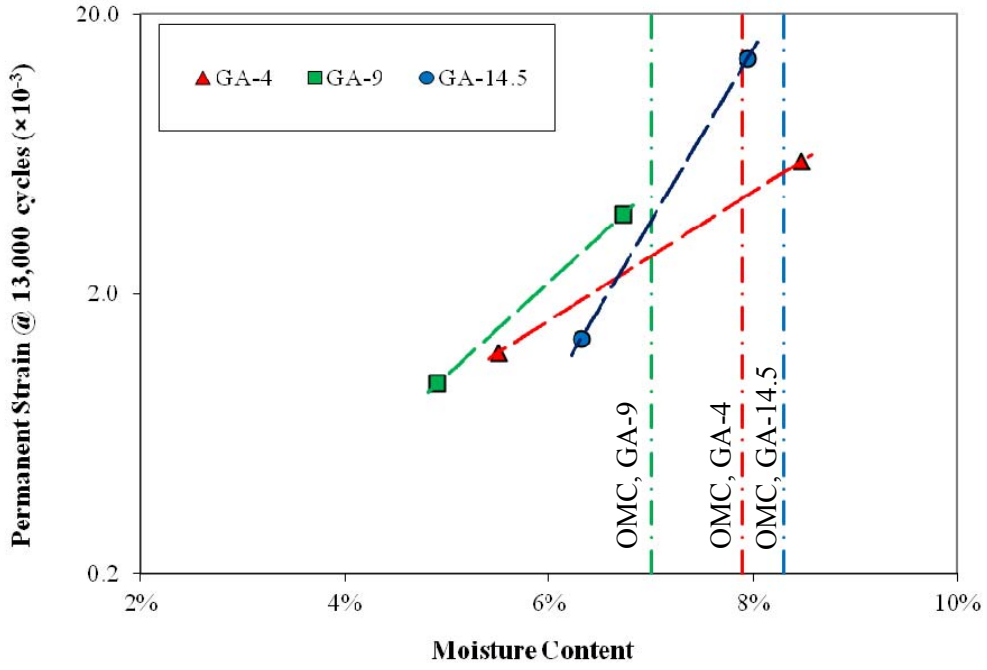

a) Gravel UGM

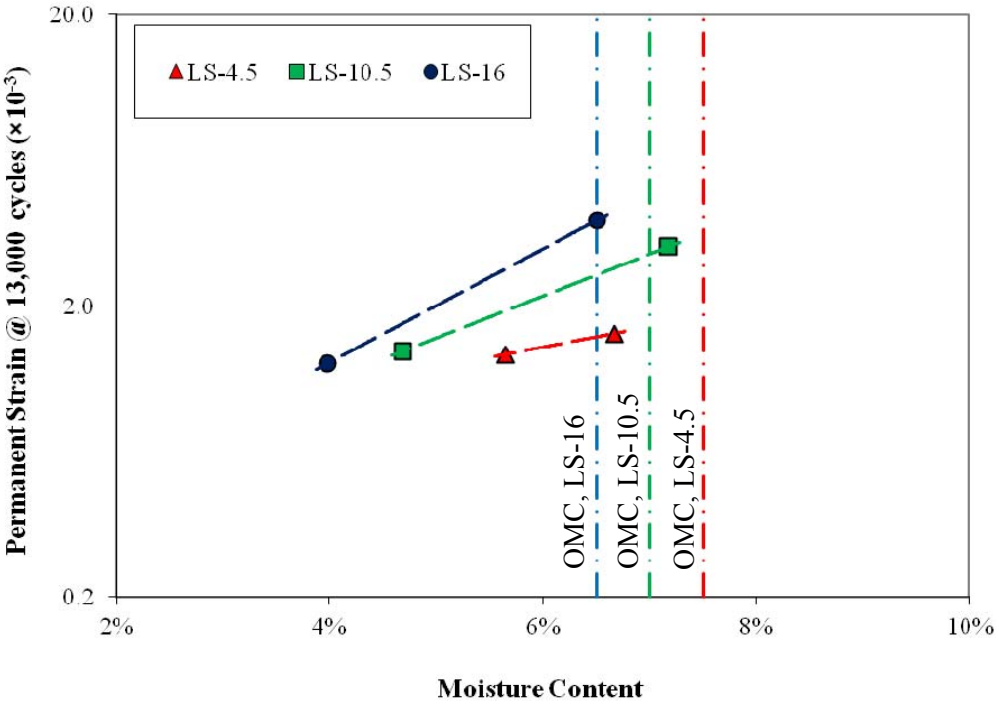

b) Limestone UGM

FIGURE 8.5: Effect of Moisture Variation on Permanent Strain after 13,000 Cycles

8.3 Effect of Fines Content and Moisture Content on Shakedown Behaviour

The deformation behaviour of UGM can be classified, according to shakedown approach, based on one of the three following criteria:

1. Accumulated permanent deformation between 3000 and 5000 cycles: as shown in Figure 8.6a, a lower accumulated permanent strain indicates more elastic behaviour of UGM. The selection of the accumulated permanent strain between 3000 and 5000 loading cycles was established based on extensive testing program of UGM (Bilodeau et al., 2011; European Committee for Standardization, 2004).
2. Change in permanent strain rate with the increase of permanent strain: as shown in Figure 8.6b, a progressive decrease in permanent strain rate with the increase of total permanent strain indicates more elastic behaviour of UGM and vice versa (Werkmeister et al., 2004).
3. Change in resilient strain with the increase of number of loading cycles: as shown in Figure 8.6c, a material with plastic shakedown or plastic creep behaviour exhibits a constant resilient strain while a significant decrease of resilient strain is observed for materials within the incremental collapse zone (Werkmeister et al., 2004).

In some cases, the boundaries between plastic shakedown, plastic creep and incremental collapse zones cannot be distinguished based on permanent strain response only (Werkmeister et al., 2004). Using both permanent strain and resilient strain responses, the

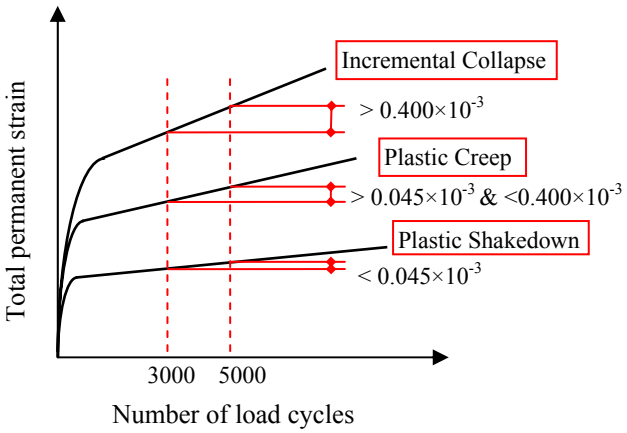

a) based on accumulated permanent strain

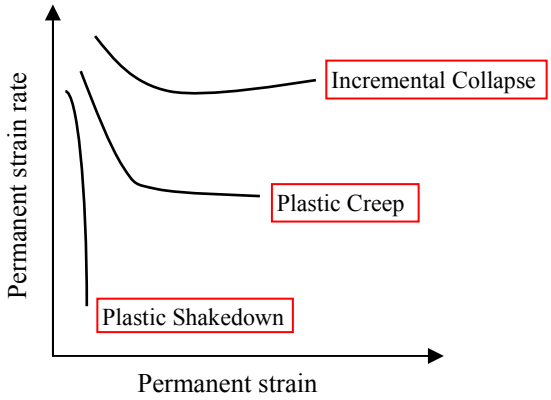

b) based on change in permanent strain rate

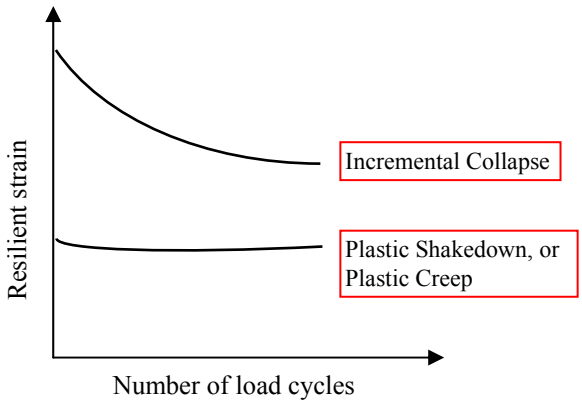

c) based on change in resilient strain

FIGURE 8.6: Three Alternative Criteria for Classification of Deformation Behaviour of UGM based on Shakedown Approach (Werkmeister et al., 2004)

three criteria described above can be applied to predict the deformation behaviour of UGM.

The deformation behaviour of UGM can be classified based on the accumulated permanent strain between 3000 and 5000 loading cycles, $\varepsilon_{p,\,3000}$ and $\varepsilon_{p,\,5000}$ respectively, as follows (Bilodeau et al., 2011; European Committee for Standardization, 2004):

- Plastic shakedown: $\varepsilon_{p,\,5000} - \varepsilon_{p,\,3000} < 0.045 \times 10^{-3}$
- Plastic creep: $0.045 \times 10^{-3} < \varepsilon_{p,\,5000} - \varepsilon_{p,\,3000} < 0.400 \times 10^{-3}$
- Incremental collapse: $\varepsilon_{p,\,5000} - \varepsilon_{p,\,3000} > 0.400 \times 10^{-3}$

Tables 8.4 to 8.6 show the deformation behaviour of gravel, limestone, and granite gradations, respectively, according to the shakedown approach. As shown in Table 8.4, the deformation behaviour of all gravel gradations is within the plastic creep zone at OMC. Below OMC, GA−9 showed more elastic behaviour than GA−4 and GA−14.5 where the deformation behaviour of the two specimens is within the plastic shakedown zone. For limestone gradations, LS−4.5 showed more elastic behaviour than LS−10.5 and LS−16 at OMC, as shown in Table 8.5. For LS-4.5 gradation, one specimen response at OMC is within the plastic shakedown zone and the second specimen behaviour is at the boundary between plastic shakedown and plastic creep zones. For the GR-9 granite gradation, the response of the two specimen at OMC is within the plastic creep zone, as shown in Table 8.6.

TABLE 8.4: Classification of Gravel Gradations According to Shakedown Behaviour

Gradation ID	MC (%)	γ_{dry} (kg/m^3)	$\varepsilon_{p,\,5000}$ ($\times 10^{-3}$)	$\varepsilon_{p,\,3000}$ ($\times 10^{-3}$)	$\varepsilon_{p,\,5000} - \varepsilon_{p,\,3000}$ ($\times 10^{-3}$)	Deformation behaviour
GA−4	5.2	2150	0.9722	0.9325	0.0397	Plastic shakedown
	5.8	2145	1.2839	1.2064	0.0775	Plastic creep
	8.3	2162	6.6964	6.4360	0.2604	Plastic creep
	8.7	2142	4.4731	4.2355	0.2377	Plastic creep
GA−9	4.7	2196	0.7611	0.7228	0.0383	Plastic shakedown
	5.2	2206	1.0157	0.9754	0.0403	Plastic shakedown
	6.5	2205	2.1852	2.0809	0.1044	Plastic creep
	7.0	2203	5.0681	4.8442	0.2239	Plastic creep
GA−14.5	6.2	2181	1.4986	1.4468	0.0518	Plastic creep
	6.5	2180	1.0900	1.0432	0.0468	Plastic creep
	7.9	2199	12.5867	12.4429	0.1438	Plastic creep
	8.0	2183	14.6968	14.5524	0.1444	Plastic creep

Figures 8.7 to 8.9 show the change in permanent strain rate with the increase of permanent strain for gravel, limestone, and granite gradations, respectively. As shown in Figure 8.7a, the permanent strain rate below OMC showed a steep decrease with a very small increase in permanent deformation for all gravel gradations. This deformation pattern indicates a plastic shakedown behaviour for all gravel gradation below OMC. From Figure 8.7b, GA−14.5 at OMC showed larger permanent strains and slower decrease in permanent strain rate than GA−4 and GA−9. This deformation pattern indicates an incremental collapse behaviour of GA−14.5. The intermediate response of

GA−4 and GA−9 at OMC, compared to all gradation behaviour below OMC and GA−14.5 behaviour at OMC, indicates plastic creep behaviour (Werkmeister et al., 2004).

TABLE 8.5: Classification of Limestone Gradations According to Shakedown Behaviour

Gradation ID	MC (%)	γ_{dry} (kg/m^3)	$\varepsilon_{p,\,5000}$ ($\times 10^{-3}$)	$\varepsilon_{p,\,3000}$ ($\times 10^{-3}$)	$\varepsilon_{p,\,5000} - \varepsilon_{p,\,3000}$ ($\times 10^{-3}$)	Deformation behaviour
LS−4.5	5.4	2142	1.1992	1.1616	0.0376	Plastic shakedown
	5.9	2186	1.3541	1.2977	0.0563	Plastic creep
	6.4	2189	1.6751	1.6157	0.0594	Plastic creep
	7.0	2187	1.3811	1.3464	0.0347	Plastic shakedown
LS−10.5	4.5	2260	1.1371	1.0940	0.0431	Plastic shakedown
	4.8	2269	1.5284	1.4961	0.0324	Plastic shakedown
	6.9	2266	2.2087	2.0491	0.1596	Plastic creep
	7.4	2275	3.7122	3.5418	0.1704	Plastic creep
LS−16	3.9	2287	1.2091	1.1575	0.0516	Plastic creep
	4.1	2298	1.1816	1.1367	0.0448	Plastic shakedown
	6.5	2301	3.3950	3.1789	0.2160	Plastic creep
	6.6	2300	3.8345	3.6052	0.2292	Plastic creep

Similar to classification of gravel gradation responses and based on Figure 8.8, the deformation behaviour of all limestone gradations below OMC is within the plastic shakedown zone. At OMC, the deformation behaviour of LS−4.5 is within the plastic shakedown zone, while the behaviour of LS−10.5 and LS−16 is within the plastic creep

zone. When compared to the behaviour of gravel and limestone gradations, the deformation behaviour of granite gradation GR-9 is at the boundary between plastic creep and incremental collapse zones, as shown in Figure 8.9.

TABLE 8.6: Classification of Granite Gradation According to Shakedown Behaviour

Gradation ID	MC (%)	γ_{dry} (kg/m^3)	$\varepsilon_{p,\,5000}$ ($\times 10^{-3}$)	$\varepsilon_{p,\,3000}$ ($\times 10^{-3}$)	$\varepsilon_{p,\,5000} - \varepsilon_{p,\,3000}$ ($\times 10^{-3}$)	Deformation behaviour
GR−9	7.1	2277	8.7736	8.5311	0.2425	Plastic creep
	7.3	2291	8.7914	8.5446	0.2468	Plastic creep

In terms of the resilient strain (ε_r) response, granular materials with plastic shakedown or plastic creep behaviour incur a constant level of resilient strain, with minor changes within the post-compaction period, during permanent deformation testing. The resilient strain level depends on UGM properties and stress level. Granular materials with incremental collapse behaviour incur a significant decrease of resilient strain with the increase of loading cycles (Werkmeister et al., 2004).

According to the resilient strain responses shown in Figures 8.10 and 8.11, all gravel and limestone gradations have either plastic shakedown or plastic creep behaviour except GA−14.5. GA−14.5 showed significant decrease in resilient strain with the increase of loading cycles at OMC which indicates an incremental collapse behaviour. Similar to GA-14.5, GR-9 showed significant decrease in resilient strain with the increase of loading cycles at OMC, as shown in Figure 8.12, which indicates an incremental collapse behaviour.

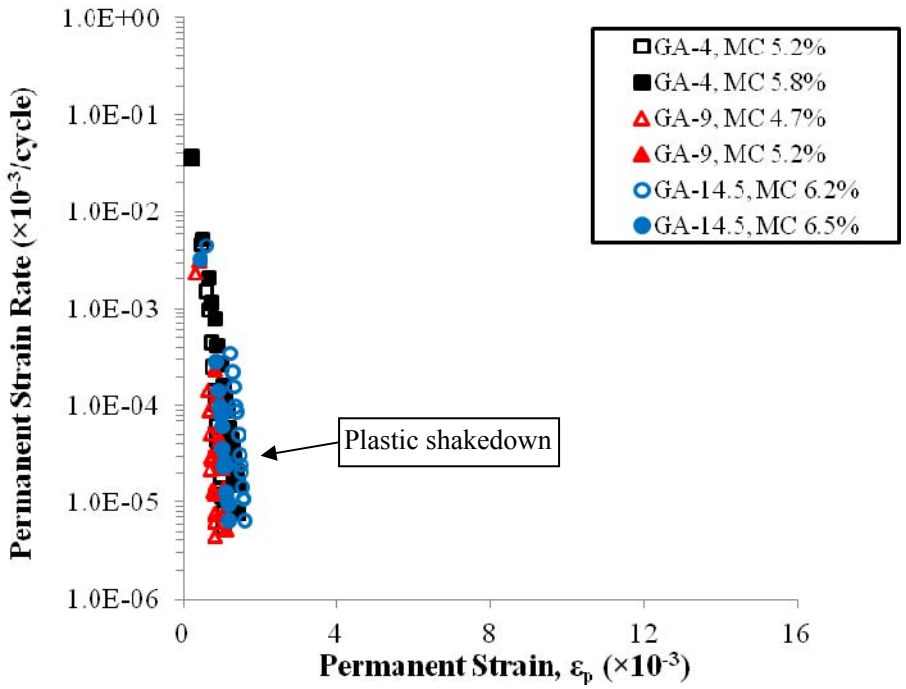

a) at 2% below OMC

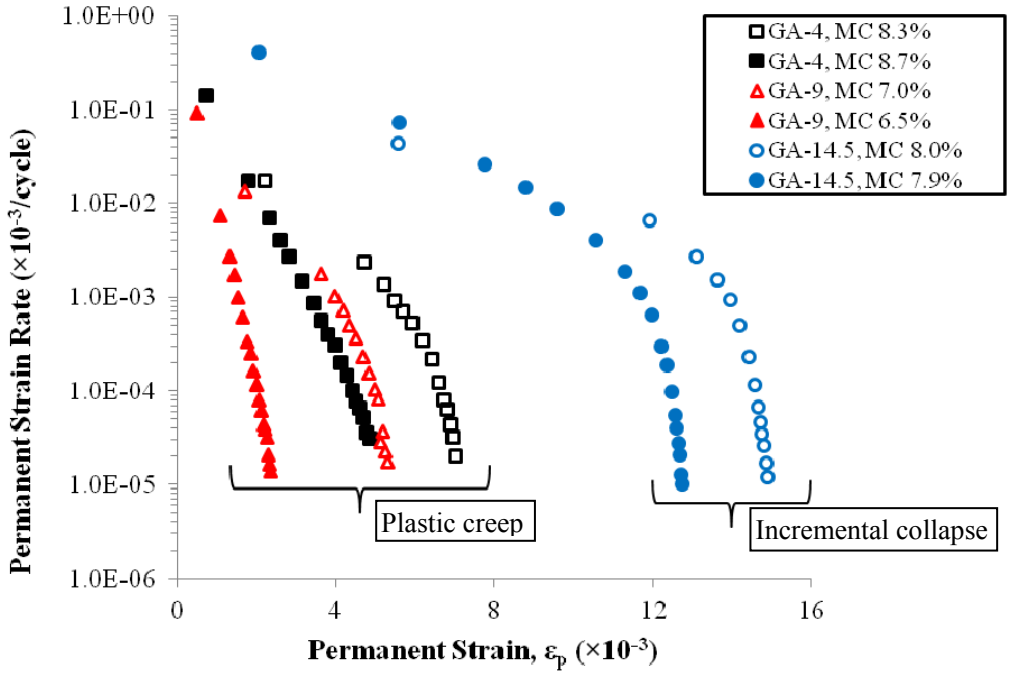

b) at OMC

FIGURE 8.7: Permanent Deformation Rate versus Permanent Strain for Gravel UGM

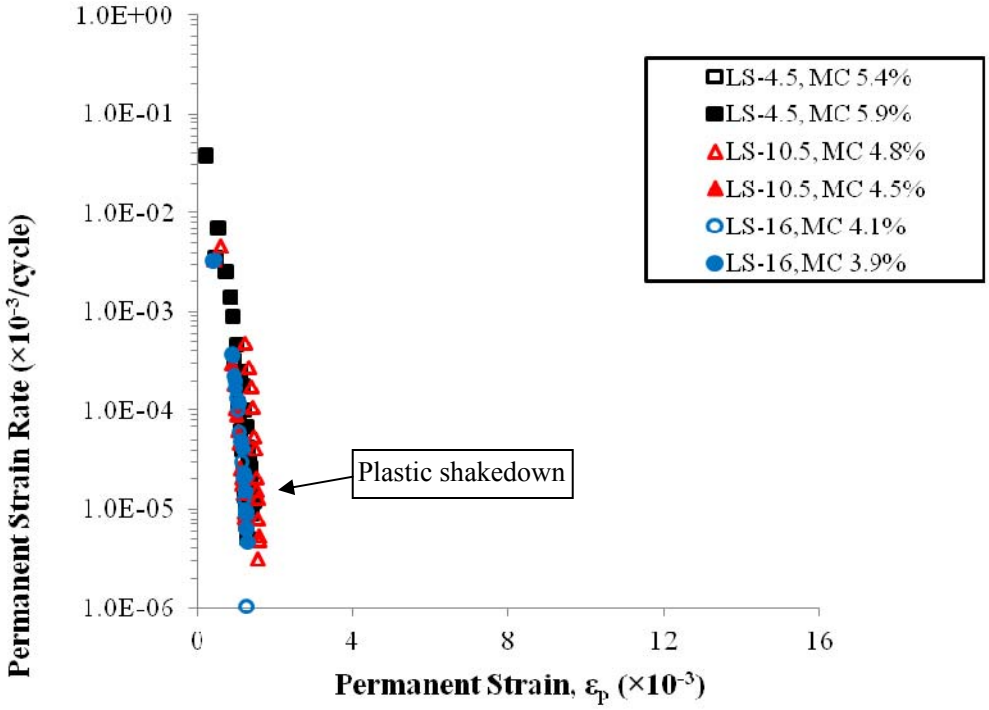

a) at 2% below OMC

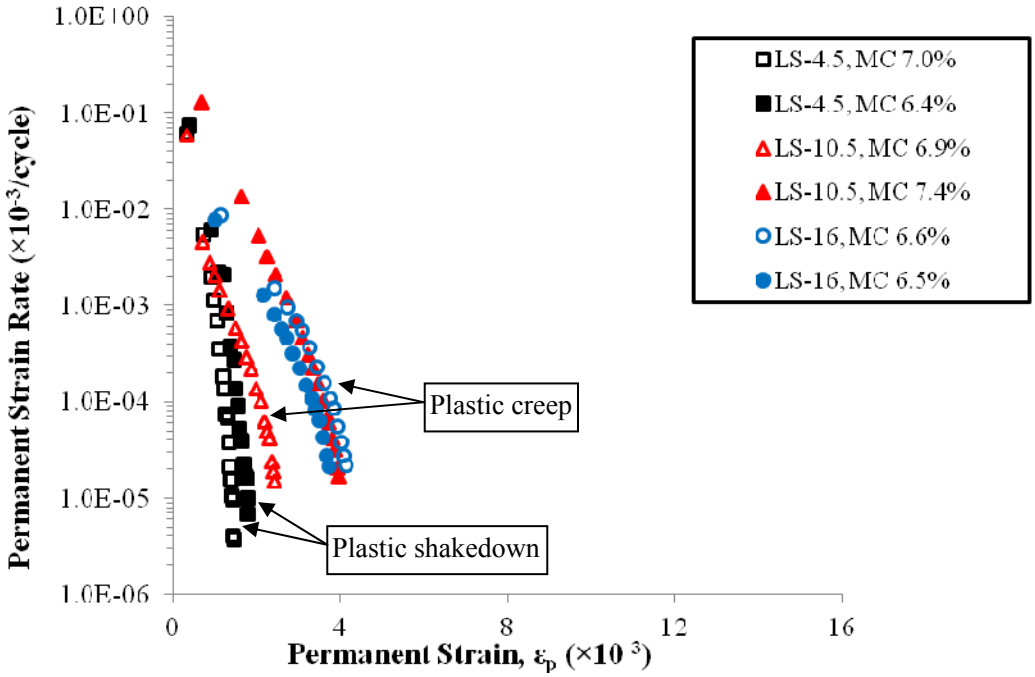

b) at OMC

FIGURE 8.8: Permanent Deformation Rate versus Permanent Strain for Limestone UGM

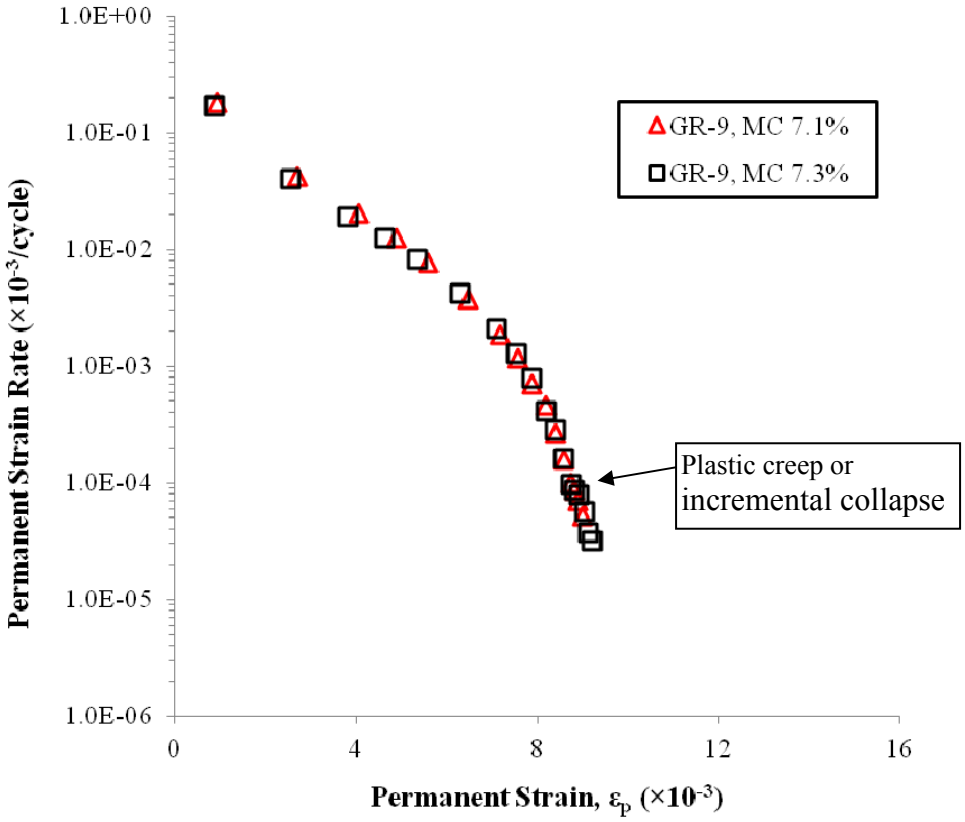

FIGURE 8.9: Permanent Strain Rate versus Permanent Strain for Granite UGM

8.4 Summary and Discussion

Permanent deformation in UGM occurs due to slip and relative motion at the interface between particles (Barber and Ciavarella, 2000). The resistance of UGM particles to slip at a given stress state depends on the friction and cohesion between the particles (shear strength). Friction between particles depends on aggregate type, shape (crushed or uncrushed), aggregate mineralogy, and gradation. Cohesion between particles is mainly controlled by the type and amount of fines in UGM. Cohesion can be due to electrostatic forces from clay fines or cementing action from calcareous fines. The shear strength of UGM is also affected by moisture content.

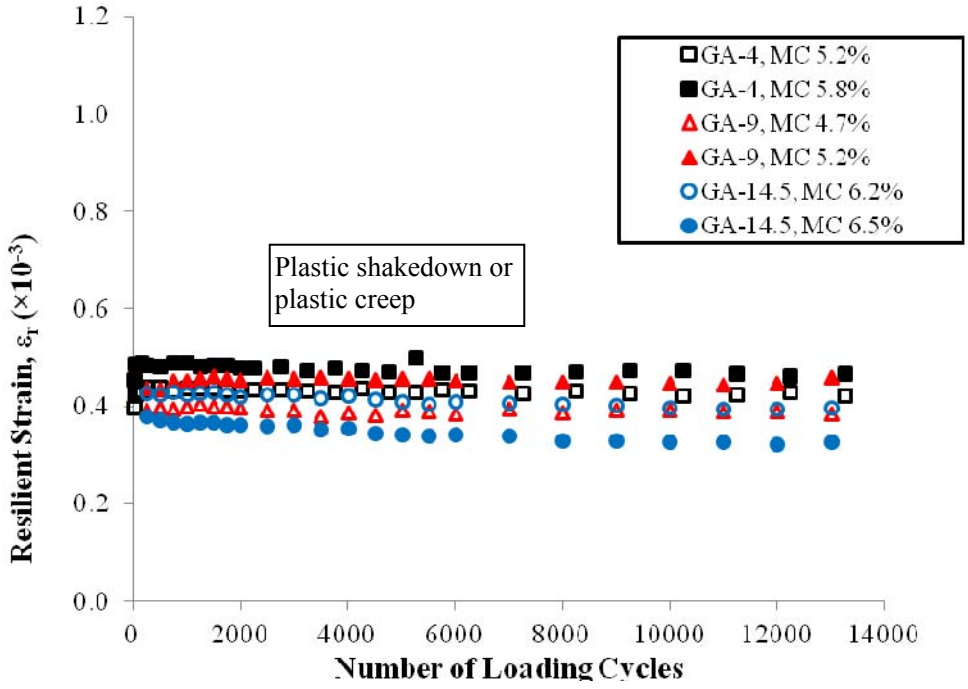

a) at 2% below OMC

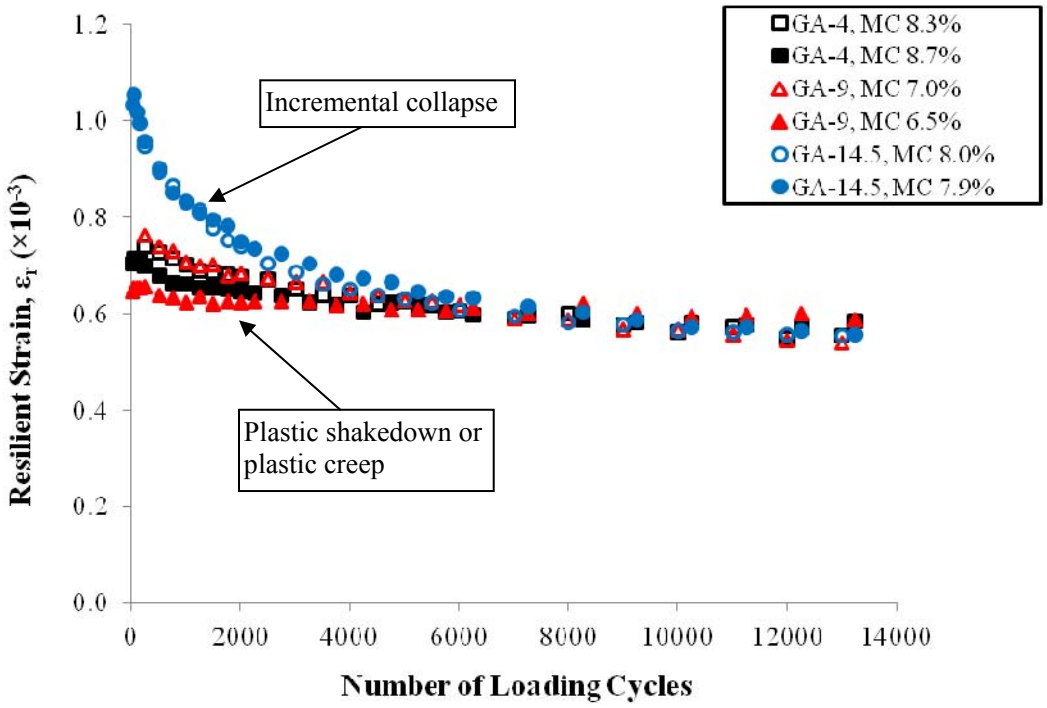

b) at OMC

FIGURE 8.10: Resilient Strain versus Number of Loading Cycles for Gravel UGM

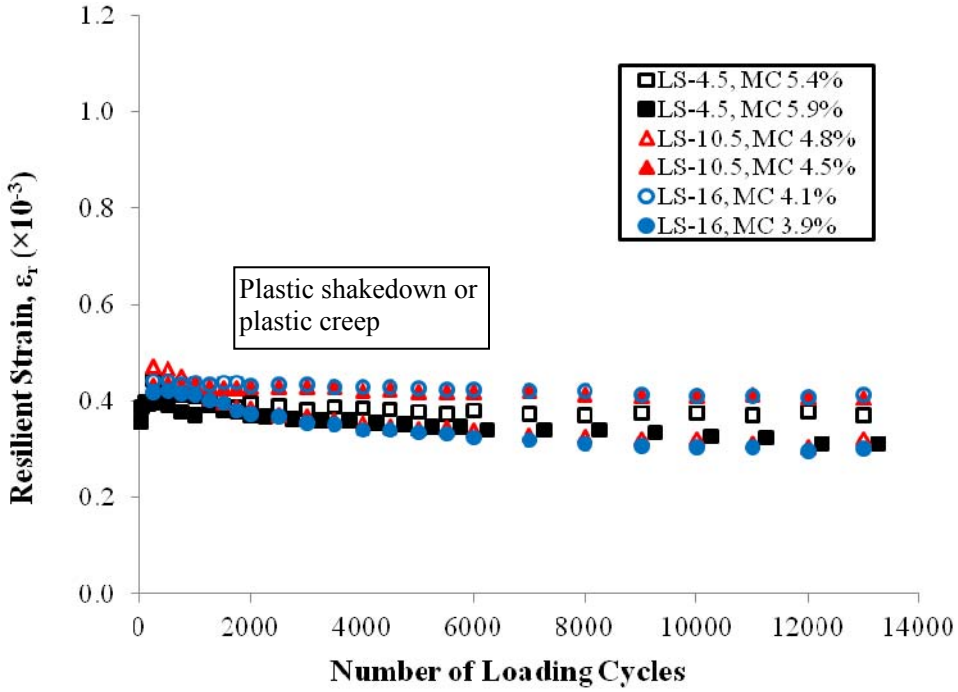

a) at 2% below OMC

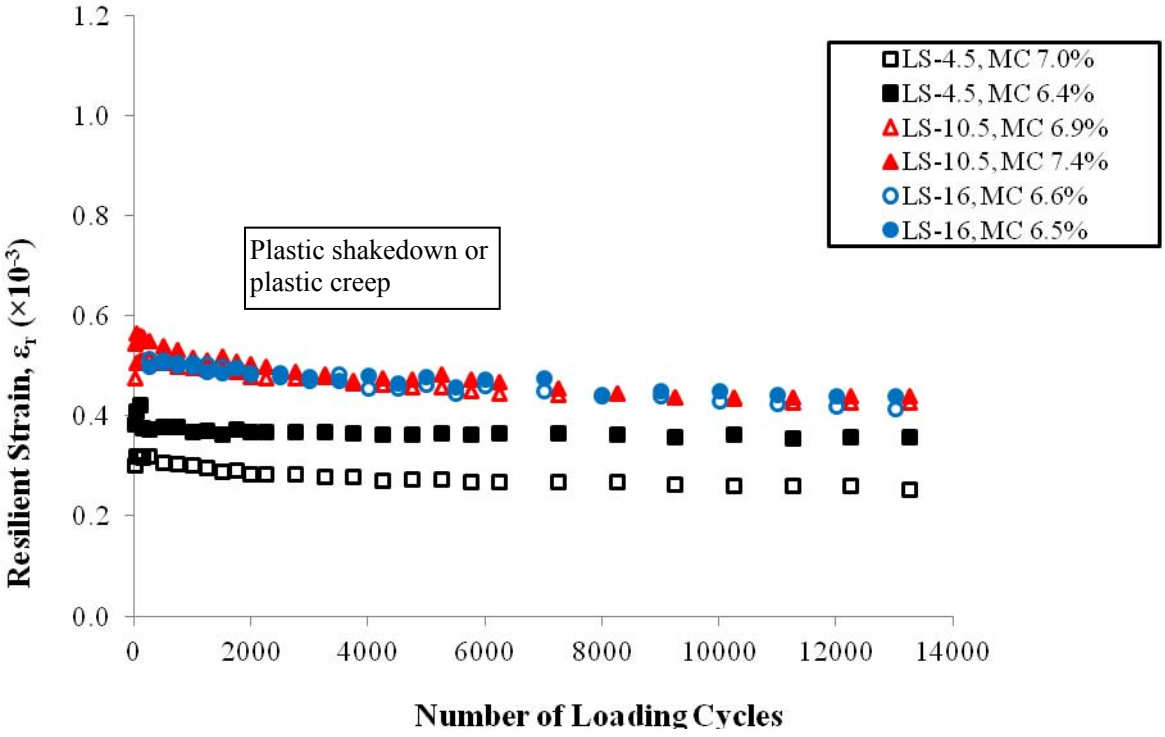

b) at OMC

FIGURE 8.11: Resilient Strain versus Number of Loading Cycles for Limestone UGM

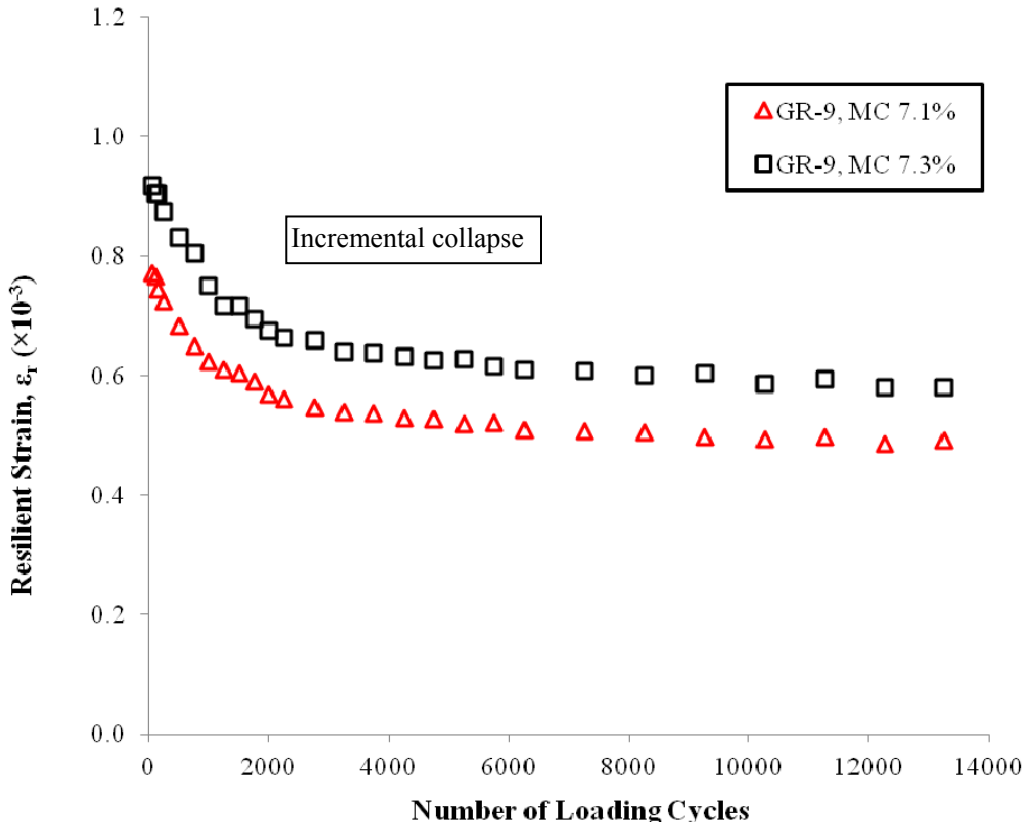

FIGURE 8.12: Resilient Strain versus Number of Loading Cycles for Granite UGM

A laboratory investigation was conducted to evaluate the effect of fines content and moisture content on permanent deformation behaviour of two types of UGM: gravel and 100% crushed limestone. Limited testing was conducted on granite UGM. It included one fines content and at OMC only. For limestone UGM, results showed that a gradation with fines content of 4.5% has better resistance to permanent deformation with less sensitivity to moisture variation than gradations with 10.5% and 16% fines. For gravel UGM, an optimum fines content of 9% showed better resistance to permanent deformation than 4% and 14.5% fines contents.

The shakedown approach was used to characterize the deformation behaviour of the tested materials. Materials were classified according to accumulated permanent deformation between 3000 and 5000 loading cycles, change of permanent strain rate with the increase of permanent strain, and change of resilient strain with the increase of number of loading cycles. Tables 8.7 to 8.9 show the classification of gravel, limestone and granite gradations, respectively, based on these three criteria.

At 2% below OMC, gravel and limestone materials had a deformation behaviour within the plastic shakedown zone. At OMC, limestone with 4.5% fines maintained its deformation response within the plastic shakedown zone, while gravel with 14.5% fines moved to the incremental collapse zone with higher plastic strains. All other gravel and limestone gradations had a deformation response within the plastic creep zone at OMC. Table 8.9 shows that the deformation response of the granite gradation is at the boundary between plastic creep and incremental collapse zones.

Tables 8.7 to 8.9 show that permanent strain and resilient strain responses must be used together to evaluate the deformation behaviour of UGM.

TABLE 8.7: Classification of Gravel Gradations based on ε_r, ε_p Rate, and Accumulated ε_p between 3000 and 5000 Loading Cycles

Gradation ID	MC (%)	Deformation behaviour classification based on		
		ε_r	ε_p rate	Accumulated ε_p between 3000 and 5000 cycles
GA−4	5.2	Plastic shakedown or plastic creep	Plastic shakedown	Plastic shakedown
	5.8	Plastic shakedown or plastic creep	Plastic shakedown	Plastic creep
	8.3	Plastic shakedown or plastic creep	Plastic creep	Plastic creep
	8.7	Plastic shakedown or plastic creep	Plastic creep	Plastic creep
GA−9	4.7	Plastic shakedown or plastic creep	Plastic shakedown	Plastic shakedown
	5.2	Plastic shakedown or plastic creep	Plastic shakedown	Plastic shakedown
	6.5	Plastic shakedown or plastic creep	Plastic creep	Plastic creep
	7.0	Plastic shakedown or plastic creep	Plastic creep	Plastic creep
GA−14.5	6.2	Plastic shakedown or plastic creep	Plastic shakedown	Plastic creep
	6.5	Plastic shakedown or plastic creep	Plastic shakedown	Plastic creep
	7.9	Incremental collapse	Incremental collapse	Plastic creep
	8.0	Incremental collapse	Incremental collapse	Plastic creep

TABLE 8.8: Classification of Limestone Gradations based on ε_r, ε_p Rate, and Accumulated ε_p between 3000 and 5000 Loading Cycles

Gradation ID	MC (%)	Deformation behaviour classification based on		
		ε_r	ε_p rate	Accumulated ε_p between 3000 and 5000 cycles
LS−4.5	5.4	Plastic shakedown or plastic creep	Plastic shakedown	Plastic shakedown
	5.9	Plastic shakedown or plastic creep	Plastic shakedown	Plastic creep
	6.4	Plastic shakedown or plastic creep	Plastic shakedown	Plastic creep
	7.0	Plastic shakedown or plastic creep	Plastic shakedown	Plastic shakedown
LS-10.5	4.5	Plastic shakedown or plastic creep	Plastic shakedown	Plastic shakedown
	4.8	Plastic shakedown or plastic creep	Plastic shakedown	Plastic shakedown
	6.9	Plastic shakedown or plastic creep	Plastic creep	Plastic creep
	7.4	Plastic shakedown or plastic creep	Plastic creep	Plastic creep
LS−16	3.9	Plastic shakedown or plastic creep	Plastic shakedown	Plastic creep
	4.1	Plastic shakedown or plastic creep	Plastic shakedown	Plastic shakedown
	6.5	Plastic shakedown or plastic creep	Plastic creep	Plastic creep
	6.6	Plastic shakedown or plastic creep	Plastic creep	Plastic creep

TABLE 8.9: Classification of Granite Gradation based on ε_r, ε_p Rate, and Accumulated ε_p between 3000 and 5000 Loading Cycles

Gradation ID	MC (%)	Deformation behaviour classification based on		
		ε_r	ε_p rate	Accumulated ε_p between 3000 and 5000 cycles
GR−9	7.1	Incremental collapse	plastic creep or Incremental collapse	Plastic creep
	7.3	Incremental collapse	plastic creep or Incremental collapse	Plastic creep

9 Assessing the Behaviour of UGM Using the Dissipated Energy Approach

9.1 Introduction

The dissipated energy approach has been utilized in the literature to characterize the behaviour of viscoelastic and elastic-plastic materials. The dissipated energy approach is a damage based criteria. It was adopted in several studies to characterize the fatigue and deformation behaviour of asphalt concrete mixtures (Ghuzlan and Carpenter 2000, 2006; Widyatmoko et al. 1999a, 1999b). Cao and Law (1992) have also used the dissipated energy approach to characterize the dynamic behaviour of clay soils under cyclic loading.

Figure 9.1 shows the change in the permanent strain rate with the increase of number loading cycles for a typical UGM. The behaviour of UGM is divided into three regions based on the change in permanent strain rate: post compaction zone, stable zone, and unstable zone. In the post compaction zone, UGM experiences a high permanent strain rate which decreases with the increase of number of loading cycles due to the continuing compaction of UGM under traffic loading. In the stable zone, UGM experiences a constant permanent strain rate with the increase of number of loading cycles. In the unstable zone, UGM experiences a stiffening behaviour with a rapid increase in permanent strain rate until failure. UGM layers must be designed to remain within the stable zone during their service life to avoid premature failure.

This chapter discusses the relationship between the dissipated energy and the deformation behaviour of the gravel and limestone materials evaluated in this study. The effect of fines content and moisture content variation on the dissipated energy is also investigated.

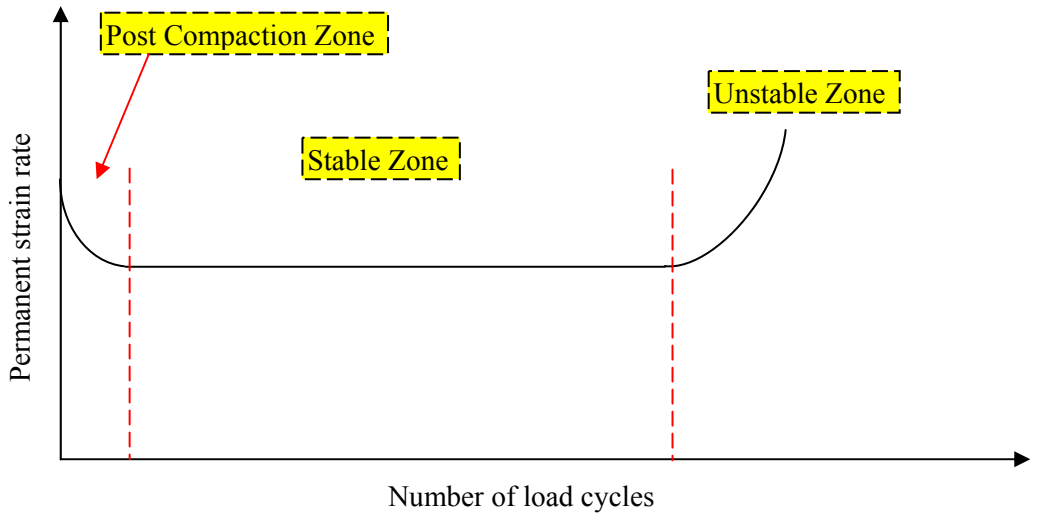

FIGURE 9.1: Permanent Strain Rate versus Number of Loading Cycles for Typical UGM

9.2 Dissipated Energy in UGM

Figure 9.2 shows a stress-strain hysteresis loop for UGM under cyclic pulse loading. According to Figure 9.2, the total energy, W_T, in any loading cycle consists of two components: elastic (stored) stain energy, W_e, and dissipated energy, W_d, as indicated by Equation 9.1.

$$W_T = W_e + W_d \quad \textbf{(9.1)}$$

When all the strain is recovered after releasing the load and the UGM has no permanent deformation, the dissipated energy consists only of the hysteretic energy, W_h. When the UGM undergo permanent strain, as shown in Figure 9.2, the dissipated energy consists of the hysteretic energy and the plastic energy, W_p, as indicated by Equation 9.2. The hysteretic energy is the dissipated energy due to the internal friction and rearrangement of UGM particles during the loading and unloading process. The plastic energy is the dissipated energy due to the irreversible movement and attrition of UGM particles under loading. Cao and Law (1992) reported that the deformation behaviour of clay soils is related to the dissipated energy under cyclic loading.

$$W_d = W_h + W_p \tag{9.2}$$

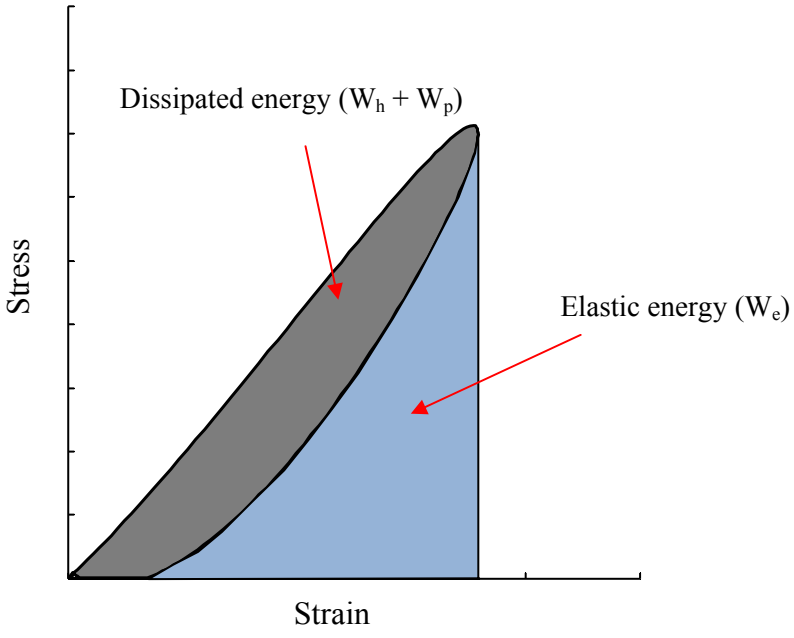

FIGURE 9.2: Stress-Strain Hysteresis Loop for UGM under Cyclic Pulse Loading

9.3 Effect of Stress Level and Fines Content on Hysteresis Loops

Figures 9.3 and 9.4 show the stress-strain hysteresis loops for gravel and limestone gradations, respectively, obtain from multistage repeated triaxial testing at different stress ratios. The stress ratio is the ratio of the deviator stress to the confining pressure as indicated by Equation 9.3.

$$Stress\ Ratio = \frac{\sigma_d}{\sigma_3} \quad \textbf{(9.3)}$$

Where:

σ_d = deviator stress, kPa

σ_3 = confining pressure, kPa

Figure 9.3 Shows that GA-14.5 had wider hysteresis loop than GA-4 and GA-9 at stress ratios 1.2 and 2.4, initial loading stages, which indicates higher dissipated energy. GA-14.5 showed also higher plastic strain than GA-4 and GA-9. The higher dissipated energy and plastic strain for GA-14.5 indicates more reversible and irreversible displacements of particles than GA-4 and GA-9. At low stress ratio, breakage of particles at interlock may exist but it has an insignificant contribution to the plastic strain which is mainly due to irreversible movement of particles. GA-14.5 showed higher plastic strain than GA-4 and GA-9 at all stress ratios, while GA-9 showed the lowest plastic strain. According to the slope of the hysteresis loops, GA-4 showed lower resilient modulus than GA-9 and GA-14.5 at all stress ratios.

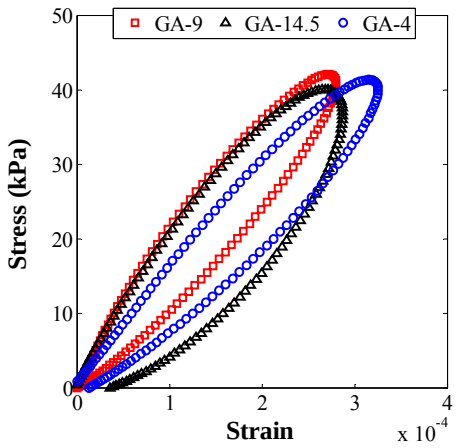

a) Stress ratio = 1.2

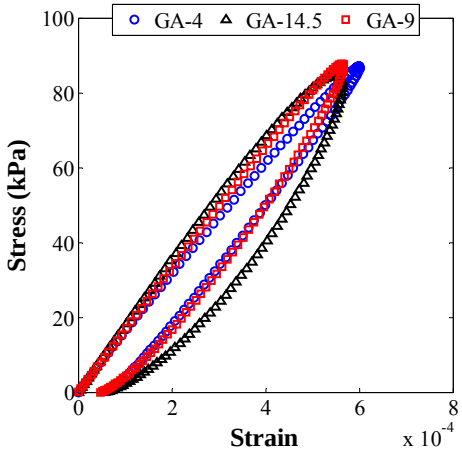

b) Stress ratio = 2.4

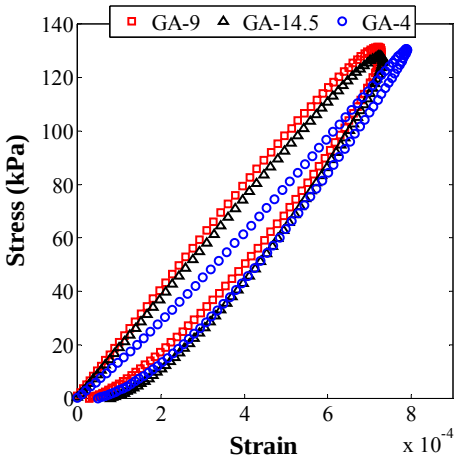

c) Stress ratio = 3.6

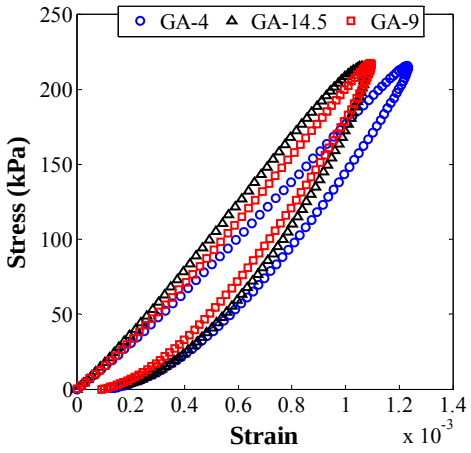

d) Stress ratio = 6.0

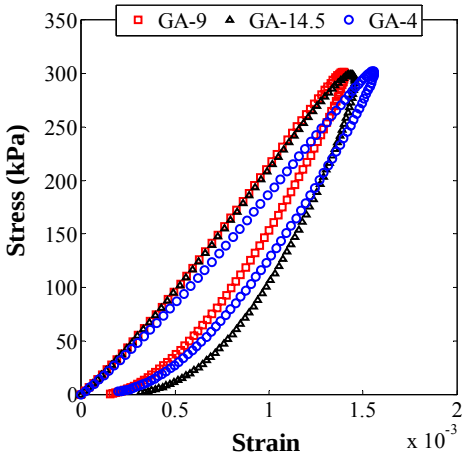

e) Stress ratio = 8.4

FIGURE 9.3: Stress-Strain Hysteresis Loops for Gravel Gradations at OMC and Confining Pressure = 36.6 kPa

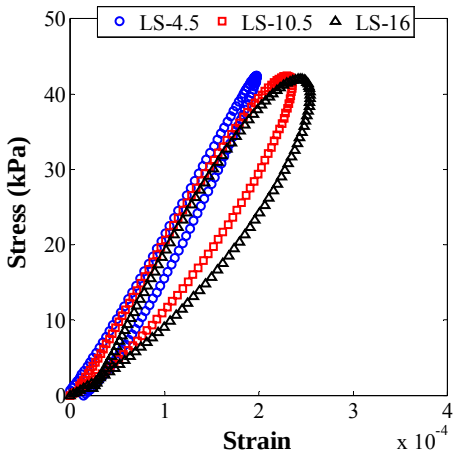

a) Stress ratio = 1.0

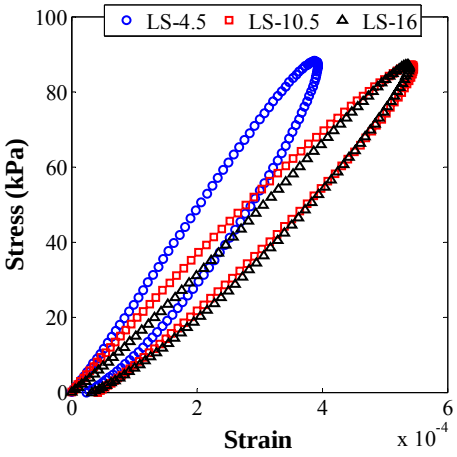

b) Stress ratio = 2.1

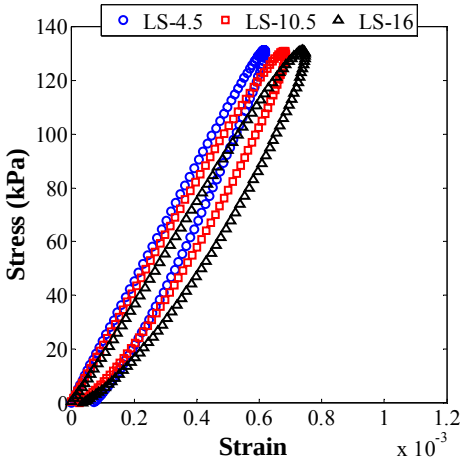

c) Stress ratio = 3.1

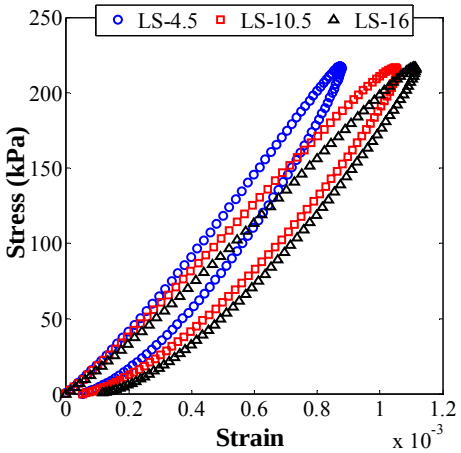

d) Stress ratio = 5.1

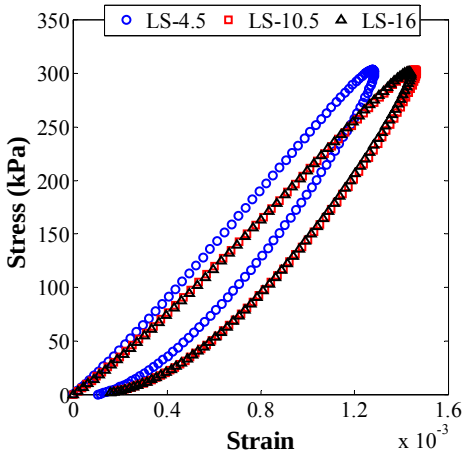

e) Stress ratio = 7.2

FIGURE 9.4: Stress-Strain Hysteresis Loops for Limestone Gradations at OMC and Confining Pressure = 42.5 kPa

Figures 9.3 (c) to 9.3 (e) show that the unloading part of the hysteresis loop at a stress ratio higher than 2.4 can be divided into two portions: elastic unloading and elastic creep unloading. The elastic unloading portion can be due to the immediate recovery of the deformation and rotation of single particles. The elastic creep unloading portion can be due to the slow recovery of the slip between particles. The recovered strain during the elastic creep unloading portion increased with the increase of the stress ratio, as shown in Figures 9.3 (c) to 9.3 (e). For GA-14.5, the slope of elastic unloading curve became steeper as the stress ratio increased to 8.4 which indicated the stiffening behaviour of the material at the transition between the stable zone and the unstable zone shown in Figure 9.1.

For limestone UGM, Figure 9.4, LS-4.5 had a narrower hysteresis loop than LS-10.5 and LS-16 at all stress ratios which indicates lower dissipated energy. LS-4.5 showed steeper hysteresis loop (lower resilient strain) than LS-10.5 and LS-16 at all stress ratios which indicates a stiffer response of the material (higher resilient modulus). Similar to gravel, Figures 9.4 (c) to 9.4 (e) show that the recovered strain during the elastic creep unloading increased with the increase of the stress ratio while the recovered strain during the elastic unloading portion remained almost constant.

9.4 Effect of Stress Level and Fines Content on Dissipated Energy for UGM

Figures 9.5 to 9.9 show the relationship between the dissipated energy ratio, DER, and the stress ratio for the gravel gradations at several confining pressures. The dissipated

energy ratio is defined according to Equation 9.4. If all the applied energy is released after unloading the material, no dissipated energy, DER equals zero. If all the applied energy is dissipated and no energy is released after unloading the material, DER equals one. A lower DER means more elastic response of the material.

$$DER = \frac{W_d}{W_T} \quad \textbf{(9.4)}$$

Where:

W_d = dissipated energy per unit volume per cycle, Joule/m^3

W_T = total energy per unit volume per cycle, Joule/m^3

Figures 9.5 to 9.9 show that DER decreased with the increase of the confining pressure. The increase of the confining pressure reduces the slip between particles which results in an increase in the material stiffness and elastic response. Figures 9.5 to 9.9 show also that the DER decreased with the decrease of moisture content which indicates more elastic response of the material. DER for GA-14.5 was more sensitivity to moisture variation than GA-4 and G-9 particularly at lower confining pressures. Overall, GA-14.5 and GA-9 showed the highest and lowest DER, respectively, at all confining pressures which indicates that GA-9 had more elastic behaviour than GA-14.5.

At OMC, DER decreased as the stress ratio increased until it reached a minimum value. As the stress ratio continued to increase beyond the minimum DER point, DER started to increase again with a lower rate. The minimum DER occurred at a stress ratio ranging

from 2 to 4.5 for the three gradations. The stress ratio corresponding to the minimum DER decreased as the confining pressure increased. The minimum DER point can be the boundary to the transition between the post compaction zone and the stable zone, as shown in Figure 9.1. In the post compaction zone, the material undergoes a progressive increase in the resilient response and a progressive decrease in the DER with the increase of stress ratio, as shown in Figures 5 and 6. This behaviour results in a decreasing trend of DER with the increase of stress ratio. In the stable zone, the resilient response of the material increases with the increase of stress ratio at a lower rate than that in the post compaction zone and the material undergoes a higher rate of permanent strain. This behaviour results in an increasing trend of DER with the increase of stress ratio. The minimum DER point represents the transition between the decreasing DER trend in the post compaction zone and the increasing DER trend in the stable zone, as shown in Figures 9.5 to 9.9.

Figures 9.10 to 9.14 show the relationship between DER and the stress ratio for the limestone gradations at several confining pressures. Similar to gravel, DER for limestone UGM decreased with the increase of the confining pressure. LS-16 showed higher DER than LS-4.5 and LS-10.5 at moisture content 2% lower than OMC. At OMC, there was not a significant difference in DER for the three gradations. The minimum DER occurred at a stress ratio ranging from 2 to 3 for the three gradations which represents the transition between the post compaction zone and the stable zone. Similar to gravel, the stress ratio corresponding to the minimum DER decreased as the confining pressure increased.

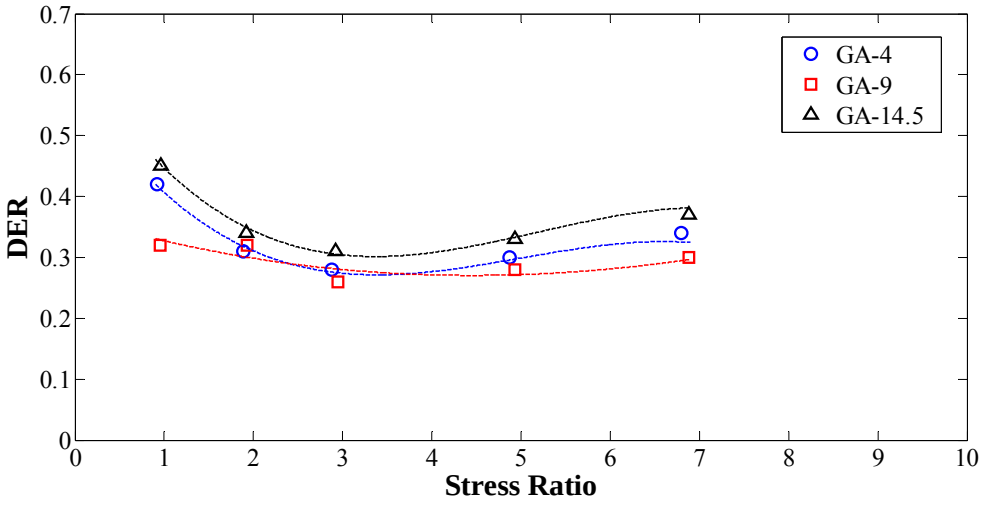

a) at 2% below OMC

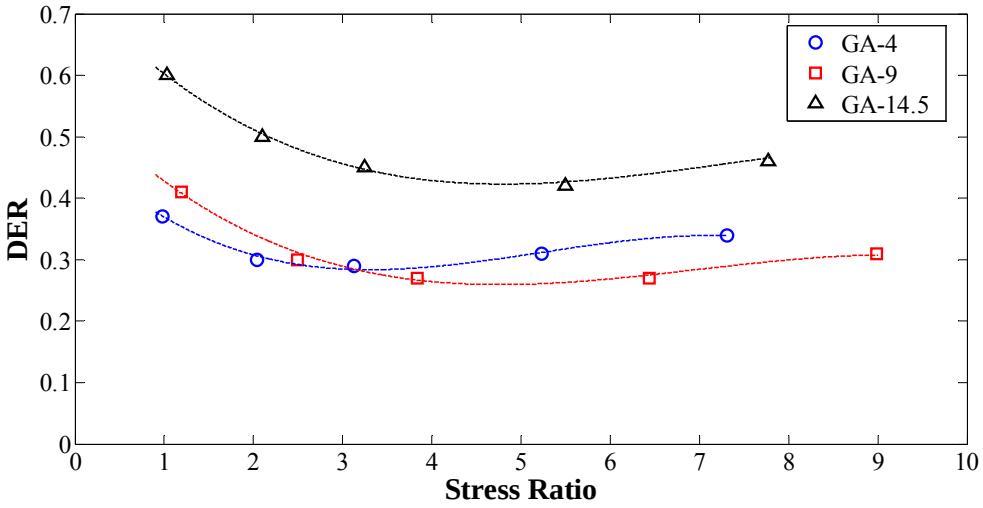

b) at OMC

FIGURE 9.5: DER versus Stress Ratio for Gravel Gradations at Confining Pressure 20.7 kPa

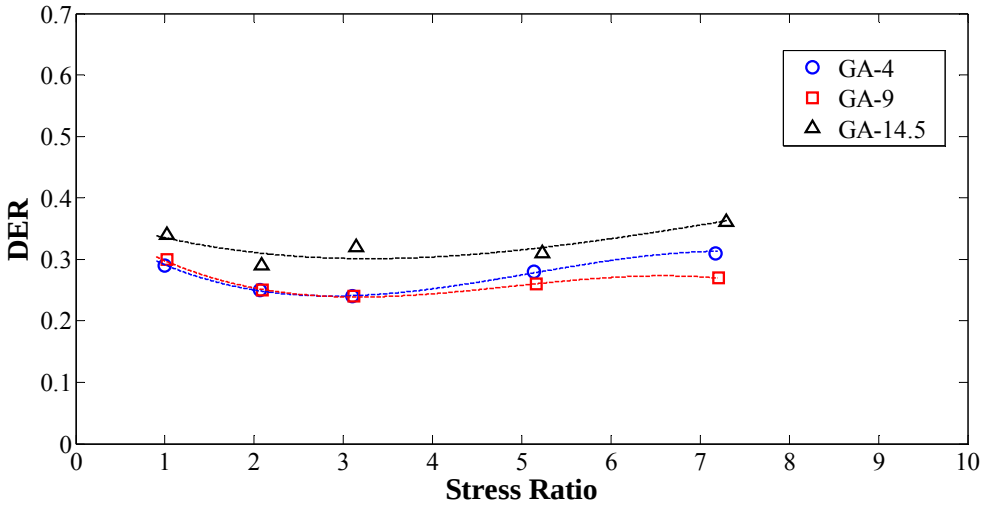

a) at 2% below OMC

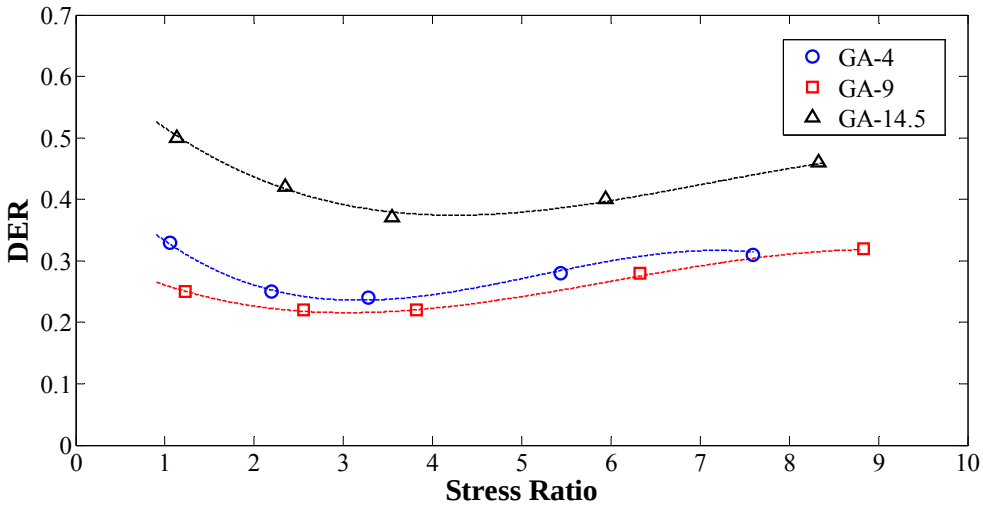

b) at OMC

FIGURE 9.6: DER versus Stress Ratio for Gravel Gradations at Confining Pressure 39.6 kPa

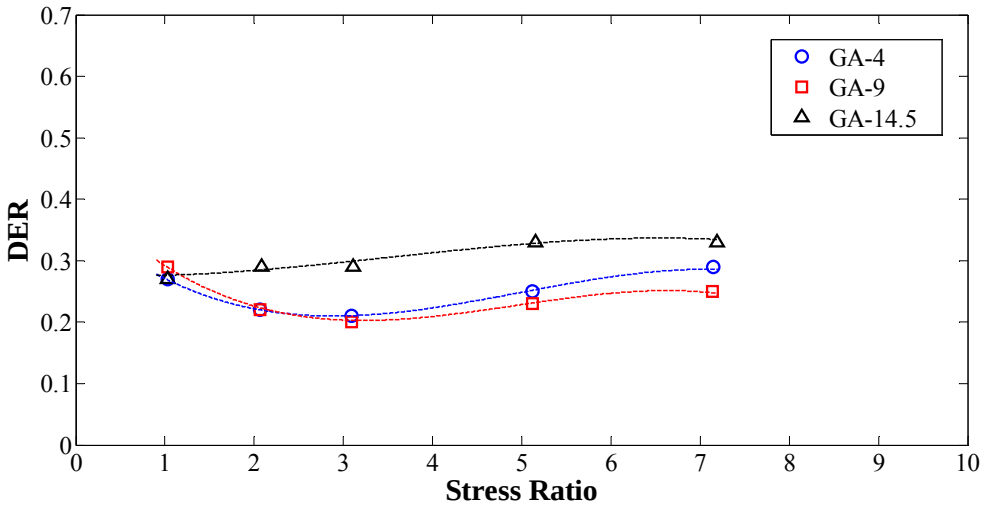

a) at 2% below OMC

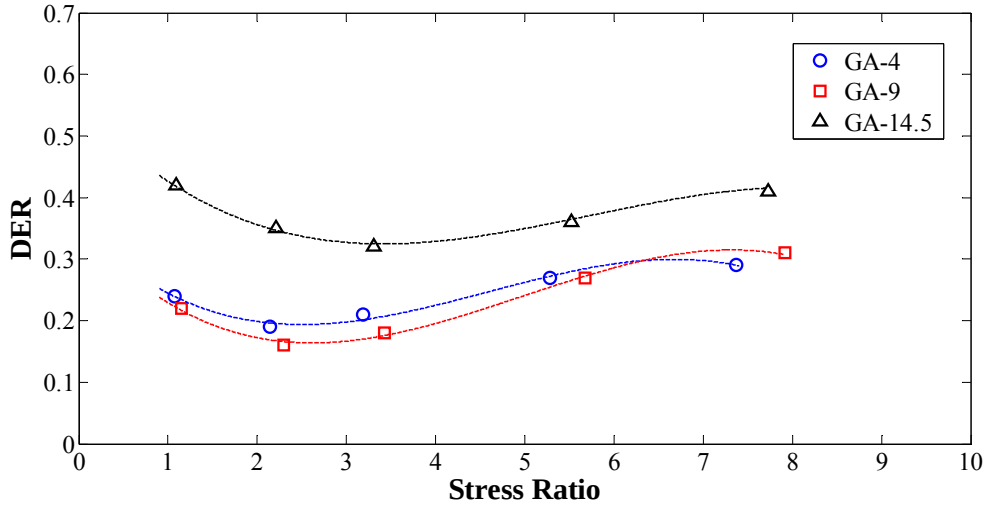

b) at OMC

FIGURE 9.7: DER versus Stress Ratio for Gravel Gradations at Confining Pressure 68.0 kPa

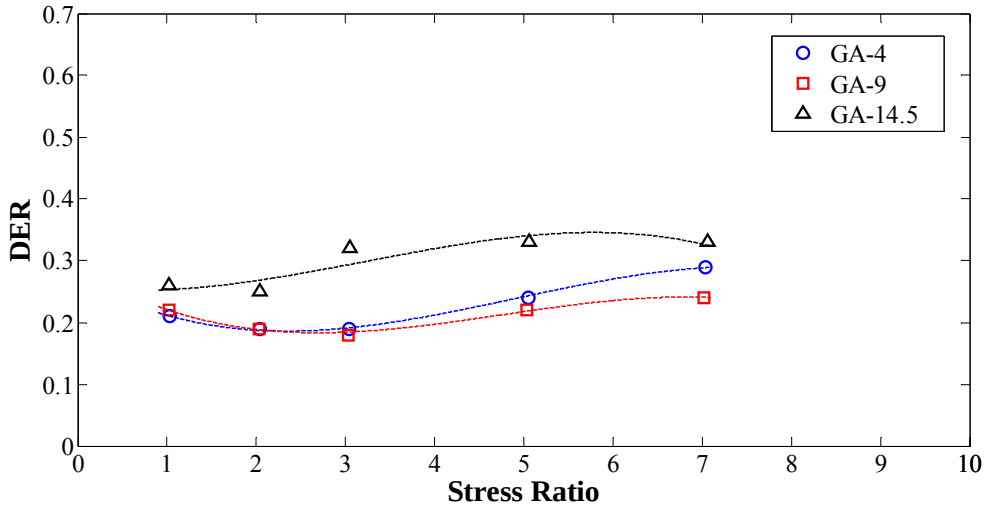

a) at 2% below OMC

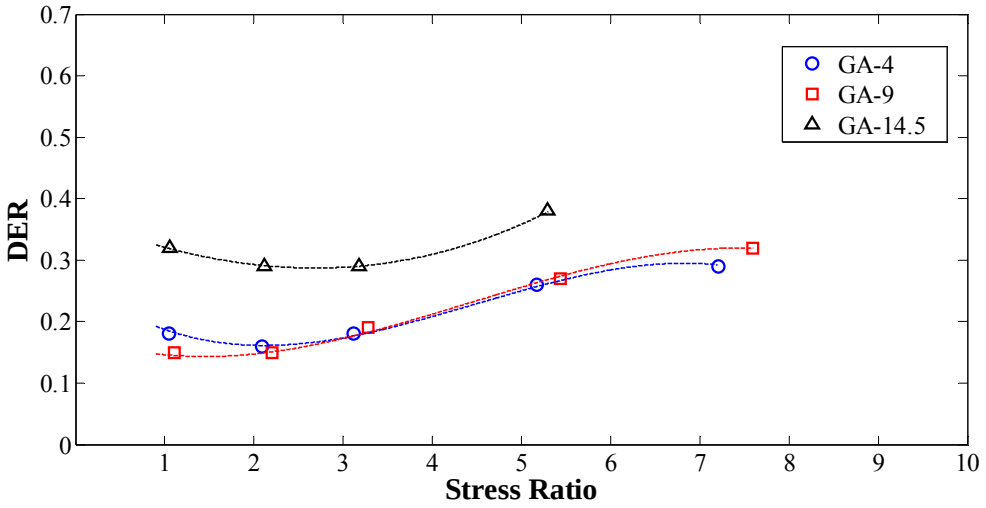

b) at OMC

FIGURE 9.8: DER versus Stress Ratio for Gravel Gradations at Confining Pressure 104.2 kPa

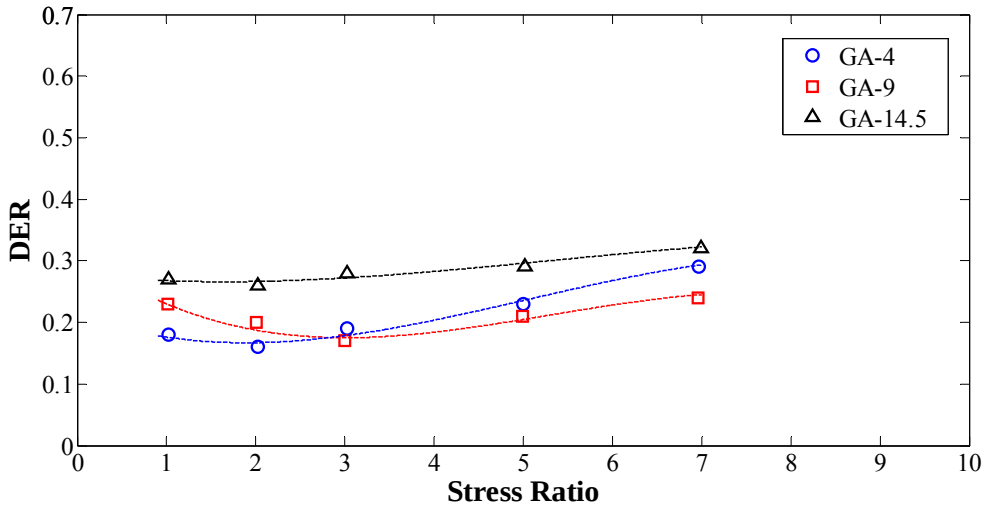

a) at 2% below OMC

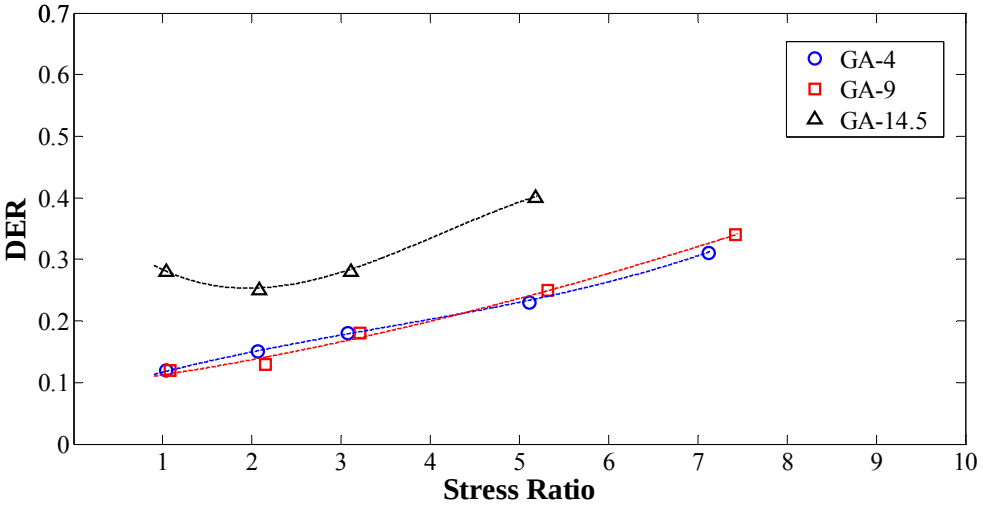

b) at OMC

FIGURE 9.9: DER versus Stress Ratio for Gravel Gradations at Confining Pressure 140.3 kPa

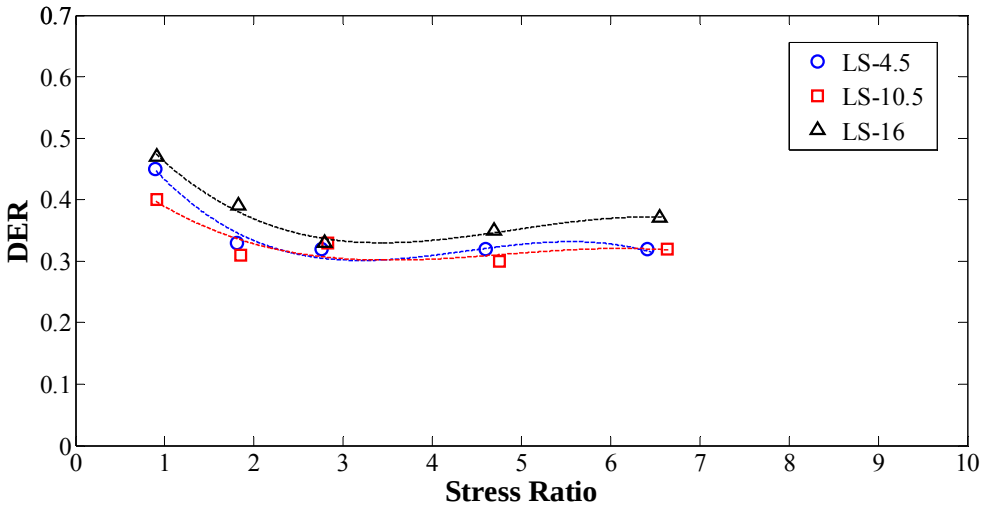

a) at 2% below OMC

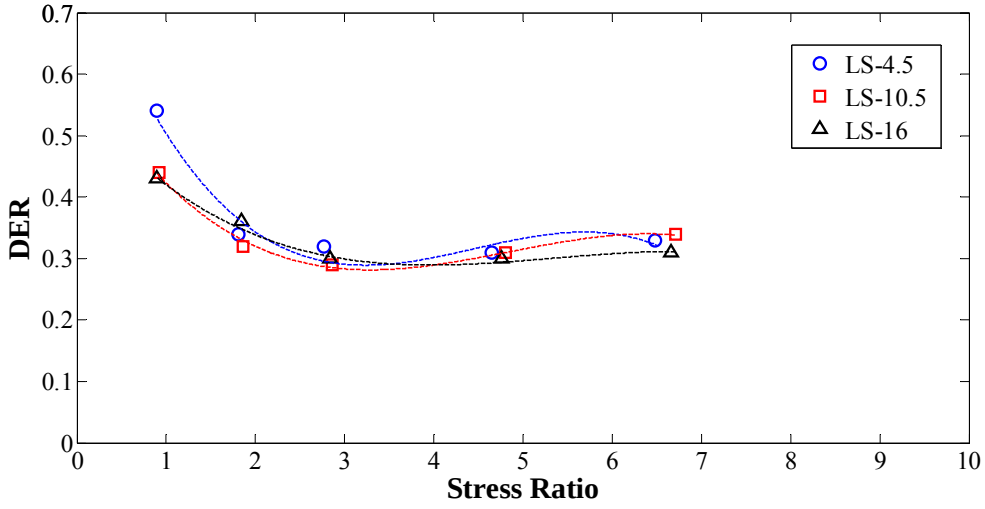

b) at OMC

FIGURE 9.10: DER versus Stress Ratio for Limestone Gradations at Confining Pressure 23.2 kPa

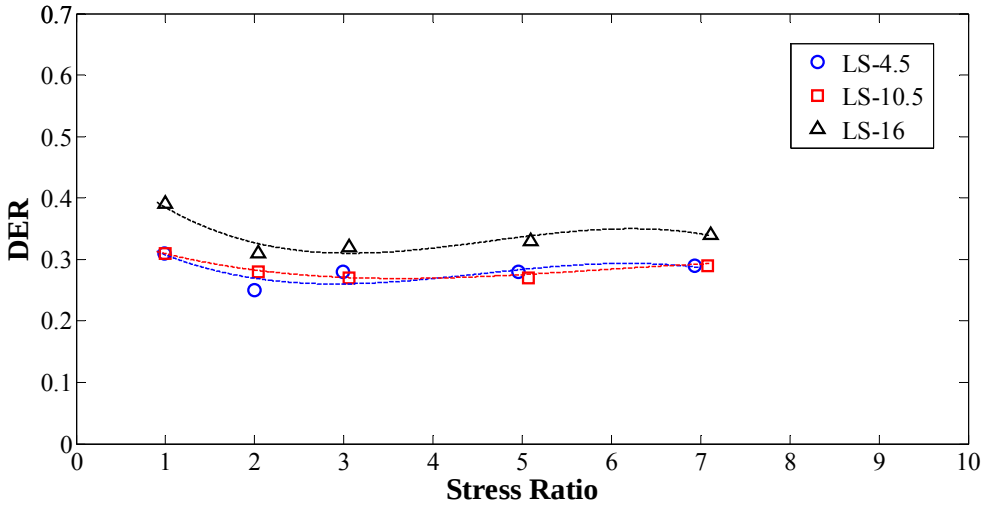

a) at 2% below OMC

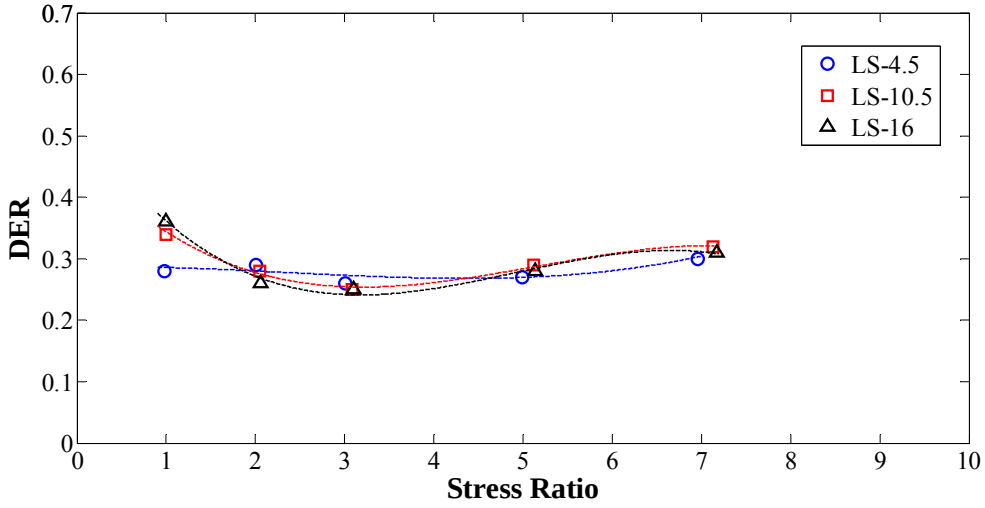

b) at OMC

FIGURE 9.11: DER versus Stress Ratio for Limestone Gradations at Confining Pressure 43.2 kPa

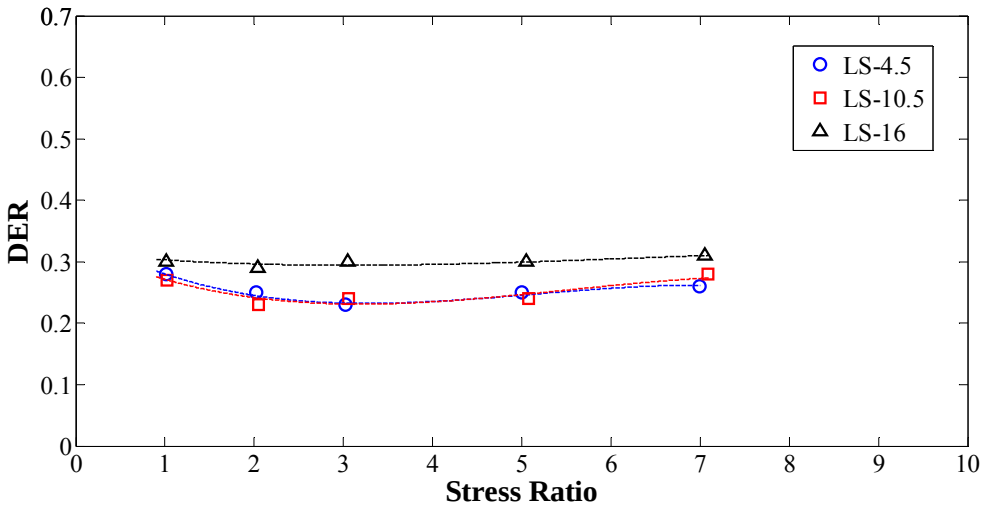

a) at 2% below OMC

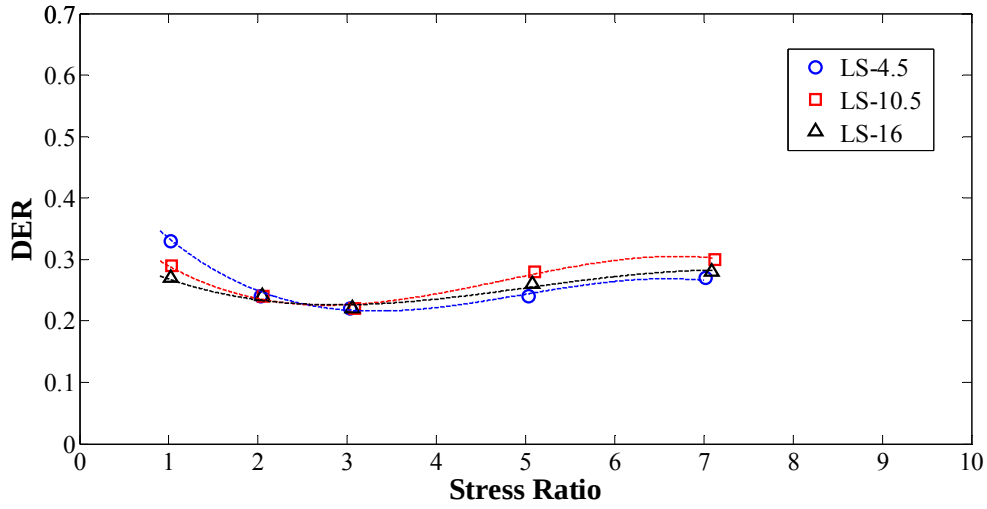

b) at OMC

FIGURE 9.12: DER versus Stress Ratio for Limestone Gradations at Confining Pressure 71.4 kPa

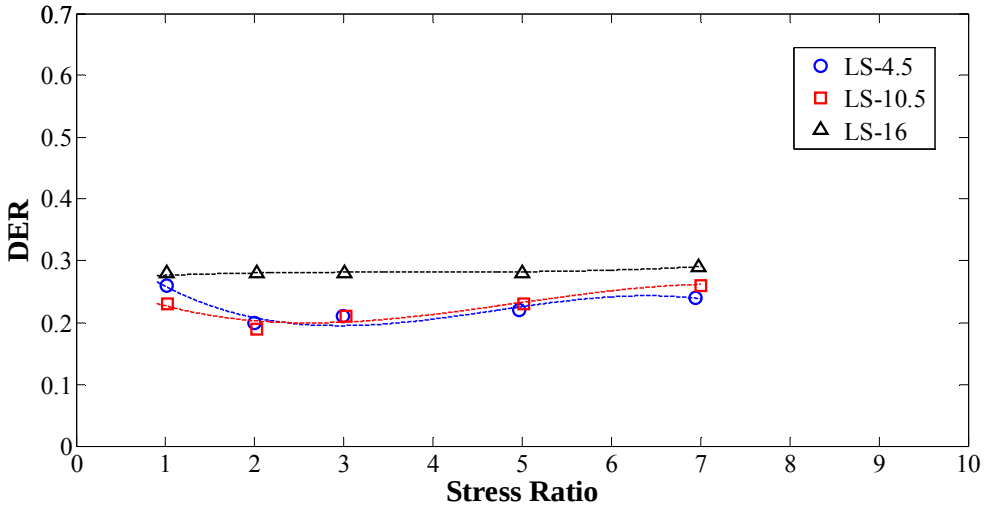

a) at 2% below OMC

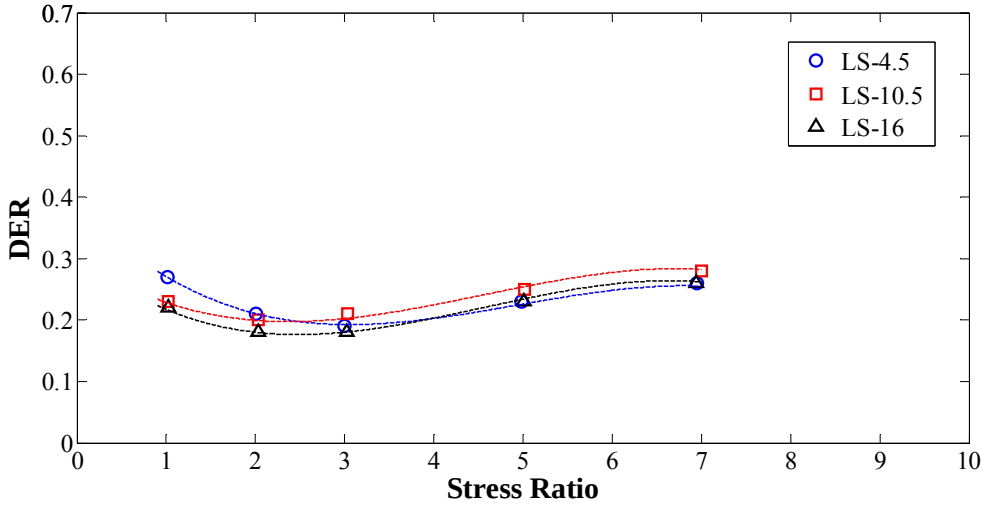

b) at OMC

FIGURE 9.13: DER versus Stress Ratio for Limestone Gradations at Confining Pressure 107.8 kPa

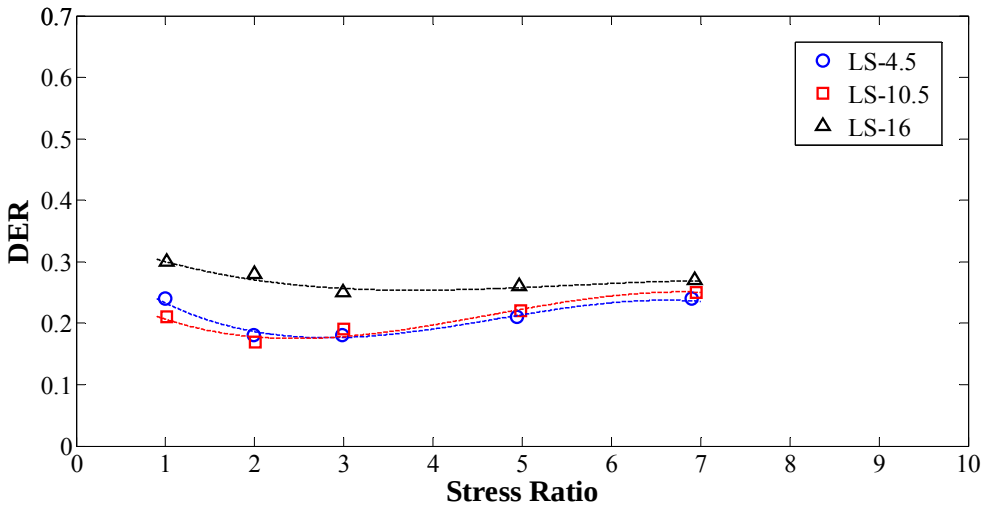

a) at 2% below OMC

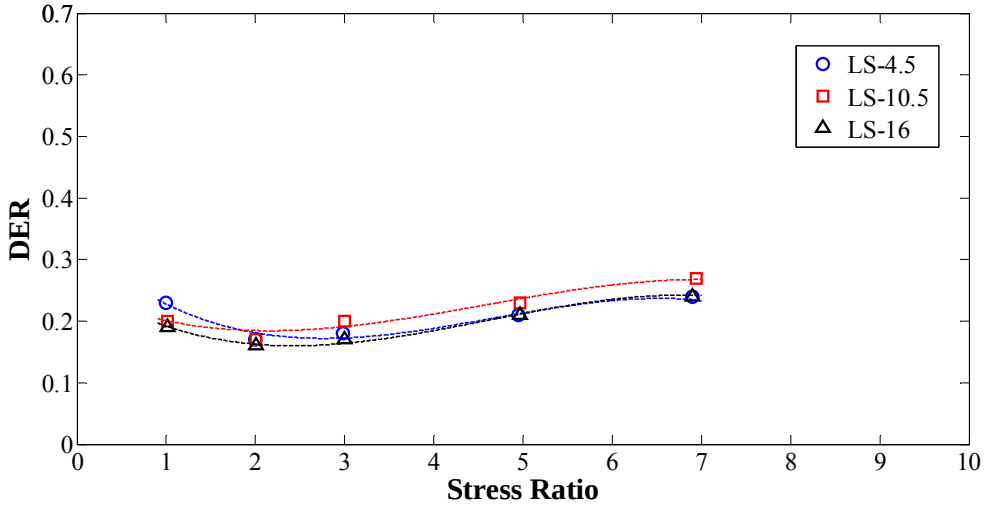

b) at OMC

FIGURE 9.14: DER versus Stress Ratio for Limestone Gradations at Confining Pressure 144.2 kPa

9.5 Effect of Number of Loading Cycles on Dissipated Energy for UGM

In the post compaction zone, Figure 9.1, the rotation and slip between UGM particles occur at a high rate (high dissipated energy per cycle) and this rate decreases rapidly as the material exits the post compaction zone. This behaviour results in a rapid decrease in the dissipated energy per cycle, with the increase of number of loading cycles, within the post compaction zone. However, in the stable zone, the rotation and slip between UGM particles occur at a lower rate than the post compaction zone and this rate remains almost constant within the zone. This behaviour results in a constant dissipated energy per cycle within the stable zone.

Figure 9.15 shows the stress-strain hysteresis loops at different number of loading cycles (N) for gravel gradations at OMC. Figure 9.15 shows that GA-14.5 had wider hysteresis loops and higher permanent strain, particularly in the first 2000 loading cycles, than GA-4 and GA-9. The wider hysteresis loops and higher permanent strain indicates that GA-14.5 incurred higher rate of rotation and slip between particles, reversible and irreversible, than GA-4 and GA-9. As the number of loading cycles increased and the cyclic stress remained constant, the slope of the hysteresis loops became steeper indicating a stiffer resilient response and lower resilient strain. On the other hand, GA-9 showed more elastic response than GA-4 and GA-14.5 where GA-9 had narrower hysteresis loops, lower dissipated energy, and lower permanent strain.

Figure 9.16 shows the dissipated energy per cycle versus the number of loading cycles for gravel gradations at 2% below OMC and OMC. For all gradations, the dissipated energy per cycle increased as the moisture content increased from 2% below OMC to OMC. At OMC, the average dissipated energy per cycle in the first 10 loading cycles was 20.6 Joule/m^3, 15.1 Joule/m^3, and 46.8 Joule/m^3 for GA-4, G-9, and GA-14.5 respectively, as shown in Table 9.1. As the number of loading cycles increased, the dissipated energy per cycle decreased at a high rate for all gradations until the dissipated energy reached a stable condition which indicated the end of the post compaction zone (Widyatmoko et al. 1999a). For GA-4 and GA-9, the post compaction zone ended after approximately 1000 loading cycles, while the post compaction zone extended up to 5000 loading cycles for GA-14.5. The extension of the post compaction zone to a higher number of loading cycles indicates that GA-14.5 was less stable than GA-4 and GA-9 when subjected to a similar loading condition.

Figure 9.17 shows the stress-strain hysteresis loops at different number of loading cycles for limestone gradations at OMC. Figure 9.17 shows that there was not a significant difference in the shape of the hysteresis loops between the three limestone gradations. This behaviour is contrary to that of the gravel gradations shown in Figure 9.15. The limestone UGM was a 100% crushed material while the gravel UGM was uncrushed. Therefore, for limestone material, the resistance to rotation and slip between UGM particles, which affect the shape of hysteresis loops, is mainly influenced by the friction and interlock between particles not the fines content. While, for gravel material, the resistance to rotation and slip between UGM particles is mainly influenced by the fines

content and aggregate matrix characteristics due to the limited friction between individual particles, as shown in Figure 9.15. Similar to gravel, the slope of the hysteresis loops became steeper indicating a stiffer resilient response as the number of loading cycles increased, except for LS-4.5 where the resilient response did not change significantly.

Figure 9.18 shows the dissipated energy per cycle versus the number of loading cycles for limestone gradations at 2% below OMC and OMC. At OMC, the average dissipated energy per cycle in the first 10 loading cycles was 9.3 Joule/m^3 and 10.1 Joule/m^3 for LS-4.5, LS-10.5, respectively, as shown in Table 9.1. The post compaction zone ended after approximately 250 loading cycles for all gradations, compared to 1000 and 5000 cycles for gravel gradations. In the post compaction zone, the dissipated energy per cycle increased as the moisture content increased from 2% below OMC to OMC. In terms of dissipated energy, there was not a significant difference between the three limestone gradations when subjected to similar cyclic stress and confining pressure for extended number of loading cycles.

TABLE 9.1: Average Dissipated Energy in the First 10 Loading Cycles and Number of Cycles at End of Post Compaction Zone at OMC

UGM type	Gradation ID	Average dissipated energy per cycle at N = 10 (Joule/m^3)	No. of cycles at end of post compaction zone
Gravel	GA-4	20.6	1000
	GA-9	15.1	1000
	GA-14.5	46.8	5000
Limestone	LS-4.5	9.3	250
	LS-10.5	10.1	250
	LS-16	N/A*	250

* Data not available

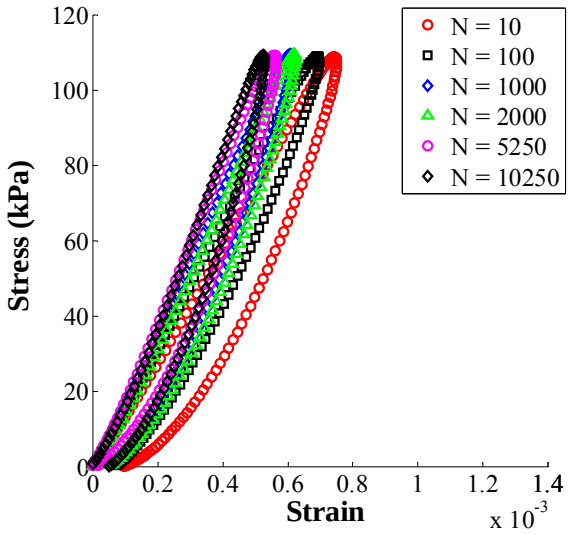

a) GA-4

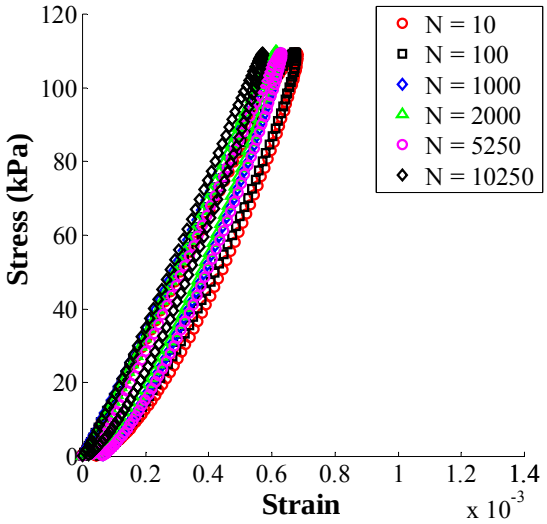

b) GA-9

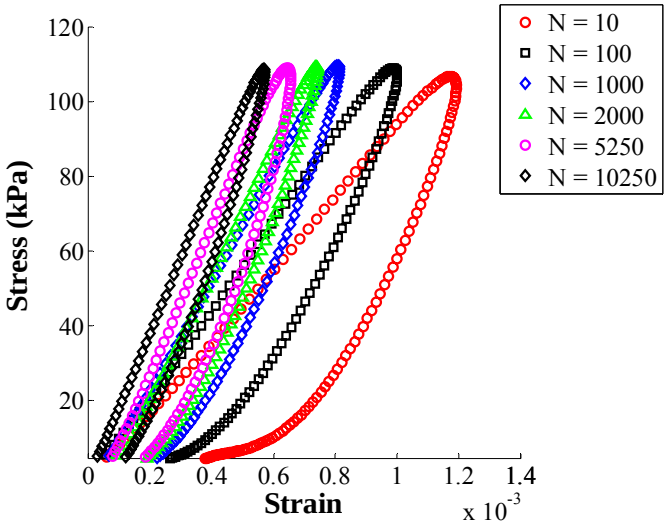

c) GA-14.5

FIGURE 9.15: Stress-Strain Hysteresis Loops for Gravel Gradations at OMC, Confining Pressure = 38.1 kPa, and Cyclic Stress = 109.3 kPa

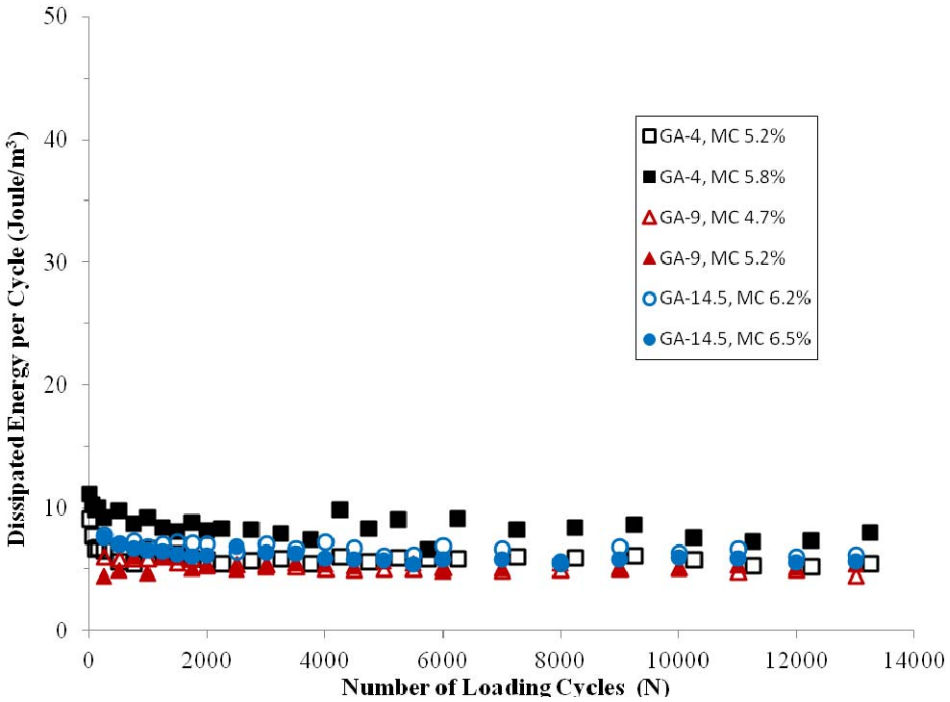

a) at 2% below OMC

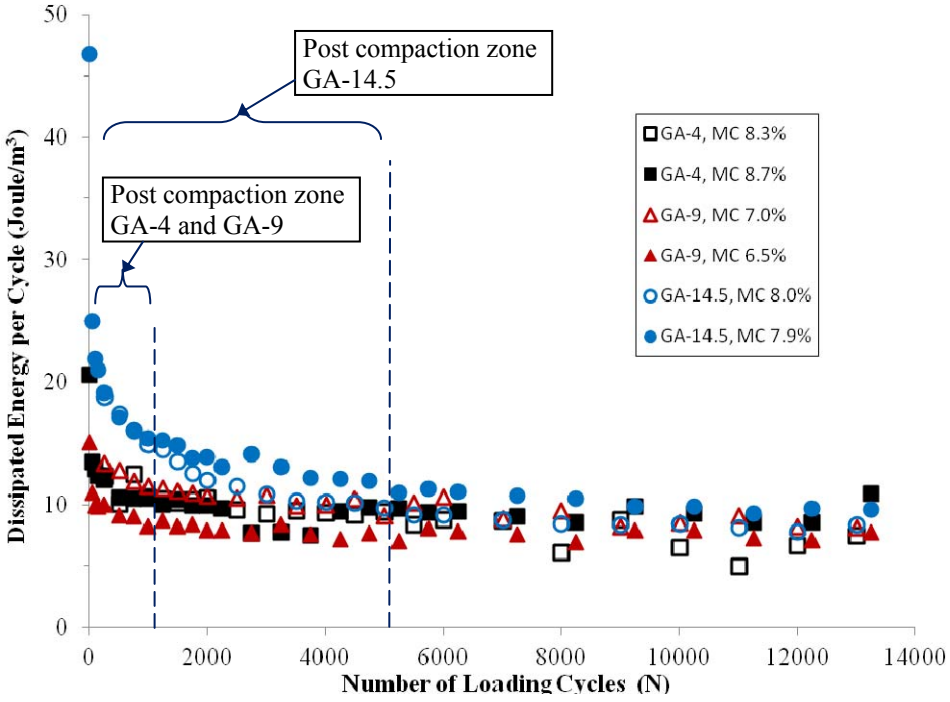

b) at OMC

FIGURE 9.16: Dissipated Energy versus Number of Loading Cycles for Gravel UGM

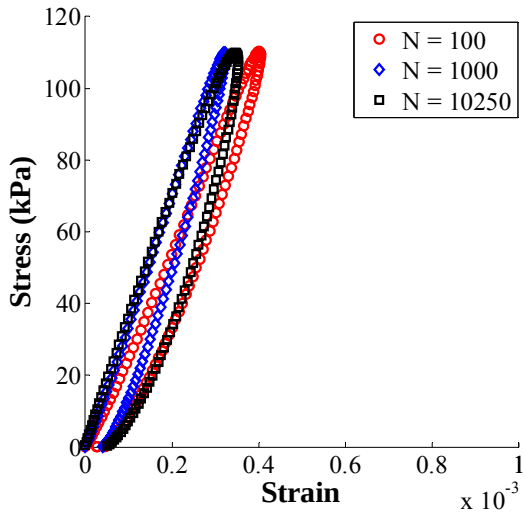

a) LS-4.5

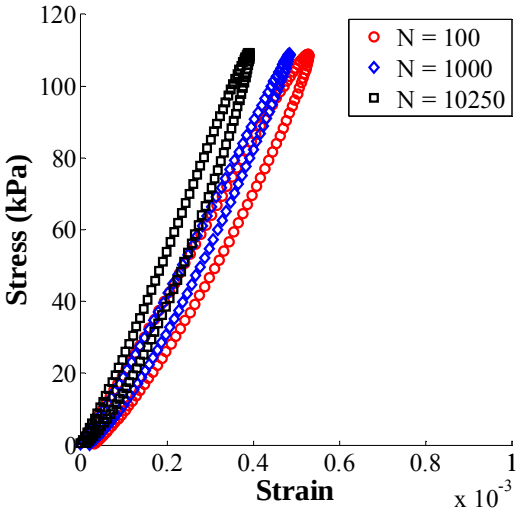

b) LS-10.5

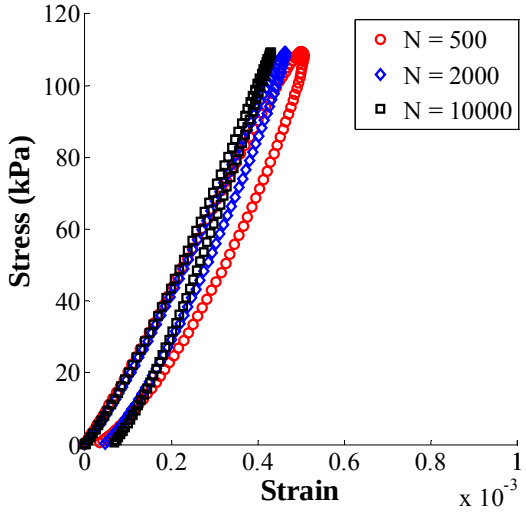

c) LS-16

FIGURE 9.17: Stress-Strain Hysteresis Loops for Limestone Gradations at OMC, Confining Pressure = 38.9 kPa, and Cyclic Stress = 109.5 kPa

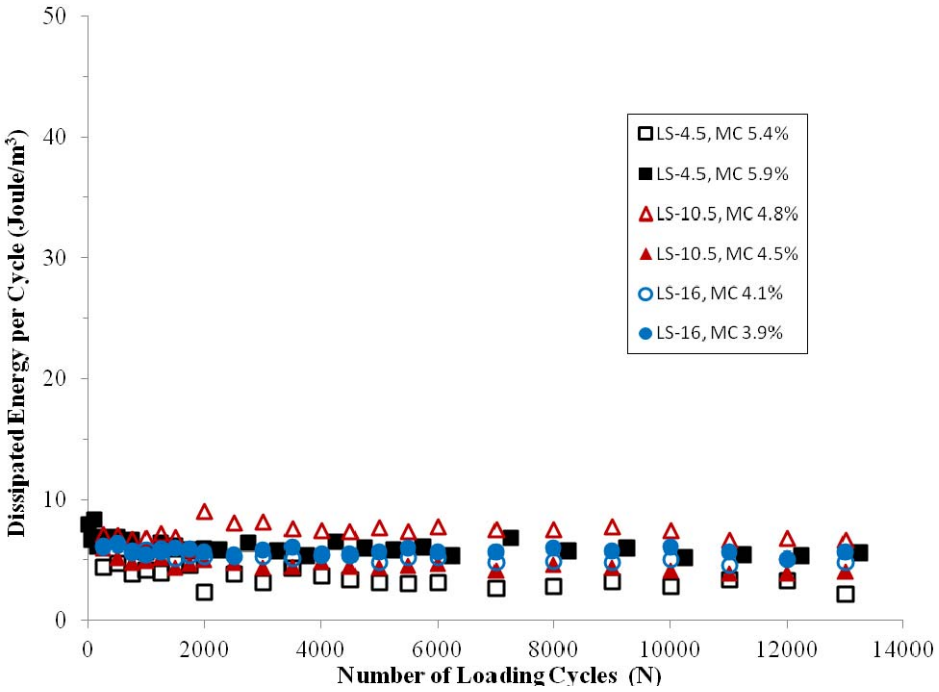

a) at 2% below OMC

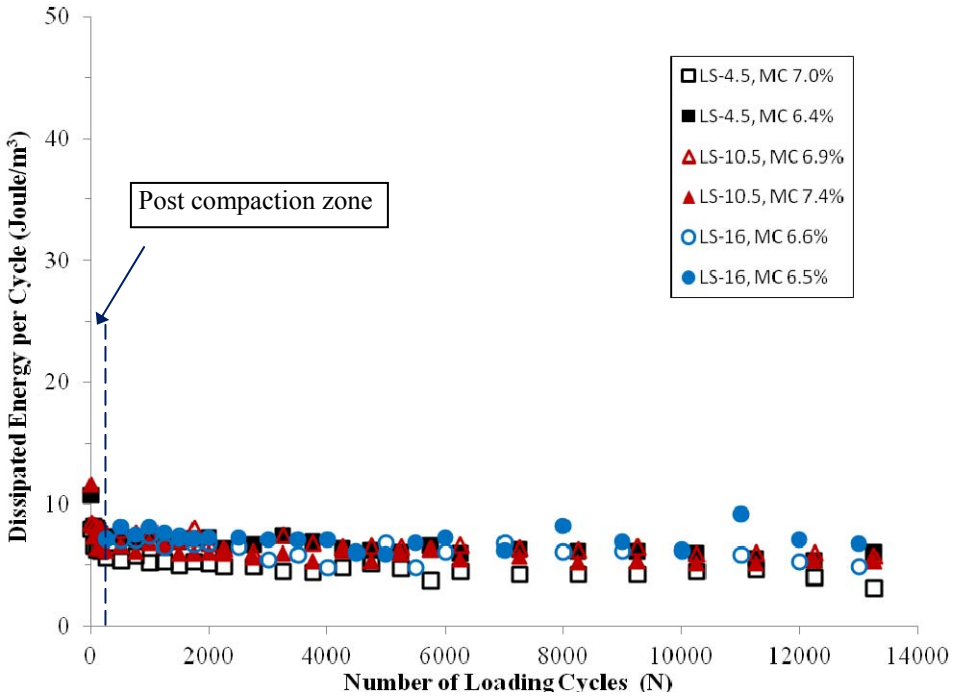

b) at OMC

FIGURE 9.18: Dissipated Energy versus Number of Loading Cycles for Limestone UGM

10 Conclusions and Recommendations

10.1 Summary

According to the Mechanistic Empirical Pavement Design Guide (Pavement ME), the design input parameters must be measured in the laboratory for Level 1 design which provides the highest level of design reliability. The resilient modulus of fine-grained soils was evaluated in the laboratory to develop Level 1 design inputs for Pavement ME. The soil samples represent three types of soil: high plastic clay, sandy clay, and silty sand/sandy silt. Soil samples were tested at four levels of moisture content that cover the dry and wet sides of Standard Proctor curve to evaluate their sensitivity to moisture variation.

Resilient modulus, permanent deformation, and permeability of UGM were evaluated in the laboratory to develop Level 1 design inputs for Pavement ME. Three samples were collected to represent three types of UGM: gravel, 100% crushed limestone, and 100% crushed granite. For gravel and limestone materials, three gradations were evaluated with different fines content to evaluate the effect of current specifications on UGM performance. Two gradations represent specification limits on allowable fines content and one gradation has less fines content than presently allowed by specifications. UGM gradations were tested at OMC and 2% below OMC to evaluate their sensitivity to moisture variation.

This research contributes to:

- Knowledge of laboratory characterization of UGM and subgrade soils resilient modulus. Although resilient modulus test is well established in several countries, few Canadian Provinces have the adequate equipment and technical experience for this test. Laboratory measured resilient modulus (Level 1) is required input for design of major projects to provide a cost-effective and sustainable design, and avoid premature failure.
- Improving the reliability of Level 2 design inputs by developing local prediction models for resilient modulus of UGM and subgrade soils. The proposed local models in this research provided a more reliable alternative to the correlation models in the literature and Pavement ME for Level 2 design. The research provides adaptable guidelines which can be used to develop new prediction models for different types of UGM and soil.
- Characterizing the effect of fines content and particle shape on the permanent deformation behaviour of UGM. The shakedown approach was used to characterize the deformation behaviour of the tested UGM. Materials were classified according to accumulated permanent deformation, change of permanent strain rate with the increase of permanent strain, and change of resilient strain with the increase of number of loading cycles. The research add to the knowledge of laboratory characterization of permanent deformation of UGM as no standard procedures have been developed yet for this test.

- Application of the dissipated energy approach to evaluate the effect of fines content, stress ratio, and number of loading cycles on the deformation behaviour of UGM. The dissipated energy approach is a damage criteria which was adopted in several studies to characterize the deformation behaviour of asphalt concrete mixtures. Three parameters were proposed to characterize the UGM performance: shape of stress-strain hysteresis loop, the amount of dissipated energy per one loading cycle, and the dissipated energy ratio..
- Developing performance-based specifications for UGM. The research provides laboratory testing data in support of updating UGM specifications. Using performance-based UGM specifications will provide durable and long lasting base layers.

10.2 Conclusions

The results of a laboratory investigation of subgrade soil performance led to the following findings:

- Resilient modulus values for High plastic clay and sandy clay soils showed medium to high sensitivity to moisture content variation, while resilient modulus values for silty sand/sandy silt soils showed low sensitivity to moisture content variation.
- The Level 3 resilient modulus values recommended by Pavement ME were higher than the measured values in the laboratory by 145% and 340% for silty sand/sandy silt, 113% and 115% for sandy clay soils, and 12% and 30% for high plastic clay soils.

- The proposed models for prediction of resilient modulus for Level 2 design input showed a good agreement with the measured resilient modulus values.
- For high plastic clay and sandy clay soils, the difference between predicted and measured resilient modulus values decreased with the decrease of resilient modulus value. The decrease in the variation between measured and predicted resilient modulus values can be due to the improved contact between ends of the test specimen and loading plates at high cyclic stresses and moisture contents.
- A significant difference was found between the measured resilient modulus values in this study and the resilient modulus values from the LTPP prediction models. The ratio between the RMSE for the LTPP prediction models and the RMSE for the prediction models proposed in this study ranged from 4 to 6.
- The proposed models showed better prediction for resilient modulus values because they were developed for more specific types of soil, while LTPP models were developed for a wide range of soils.

The results of a laboratory investigation of UGM performance led to the following findings:

- For the 100% limestone UGM, the resilient modulus increased as the fines content decreased and became less sensitive to moisture content variation. For the gravel UGM, a gradation with 9.0% fines showed higher resilient modulus than 4.0% fines and 14.5% fines.

- The Level 3 resilient modulus values recommended by Pavement ME were higher than the measured values in the laboratory by 55% and 113% for the tested UGM.

- The proposed models for predicting UGM modulus values for Level 2 design input showed better prediction than the LTTP models. The coefficient of variation of the RMSE for the LTPP models was more than 250% the coefficient of variation of the RMSE for the proposed models for gravel and limestone UGM.
- UGM must have adequate friction and cohesion between particles to support the design traffic loading without undergoing excess permanent deformation where permanent deformation is resisted by shear strength of the material.
- For 100% crushed limestone base material, using the minimum amount of fines increases rutting resistance and reduce sensitivity of permanent deformation to moisture variation.
- Gravel base material has less friction between particles than 100% crushed material. In this case, fines are required to provide adequate resistance to slip between particles under traffic loading. An intermediate level of fines content, 9% for the tested gravel material in this study, provided better resistance to permanent deformation and lower sensitivity to moisture variation.
- Deformation behaviour of UGM must be evaluated based on permanent strain and resilient strain responses together. The boundaries between plastic shakedown, plastic creep and incremental collapse zones cannot be distinguished based on permanent strain response only. Accumulated permanent strain, change in permanent strain rate, and change in resilient strain shall be used together to evaluate the performance of UGM.

- The dissipated energy approach can be used to determine the stress ratio for the boundary between post compaction and stable zone from multistage triaxial testing.
- For the 100% crushed limestone material, the post compaction zone ended after approximately 250 loading cycles for all gradations and was not sensitive to fines content.
- For the gravel material, the length of the post compaction zone was sensitive to fines content variation (1000 cycles for GA-4 and GA-9, 5000 cycles for GA-14.5), and higher than that of the limestone gradations.
- The hydraulic conductivity of UGM increased as the fines content decreased. Reducing the fines content to 4.0% for gravel and 4.5% to 10.5% for limestone improved the pavement quality of drainage to "good to fair" from "fair to poor".
- The calculated hydraulic conductivity from Pavement ME Level 2 equation was higher than the laboratory measured value (the difference was 693% for GA-14.5). Pavement ME equation does not account for the effect of fines content on the hydraulic conductivity for nonplastic fines.

10.3 Recommendations and Applications

The following recommendations are based on the results of a laboratory investigation of subgrade soil and UGM performance:

1. In addition to the dependency of resilient modulus on the stress-state of the soil, test results showed that the resilient modulus of sandy clay and high plastic clay soils

sample are sensitive to moisture variation. When determining the design values for subgrade resilient modulus the following must be taken into account:

- the moisture content of subgrade soil at time of construction
- road drainage system and the seasonal variation of subgrade moisture content

2. The Level 3 resilient modulus values recommended Pavement ME for soil and UGM must be calibrated by transportation agencies according to the typical soil and UGM types available in their region.
3. Transportation agencies must calibrate their own prediction models (for resilient modulus, hydraulic conductivity,...) to determine Level 2 design input according to the typical soil and UGM types available in their region. Using Pavement ME or other models available in the literature can result in over designing or under designing the pavement structure.
4. UGM specifications must be related to laboratory performance of the material and function of the UGM layer. Transportation agencies can develop performance-based specifications for UGM based on the layer function (drainable layer, high stiffness, or both) and use the corresponding properties for design (resilient modulus, permanent deformation, hydraulic conductivity,...). Other design alternative shall be considered when the locally available UGM does not meet the required performance.

10.4 Recommendations for Future Work

The resilient and permanent deformation behaviours of selected materials were investigated in this research. The following points need to be covered in future research:

- In this study, permanent deformation tests were conducted for 13,000 cycles. The reason for selecting this number of loading cycles was to examine the early permanent deformation behaviour of UGM in a practical method compatible with laboratory testing constraints. The deformation pattern of gravel material with 14.5% fines at OMC indicated an incremental collapse behaviour according to the adopted criteria in this study. However, this behaviour should be confirmed by testing the material to a substantially higher number of loading cycles.
- The research showed that the shape of aggregate (100% crushed versus uncrushed) influenced the resilient and permanent deformation behaviour of UGM. Further resilient and permanent behaviour tests are required for UGM with different number of fractured faces (less than 100%). The testing data should be used to update the local prediction models for resilient modulus by including an aggregate shape index in the models. The test data should also be used to update the aggregate shape requirements in UGM specifications.
- One of the objectives of this research was to provide testing date in support of updating specifications for UGM. The research investigated the influence of aggregate shape and fines content on the performance of two types of UGM. Further investigation is needed to study the influence of other parameters (toughness, durability, shale content,...) on the deformation behaviour of UGM.
- This research showed that the dissipated energy approach can be used to evaluate the deformation behaviour of UGM. Further testing is required to a substantially higher number of loading cycles and at different stress levels. The testing data can be used to develop threshold values (based on dissipated energy) which are

related to the boundaries between different deformation behaviour categories (i.e., plastic shakedown, plastic creep, and incremental collapse). These threshold values can be used to predicted the long term deformation behaviour of UGM from the accelerated triaxial testing.

References

1. AASHTO Standards T307-99. Determining the Resilient Modulus of Soils and Aggregate Materials. American Association of State Highway and Transportation Officials, 2003.
2. Alberta Ministry of Transportation (AT). Standard Specifications for Highway Construction. Alberta, 2010.
3. American Association of State Highway and Transportation Officials. AASHTO Guide for Design of Pavement Structures. Washington, D.C., 1993.
4. American Association of State Highway and Transportation Officials. AASHTO Guide for Design of Pavement Structures: Volume 2. Washington, D.C., 1986.
5. ASTM Standard D5856-95. Standard Test Method for Measurement of Hydraulic Conductivity of Porous Material Using a Rigid-Wall, Compaction-Mold Permeameter. ASTM, 2007.
6. Babic′, B., Prager, A., and Rukavina, T. Effect of Fines Particles on Some Characteristics of Granular Base Courses. Materials and Structures, Springer, Vol. 33, pp.419-424, 2000.
7. Barber, J.R., and Ciavarella, M. Contact Mechanics. International Journal of Solids and Structures, Elsevier Science, Vol. 37, issues 1-2, pp.29-43, 2000.
8. Bilodeau, J.-P., and Doré, G. Relating Resilient Behaviour of Compacted Unbound Base Granular Materials to Matrix and Interlock Characteristics. Journal of Construction and Building Materials, Vol. 37, pp. 220–228, 2012a.

9. Bilodeau, J.-P., and Doré, G. Water Sensitivity of Resilient Modulus of Compacted Unbound Granular Materials Used as Pavement Base. International Journal of Pavement Engineering, Vol. 13,No. 5, pp. 459–471, 2012b.

10. Bilodeau, J-P., Dore, G., and Schwarz, C. Effect of Seasonal Frost Conditions on the Permanent Strain Behaviour of Compacted Granular Materials Used as Base Course. International Journal of Pavement Engineering, Taylor & Francis, Vol. 12, No. 5, pp.507-518, 2011.

11. Bilodeau, J.-P., Doré, G., and Pierre, P. Gradation Influence on Frost Susceptibility of Base Granular Materials. International Journal of Pavement Engineering, Taylor & Francis, Vol. 9, No. 6, pp. 397–411, 2008.

12. British Columbia Ministry of Transportation and Infrastructure (BCMOTI). 2012 Standard Specifications for Highway Construction. November 2011.

13. Boulbibane, M., Collins, I.F., Ponter, A. R.S., and Weichert, D. Shakedown of Unbound Pavements. Road Materials and Pavement Design, Taylor & Francis, Vol. 6:1, pp.81-96, 2005.

14. Burczyk, J. M., Ksaibati, K., Andeson-Specher , R., and Farrar, M. J. Factors Influencing Determination of a Subgrade Resilient Modulus Value. Journal of Transportation Research Record, TRB, National Research Council, No. 1462, pp. 72-78, 1994.

15. Carmichael III, R. F., and Stuart, E. Predicting Resilient Modulus: A Study to Determine the Mechanical Properties of Subgrade Soils. Journal of Transportation Research Record, TRB, National Research Council, No. 1043, pp. 145-148, 1985.

16. Cao, Y.L., and Law, K.T. Energy Dissipation and Dynamic Behaviour of Clay under Cyclic Loading. Canadian Geotechnical Journal, Canadian Science Publishing, NRC Research Press, Vol. 29, pp. 103-111, 1992.

17. Cerni, G., Cardone, F., Virgili, A., and Camilli, S. Characterisation of Permanent Deformation Behaviour of Unbound Granular Materials Under Repeated Triaxial Loading. Journal of Construction and Building Materials, Elsevier Science, Vol. 28, Issue 1, pp.79-87, 2012.

18. Christopher, B.R., Schwartz, C., and Boudreau, R. Geotechnical Aspects of Pavements. National Highway Institute, Federal Highway Administration, U.S. Department of Transportation, Washington, D.C., 2006.

19. Dai, S., and Zollars, J. Resilient Modulus of Minnesota Road Research Project Subgrade Soil. Journal of Transportation Research Record, TRB, National Research Council, No. 1786, pp. 20-28, 2002.

20. Drumm, E. C., Boateng-Poku, Y., and Pierce, T. J. Estimation of Subgrade Resilient Modulus from Standard Tests. Journal of Geotechnical Engineering, American Society of Civil Engineering (ASCE), Vol. 116, No. 5, pp. 774-789, 1990.

21. European Committee for Standardization. Unbound and Hydraulically Bound Mixtures - Part 7: Cyclic Load Triaxial Test for Unbound Mixtures. EN 13286-7, 2004.

22. Farrar, M., and Turner, J. Resilient Modulus of Wyoming Subgrade Soils. Mountain Plains Consortium, Report No. MPC-91-1, 1991.

23. Fredlund, D.G. Use of Soil-Water Characterization Curves in Implementation of Unsaturated Soil Mechanics. Proceedings of the Third International Conference on Unsaturated Soils, UNSAT 2002, REcife, Brazil, 2002.

24. Fredlund, D.G., and Xing, A. Equations for the Soil-Water Characterization Curves. Canadian Geotechnical Journal, Canadian Science Publishing, NRC Research Press, Vol. 31, pp. 521-532, 1994.

25. Frost, M.W., Fleming, P.R., and Rogers, D.F. Cyclic Triaxial Tests on Clay Subgrades for Analytical Pavement Design. Journal of Transportation Engineering, American Society of Civil Engineers (ASCE), Vol. 130, No. 3, pp.378-386, 2004.

26. Gandara, J.A., Kancherla, A., Alvarado, G, Nazarian, S., and Scullion, T. Impact of Aggregate Gradation on Base Material Performance. Report No. TX-1502-2, Center for Transportation Infrastructure Systems, the University of Texas at El Paso, 2005.

27. Garcia-Rojo, R., and Herrmann, H.J. Shakedown of Unbound Granular Material. Granular Matter, Springer, Vol. 7, Issue 2-3, pp.109-118, 2005.

28. George, K. P. Resilient Modulus Prediction Employing Soil Index Properties, Final Report. Federal Highway Administration, U.S. Department of Transportation, FHWA/MS-DOT-RD-04-172, Washington, D.C., 2004.

29. Ghabchi, R., Zaman, M., Khoury, N., Kazmee, H., and Solanki, P. Effect of Gradation and Source Properties on Stability and Drainability of aggregate bases: Laboratory and Field Study. International Journal of Pavement Engineering, Taylor and Francis, Vol. 14, No. 3, pp. 274–290, 2013.

30. Ghuzlan, K.A., and Carpenter, S.H. Fatigue Damage Analysis in Asphalt Concrete Mixtures Using the Dissipated Energy Approach. Canadian Journal of Civil Engineering, Canadian Science Publishing, NRC Research Press, Vol. 33, pp. 890-901, 2006.

31. Ghuzlan, K.A., and Carpenter, S.H. Energy-Derived, Damage-Based Failure Criterion for Fatigue Testing . Journal of Transportation Research Record, TRB, National Research Council, No. 1723, pp. 141-149, 2000.

32. Guan, Y., Drumm, E. C., and Jackson, N. M. Weighting Factors for Seasonal Subgrade Resilient Modulus. Journal of Transportation Research Record, TRB, National Research Council, No. 1619, pp. 94-101, 1998.

33. Gudishala, R. Development of Resilient Modulus Prediction Models for Base and Subgrade Pavement Layers from In Situ Devices Test Results. Master's Thesis, Louisiana State University, 2004.

34. Harrigan, E.T., and Witczak, M.W. Laboratory Determination of Resilient Modulus for Flexible Pavement Design. National Cooperative Highway Research Program: Research Results Digest, No. 285, Transportation Research Board of the National Academies, Washington, D.C., 2004.

35. Illinois Department of Transportation (IDOT). Standard Specifications for Road and Bridge Construction. pp. 735-740, 2012.

36. Johnson, . K. L. Contact mechanics. Cambridge University Press, New York, 1985.

37. Kancherla, A. Resilient Modulus and Permanent Deformation Testing of Unbound Granular Materials. Master's Thesis, Texas A&M University, 2004.

38. Kansas Department of Transportation (KDOT). Standard Specifications for State Road and Bridge Construction. 1100:14, 2007.

39. Konrad, J-M., and Robert, C. Resilient Modulus Testing Using Conventional Geotechnical Triaxial Equipment. American Society for Testing and Materials (ASTM) International, Special Technical Publication No. 1437, pp. 165-175, 2003.

40. Lekarp, F., Isacsson, U., and Dawson, A. State of the Art. I: Resilient Response of Unbound Aggregates". Journal of Transportation Engineering, American Society of Civil Engineering (ASCE), Vol. 126, No. 1, pp. 66-75, 2000a.

41. Lekarp, F., Isacsson, U., and Dawson, A. State of the Art. II: Permanent Response of Unbound Aggregates". Journal of Transportation Engineering, American Society of Civil Engineering (ASCE), Vol. 126, No. 1, pp. 76-83, 2000b.

42. Long Term Pavement Performance (LTPP) Program. Protocol P46: Resilient Modulus of Unbound Granular Base/Subbase Materials and Subgrade Soils. Federal Highway Administration, U.S. Department of Transportation, Washington, D.C., 1996.

43. Manitoba Infrastructure and Transportation (MIT). Specifications for Aggregate for Granular Base Course. March 2002.

44. May, R.W., and Witczak, M.W. Effective Granular Material Modulus to Model Pavement Responses. Transportation Research Record: Journal of the Transportation Research Board, Transportation Research Board (TRB), Volume 810, pp.1-9, 1981.

45. Mishra, D. Aggregate Characteristics Affecting Response and Performance of Unsurfaced Pavements on Weak Subgrades. Ph.D. Dissertation, University of Illinois at Urbana-Champaign, 2012.

46. Mohammad, L.N., Herath, A., Gudishala, R., Nazzal, M., Abu-Farsakh, M.Y., and Alshibli, K. Development of Models to Estimate the Subgrade and Subbase Layers' Resilient Modulus from In Situ Devices Test Results for Construction Control. Louisiana Transportation Research Center, Report No. FHWA/LA.05/406, Baton Rouge, Louisiana, 2008.

47. Mohammad, L.N., Gaspard, K., Herath, A., and Nazzal, M. Comparative Evaluation of Subgrade Resilient Modulus from Non-destructive, In-situ, and Laboratory Methods. Louisiana Transportation Research Center, Report No. FHWA/LA.06/417, Baton Rouge, Louisiana, 2007.

48. Mohammad, L. N., Puppala, A. J., and Alavilli, P. Influence of Testing Procedures and LVDT Location on Resilient Modulus of Soils. Journal of Transportation Research Record, TRB, National Research Council, No. 1462, pp. 91-101, 1994.

49. National Cooperative Highway Research Program (NCHRP). Guide for Mechanistic-Empirical Design of New and Rehabilitated Pavement Structures. NCHRP 1-37A, Transportation Research Board of the National Academies, Washington, D.C., 2004.

Available form: http://onlinepubs.trb.org/onlinepubs/archive/mepdg/guide.htm [accessed May 2014].

50. National Cooperative Highway Research Program (NCHRP). Guide for Mechanistic-Empirical Design of New and Rehabilitated Pavement Structures, Appendix CC-1: Correlation of CBR Values with Soil Index Properties. Transportation Research Board, National Research Council, Washington, D.C., 2001.

51. Nazarian, S., Mazari, M., Abdallah, I., Puppala, A.J., Mohammad, L.N., and Abu-Farsakh, M.Y. Modulus-Based Construction Specification for Compaction of Earthwork and Unbound Aggregate. National Cooperative Highway Research Program (NCHRP), Final Report, Washington, D.C., 2014.

52. Nazzal, M.D., Mohammad, L.N., and Austin, A. Evaluation of the Shakedown Behavior of Unbound Granular Base Materials. Geo-Frontiers 2011, American Society of Civil Engineers (ASCE), pp.4752-4761, 2011.

53. Nazzal, M.D., Mohammad, L.N., and Gaspard, K. Development of Resilient Modulus Prediction Models for Louisiana Subgrade Soils. 87th Annual Meeting of the Transportation Research Board, Washington D.C., 2008.

54. Nebraska Department of Roads (NDOR). Standard Specifications for Highway Construction. pp.802-803, 2007.

55. North Dakota Department of Transportation (NDOT). Standard Specifications for Road and Bridge Construction. pp. 542-545, 2008.

56. Ontario Ministry of Transportation (MTO). OPSS 1010 - Material Specifications for Aggregates - Base, Subbase, Select Subgrade, and Backfill Material. Ontario Provincial Standard Specification, November 2003.

57. Pérez, I., Medina, L., and Romana, M.G. Permanent Deformation Models for a Granular Material Used in Road Pavements. Journal of Construction and Building Materials, Elsevier Science, Vol. 20, pp.790-800, 2006.

58. Puppala, A. J., Saride, S., and Chomtid, S. Experimental and Modeling Studies of Permanent Strains of Subgrade Soils. Journal of Geotechnical and Geoenvironmental Engineering, American Society of Civil Engineering (ASCE), Vol. 135, No. 10, pp. 1379-1389, 2009.

59. Rahim, A. M., and George, K. P. Subgrade Soil Index Properties to Estimate Resilient Modulus. 83rd Annual Meeting of the Transportation Research Board, Washington D.C., 2004.

60. Richardson, D.N. Drainability Characteristics of Granular Pavement Base Material. Journal of Transportation Engineering, American Society of Civil Engineers (ASCE), Vol. 123, No. 5, pp.385-392, 1997.

61. Saeed, A. Performance-Related Tests of Recycled Aggregates for Use in Unbound Pavement Layers. National Cooperative Highway Research Program (NCHRP), NCHRP Report 598, Project 4-31, Transportation Research Board of the National Academies, Washington, D.C., 2008.

62. Santha, B. L. Resilient Modulus of Subgrade Soils: Comparison of Two Constitutive Equations. Journal of Transportation Research Record, TRB, National Research Council, No. 1462, pp. 79-90, 1994.

63. Saskatchewan Department of Highways and Transportation (SKDHT). 3500 - Specification for Base Aggregate and Base Mix. 2004.

64. Sharp, R.W. Pavement Design Based on Shakedown Analysis. Transportation Research Record: Journal of the Transportation Research Board, Transportation Research Board (TRB), Vol. 1022, pp.99-107, 1985.

65. Soliman, H., and Shalaby, A. Characterizing the Elastic Behavior of Fine-Grained Subgrade Soils under Traffic Loading. The International Journal of Pavement Engineering, Taylor & Francis, Vol. 15, Issue 8, pp. 698-707, 2014.

66. Soliman, H., and Shalaby, A. Sensitivity of Subgrade Resilient Modulus to Moisture Variation. Presented at the Annual Conference of the Transportation Association of Canada, Halifax, Nova Scotia, 2010.

67. Soliman, H., Shalaby, A., Kass, S., and Ng, T. N. Characterizing the Soil Resilient Modulus for Typical Manitoba Soils. Presented at the Annual Conference of the Transportation Association of Canada, Vancouver, British Columbia, 2009.

68. South Dakota Department of Transportation (SDDOT). Standard Specifications for Road and Bridge Construction. pp. 459-460, 2004.

69. Tao, M., Mohammad, L.N., Nazzal, M.D., Zhang, Z., and Wu, Z. Application of Shakedown Theory in Characterizing Traditional and Recycled Pavement Base Materials. Journal of Transportation Engineering, American Society of Civil Engineers (ASCE), Vol. 136, No. 3, pp.214-222, 2010.

70. Tian, P., Zaman, M., and Laguros, J. Gradation and Moisture Effects on Resilient Moduli of Aggregate Bases. Transportation Research Record: Journal of the Transportation Research Board, Transportation Research Board (TRB), Vol. 1619, pp. 75-84, 1998.

71. Tseng, K-H., and Lytton, R.L. Prediction of Permanent Deformation in Flexible Pavement Materials. Implication of Aggregates in Design, Construction, and Performance of Flexible Pavements, ASTM STP 1016, H.G. Schreuders and C.R. Marek, Eds., American Society for Testing and Materials, Philadelphia, pp. 154-172, 1989.

72. Tutumluer, E. Practices for Unbound Aggregate Pavement Layers: A Synthesis of Highway Practice. National Cooperative Highway Research Program (NCHRP), NCHRP Synthesis 445, Transportation Research Board of the National Academies, Washington, D.C., 2013.

73. Tutumluer, E. and Seyhan, U. Effects of Fines Content on the Anisotropic Response and Characterization of Unbound Aggregate Bases. Proceedings of the 5th International Symposium on Unbound Aggregates in Roads (UNBAR5), Unbound Aggregates in Road Construction, Edited by A.R. Dawson, A.A. Balkema Publishers, University of Nottingham, U.K.,pp. 153–161, 2000.

74. Uzan, J. Characterization of Granular Material. Transportation Research Record: Journal of the Transportation Research Board, Transportation Research Board (TRB), Vol. 1022, pp.52-59, 1985.

75. Von Quintus, H., and Killingsworth, B. Analyses Relating to Pavement Material Characterizations and Their Effects on Pavement Performance, Final Report. Federal Highway Administration, U.S. Department of Transportation, FHWA-RD-97-085, Washington, D.C., 1998.

76. Werkmeister, S., Dawson, A.R., and Wellner, F. Permanent Deformation Behaviour of Granular Materials. Road Materials and Pavement Design, Taylor & Francis, Vol. 6:1, pp.31-51, 2005.

77. Werkmeister, S., Dawson, A.R., and Wellner, F. Pavement Design Model for Unbound Granular Materials. Journal of Transportation Engineering, American Society of Civil Engineers (ASCE), Vol. 130, No. 5, pp.665-674, 2004.

78. Werkmeister, S., Numrich, R., Dawson, A.R., and Wellner, F. Design of Granular Pavement Layers Considering Climatic Conditions. Transportation Research Record: Journal of the Transportation Research Board, Transportation Research Board (TRB), Vol. 1837, pp. 61-70, 2003.

79. Werkmeister, S., Dawson, A.R., and Wellner, F. Permanent Deformation Behavior of Granular Materials and the Shakedown Concept. Transportation Research Record: Journal of the Transportation Research Board, Transportation Research Board (TRB), Vol. 1757, pp.75-81, 2001.

80. Widyatmoko, I., Ellis, C., and Read, J.M. Energy Dissipation and the Deformation Resistance of Bituminous Mixtures. Materials and Structures, Springer, Vol. 32, pp.218-223, 1999a.

81. Widyatmoko, I., Ellis, C., and Read, J.M. The Application of the Dissipated Energy Method for Assessing the Performance of Polymer-Modified Bituminous Mixtures. Materials and Structures, Springer, Vol. 32, pp.304-310, 1999b.

82. Yau, A., and Von Quintus, H. Study of LTPP Laboratory Resilient Modulus Test Data and Response Characteristics – Final Report. Long Term Pavement

Performance (LTPP) Program, Federal Highway Administration, U.S. Department of Transportation, Washington, D.C., 2001.

Contributions

1. Soliman, H., and Shalaby, A. Permanent Deformation Behavior of Unbound Granular Base Materials with Varying Moisture and Fines Content. Journal of Transportation Geotechnics, Elsevier Science, 2015.
   DOI: 10.1016/j.trgeo.2015.06.001.
2. Soliman, H., and Shalaby, A. Characterizing the Elastic Behavior of Fine-Grained Subgrade Soils under Traffic Loading. The International Journal of Pavement Engineering, Taylor & Francis, Vol. 15, Issue 8, pp. 698-707, 2014.
3. Soliman, H., and Shalaby, A. Validation of Long Term Pavement Performance Prediction Models for Resilient Modulus of Unbound Granular Materials. Transportation Research Record: Journal of the Transportation Research Board, Transportation Research Board of the National Academies, Washington, D.C., 2015, Submitted.
4. Soliman, H., and Shalaby, A. Utilizing the Dissipated Energy Approach for Assessing the Behaviour of Unbound Granular Materials with Varying Fines Content. Journal of Construction and Building Materials, Elsevier Science, 2015, In progress.
5. Soliman, H., Shalaby, A., and Kass, S. Overview of Specifications for Unbound Granular Base Materials in Selected Canadian Provinces and Neighbouring States. The Annual Conference of the Transportation Association of Canada, Montreal, 2014.

6. Soliman, H., and Shalaby, A. Developing Pavement Design Inputs for Fine-Grained Subgrade Soils in Manitoba. 90th Annual Meeting of the Transportation Research Board, Washington D.C., 2011.

7. Soliman, H., and Shalaby, A. Sensitivity of Subgrade Resilient Modulus to Moisture Variation. The Annual Conference of the Transportation Association of Canada, Halifax, 2010.

8. Soliman, H., Shalaby, A., Kass, S., and Ng, T. Characterizing the Soil Resilient Modulus for Typical Manitoba Soils. The Annual Conference of the Transportation Association of Canada, Vancouver, 2009.